

UNIVERSIDADE ESTADUAL DE CAMPINAS
SISTEMA DE BIBLIOTECAS DA UNICAMP
REPOSITÓRIO DA PRODUÇÃO CIENTÍFICA E INTELLECTUAL DA UNICAMP

Versão do arquivo anexado / Version of attached file:

Versão do Editor / Published Version

Mais informações no site da editora / Further information on publisher's website:

<https://journals.aps.org/prd/abstract/10.1103/PhysRevD.109.112001>

DOI: 10.1103/PhysRevD.109.112001

Direitos autorais / Publisher's copyright statement:

©2024 by American Physical Society. All rights reserved.

DIRETORIA DE TRATAMENTO DA INFORMAÇÃO

Cidade Universitária Zeferino Vaz Barão Geraldo

CEP 13083-970 – Campinas SP

Fone: (19) 3521-6493

<http://www.repositorio.unicamp.br>

Combined search for electroweak production of winos, binos, higgsinos, and sleptons in proton-proton collisions at $\sqrt{s} = 13$ TeV

A. Hayrapetyan *et al.*^{*}
(CMS Collaboration)



(Received 2 February 2024; accepted 19 March 2024; published 6 June 2024)

A combination of the results of several searches for the electroweak production of the supersymmetric partners of standard model bosons, and of charged leptons, is presented. All searches use proton-proton collision data at $\sqrt{s} = 13$ TeV recorded with the CMS detector at the LHC in 2016–2018. The analyzed data correspond to an integrated luminosity of up to 137 fb^{-1} . The results are interpreted in terms of simplified models of supersymmetry. Two new interpretations are added with this combination: a model spectrum with the bino as the lightest supersymmetric particle together with mass-degenerate Higgsinos decaying to the bino and a standard model boson, and the compressed-spectrum region of a previously studied model of slepton pair production. Improved analysis techniques are employed to optimize sensitivity for the compressed spectra in the wino and slepton pair production models. The results are consistent with expectations from the standard model. The combination provides a more comprehensive coverage of the model parameter space than the individual searches, extending the exclusion by up to 125 GeV, and also targets some of the intermediate gaps in the mass coverage.

DOI: [10.1103/PhysRevD.109.112001](https://doi.org/10.1103/PhysRevD.109.112001)

I. INTRODUCTION

The standard model (SM), despite its success in describing the fundamental particles and their interactions, leaves several open questions in particle physics unanswered. Various extensions of the SM, such as supersymmetry (SUSY) [1–5], have been developed to address these questions. Supersymmetry potentially provides a solution to the hierarchy problem [6–8], as well as the unification of the gauge couplings at high energy scales [3,9]. Moreover, if R -parity [10] is conserved, the lightest SUSY particle (LSP) would be stable, and a potential dark matter candidate [11,12].

Supersymmetry introduces a fermionic (bosonic) superpartner for each boson (fermion) of the SM. The superpartners of the leptons are called sleptons; $\tilde{\ell}$ denotes the superpartner of lepton ℓ . Those of the SM $SU(2)_L$ and $U(1)$ gauge fields before electroweak (EW) symmetry breaking are the winos and binos, respectively, collectively called gauginos. In the minimal SUSY theory, MSSM [2,13,14], a new complex Higgs doublet is added to the SM. The MSSM thus contains five Higgs bosons along with the four Higgsino superpartners of the two Higgs doublets. The

bino, winos, and Higgsinos can mix among one another to form in total eight mass eigenstates (collectively, electroweakinos): two chargino pairs ($\tilde{\chi}_{1,2}^\pm$) and four neutralinos ($\tilde{\chi}_{1-4}^0$). While in some models $\tilde{\chi}_1^0$ is taken as the LSP, this assumption is not required. For example, models motivated by gauge-mediated SUSY breaking (GMSB) [15,16] introduce a Nambu-Goldstone boson goldstino (\tilde{G}) that may be identified with two of the chirality components of the superpartner of a graviton (gravitino), and be considered the LSP.

Interactions among the charginos, neutralinos, and sleptons occur with the same EW couplings as those of their SM partners. At the CERN LHC, the cross sections for production of these particles are correspondingly small compared with those for the SUSY partners of the strongly interacting SM particles (squarks and gluinos). Nevertheless, if the squarks and gluinos are more massive than the EW SUSY particles, the EW superpartners might be the only SUSY particles accessible at the LHC.

The ATLAS [17–44] and CMS [45–77] Collaborations have carried out extensive search programs that target final states that could result from the production and decay of EW interacting SUSY particles. The proton-proton (pp) collision energy \sqrt{s} for Ref. [17] (ATLAS) was 7 TeV; for Refs. [18,19] (ATLAS) and [45–47] (CMS) it was 8 TeV; for all other searches it was 13 TeV. Given that the SUSY particle decays could result in more than one final state, these programs benefit from combining individual searches to maximally exploit the available data, and both collaborations have performed combined searches for EW

^{*}Full author list given at the end of the article.

Published by the American Physical Society under the terms of the [Creative Commons Attribution 4.0 International license](https://creativecommons.org/licenses/by/4.0/). Further distribution of this work must maintain attribution to the author(s) and the published article's title, journal citation, and DOI. Funded by SCOAP³.

particles at $\sqrt{s} = 8$ TeV, by ATLAS [19] and CMS [45,47], and at 13 TeV, by ATLAS [37,44] and CMS [53].

In this paper we present the results of a combination of the EW SUSY searches reported in Refs. [71–76]. The data were collected at the LHC in 2016–2018 and correspond to an integrated luminosity of 137 fb^{-1} , except as noted in the following sections. The interpretation of results was performed using simplified model spectra (SMS) of SUSY [78–81], which assume that all SUSY particles other than those directly involved in the specified process are decoupled, being too massive to be produced or be involved in the decays. Additionally, R -parity is assumed to be conserved, ensuring that the initial production process gives rise to pairs of superpartners. Both compressed and uncompressed mass spectra scenarios were targeted; in the former the mass-splitting Δm between the lightest and next-to-lightest supersymmetric particles is $\mathcal{O}(10)$ GeV and smaller, resulting in an experimentally challenging final state in which the observable decay products have low momentum. Here we present an improved and extended reanalysis of the search of Ref. [73]: a novel signal extraction method is employed, along with a signal selection optimized to search for slepton pair production in models with compressed spectra. We also consider two additional interpretations beyond those covered in the Refs. [71–76], one of them enabled by the updates provided for the search of Ref. [73]. Together with the increased sensitivity resulting from the combined search itself, these provide a more comprehensive coverage of the model parameter space than the original individual searches. Tabulated results are provided in the HEPData record for this analysis [82].

This paper is organized as follows. The specific SMS scenarios studied in this combination are discussed in Sec. II. The CMS detector is briefly described in Sec. III, while Sec. IV contains summaries of the event reconstruction methods as well as the simulation of the different background and signal processes. Individual searches used as input are detailed in Sec. V, together with the updates provided for this combination where applicable. The general strategy used to combine the input analyses is described in Sec. VI, followed by the description of the treatment of systematic uncertainties in Sec. VII. The interpretation of the combined data under the considered SMS scenarios is provided in Sec. VIII, and a summary of the results is provided in Sec. IX.

II. SIGNAL MODELS AND SEARCH STRATEGY

In this section we introduce the specific SUSY models used to interpret the results of the combined search, together with a summary of the component searches. Each search is characterized by its topology, that is, the combination of SM particles directly emitted in the decay chains of SUSY particles in a given production and decay process. For example, the associated production of $\tilde{\chi}_1^\pm$ and

$\tilde{\chi}_2^0$, with the $\tilde{\chi}_1^\pm$ ($\tilde{\chi}_2^0$) decaying to a W (Z) boson and a $\tilde{\chi}_1^0$, falls within the WZ topology.

Each SMS model is defined in terms of the initially produced pair of SUSY particles, here the $\tilde{\chi}$ or $\tilde{\ell}$, and their decay chains, leading to the observable topologies. For the interpretations we make assumptions for the production cross sections and branching fractions, motivated by predictions from theoretical models of soft SUSY breaking. A review of these predictions for the electroweakino sector can be found in Ref. [83]. In these models the mixing matrix relating the gauge to mass eigenstates is approximately diagonal, so that we may identify the $\tilde{\chi}$ states as binolike, winolike, and Higgsino-like multiplets. The mass splitting within these multiplets is small, while the hierarchy among the multiplets is dependent on the SUSY-breaking picture assumed. For example, in “natural” SUSY models [84–86], the Higgsino-like multiplet tends to lie lowest among the $\tilde{\chi}$ states. As a representative of this class we consider the GMSB model [16,87–93]. Spectra with a binolike LSP are favored by alternative approaches to naturalness [94] among other models. The next-to-lightest SUSY particle (NLSP) states can be either winolike, with the Higgsino-like states decoupled, or vice-versa; we consider both of these cases below.

The following subsections provide detailed descriptions of the models: three for electroweakino production and decay, and one that instead assumes that only the slepton states are accessible. Of these, the Higgsino-bino and slepton interpretations are in addition to those considered in the previous CMS combination paper [53].

A. Models for the production of electroweakinos

We consider three SMS models for the production and decay of electroweakinos in which the NLSP decays to the LSP with the emission of a W , Z , or H boson. Here “ H boson” refers to the observed 125 GeV scalar (Higgs) boson, assumed to be the lightest CP -even state of the extended Higgs sector.

The first of these models is a wino-bino model, Fig. 1, in which the lightest chargino $\tilde{\chi}_1^\pm$ is produced in association with the next-to-lightest neutralino $\tilde{\chi}_2^0$. In computing the production cross section we take the $\tilde{\chi}_1^\pm$ and $\tilde{\chi}_2^0$ to be

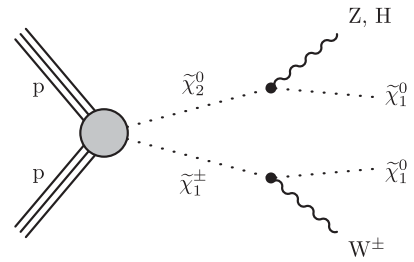


FIG. 1. Wino-bino model: production of $\tilde{\chi}_2^0$ and $\tilde{\chi}_1^\pm$, with the $\tilde{\chi}_2^0$ decaying to either a Z or H boson and a $\tilde{\chi}_1^0$, and the $\tilde{\chi}_1^\pm$ decaying to a W boson and a $\tilde{\chi}_1^0$.

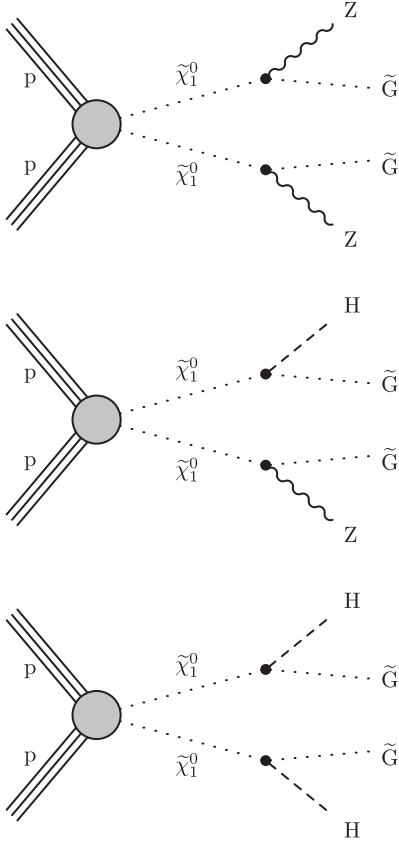


FIG. 2. GMSB model: pair production of $\tilde{\chi}_1^0\tilde{\chi}_1^0$. The $\tilde{\chi}_1^0$ particles each decay to a \tilde{G} with the emission of an SM gauge boson: (left) both Z , (middle) one Z and the other H , and (right) both H . Soft fermions from decays of nearly degenerate neutralinos and charginos are omitted from these diagrams.

degenerate in mass and winolike. We consider mass splittings between the NLSP and LSP up to the kinematic limit of the experiment, but also include a search, “2/3 ℓ soft” [73], targeting the compressed limit in which the gaugino mass spectrum is approximately degenerate (gaugino mass universality [83]). In addition, allowing also for Higgsino-gaugino mixing of the neutral states, and in the spirit of the more general SMS approach, we search for both $Z\tilde{\chi}_1^0$ and $H\tilde{\chi}_1^0$ decays of the $\tilde{\chi}_2^0$, as indicated in Fig. 1.

The other two electroweakino production models are characterized by a SUSY mass spectrum in which the light Higgsinos, including the NLSP, are nearly degenerate in mass and heavier than the LSP. In these models multiple production mechanisms leading to the same final state enhance the total effective cross section.

The first of these, the GMSB model, is motivated by a specific GMSB scenario [16] in which the light Higgsinos are nearly degenerate in mass, and the \tilde{G} is the LSP. The coupling of \tilde{G} is suppressed by the SUSY breaking scale [15], so that the $\tilde{\chi}_1^0$ NLSP is metastable. We assume that nonetheless the $\tilde{\chi}_1^0$ decays promptly on the measurement scale. Thus the production of $\tilde{\chi}_1^0$ pairs occurs both directly

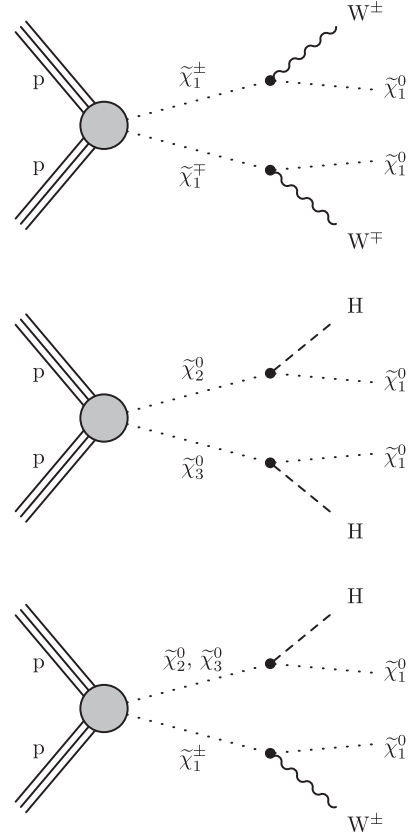


FIG. 3. Higgsino-bino model: (left) the production of a pair of charginos followed by their decays to W bosons and the LSP, (middle) the production of a pair of neutralinos followed by decays to H bosons and the LSP, and (right) the production of chargino-neutralino pairs followed by decay of the chargino (neutralino) to a W (H) boson and the LSP.

and as a result of cascade decays following production of the combinations $\tilde{\chi}_1^\pm\tilde{\chi}_1^0$, $\tilde{\chi}_1^\pm\tilde{\chi}_2^0$, $\tilde{\chi}_1^\pm\tilde{\chi}_1^\mp$, and $\tilde{\chi}_1^0\tilde{\chi}_2^0$. Because of the small mass splitting among the Higgsinos, low-momentum SM fermions emitted in these decays have a negligible impact on the kinematics of the event. We consider in total three topologies as illustrated in Fig. 2. The Z decays (Fig. 2, left) of Higgsino-like $\tilde{\chi}$ states are included in the search topology, allowing for any admixture of gauginos into these states.

The second Higgsino model, the Higgsino-bino model, assumes a binolike LSP, and again mass-degenerate light Higgsinos. The production mechanisms considered are: $\tilde{\chi}_1^\pm\tilde{\chi}_2^0$, $\tilde{\chi}_1^\pm\tilde{\chi}_3^0$, $\tilde{\chi}_1^\pm\tilde{\chi}_1^\mp$, and $\tilde{\chi}_2^0\tilde{\chi}_3^0$. The charged Higgsinos decay to a W boson and the LSP with 100% branching fraction, and for this process we assume that the neutral ones decay exclusively to $H + \text{LSP}$. This scenario is motivated by an alternate approach to natural SUSY [94] that seeks to evade constraints on the superpartner masses from earlier LHC searches by considering relatively large wino-bino mass splittings. The topologies contributing the Higgsino-bino interpretation are shown in Fig. 3.

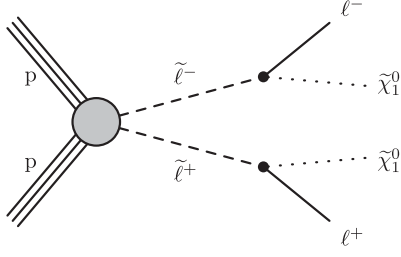


FIG. 4. Slepton-neutralino model: direct slepton pair production, with each slepton decaying into a lepton and a $\tilde{\chi}_1^0$ LSP.

B. Model for the production of sleptons

We also target the production of a pair of charged sleptons [95–97], each of which decays to a lepton and a $\tilde{\chi}_1^0$ LSP. The diagram for the process described by the slepton-neutralino model is shown in Fig. 4, and the model assumes equal masses for the superpartners $\tilde{e}_{L,R}$ and $\tilde{\mu}_{L,R}$ of the electrons and muons, respectively, while the $\tilde{\tau}$ states are considered to be decoupled. A dedicated analysis, presented here for the first time, addresses the compressed region of model parameter space that was not covered in a previous slepton search [71] by the CMS Collaboration.

C. Search strategies

Here we give an overview of the strategies pursued by the analyses that are included in this combination. Each is the subject of a more detailed summary given in Sec. V. The contributing searches are

- (1) “ $2/3\ell$ soft” [73], targeting the region of SUSY parameter space in which the mass difference between the NLSP and LSP is small. At least one pair of opposite-sign, low-transverse momentum (p_T) electrons or muons (“light leptons”) is required, together with jets.
- (2) “ 2ℓ ” [71], requiring two opposite-sign, same-flavor (OSSF) light leptons. We consider two categories:
 - (a) “ 2ℓ on- Z ,” in which the pair mass is consistent with the leptons’ origin in the decay of a Z boson, and
 - (b) “ 2ℓ nonresonant,” requiring that the lepton pair mass lie outside the Z mass peak region.
- (3) “ $2SS\ell/\geq 3\ell$ ” [74], selecting either two same-sign light leptons or at least three leptons, which may include one or more hadronically decaying tau leptons.
- (4) “ $1\ell 2b$ ” [72], requiring a light lepton consistent with arising from the decay of a W boson, and two b quarks that form an H boson candidate.
- (5) “ $4b$ ” [75], requiring two resolved or merged pairs of b -tagged jets that form H boson candidates.
- (6) “Hadr. WX” [76], selecting events with at least two merged (large-radius) jets from hadronically decaying W , Z , and H bosons.

In each of these searches a threshold on missing transverse momentum (p_T^{miss}) is imposed, since the presence of undetected LSPs in the final state is characteristic of the SUSY models considered.

Extensions are presented in this paper of the “ $2/3\ell$ soft” analysis reported in Ref. [73]: a more optimal binning of the search regions (SRs) is applied to the WZ topology, and a new variable tailored to search for slepton pair production is exploited. Adjustments are made to the SR and control-region (CR) definitions of the “ $2SS\ell/\geq 3\ell$ ” analysis to remove overlap with the event selection of the “ $2/3\ell$ soft” analysis.

The combination is performed with a simultaneous maximum likelihood (ML) fit to the SR and CR data from the input searches, described in Sec. VIII. In reference to background yields, we use the term “postfit” to refer to this fit for the background-only hypothesis with all SRs and CRs included.

III. THE CMS DETECTOR

The central feature of the CMS apparatus is a superconducting solenoid, 6 m in internal diameter and 13 m in length, that provides a magnetic field of 3.8 T. Within the solenoid volume are various particle detection systems. Charged-particle trajectories are measured by the silicon pixel and strip trackers. A lead tungstate crystal electromagnetic calorimeter (ECAL) and a brass and scintillator hadron calorimeter (HCAL) surround the tracker volume, each composed of a barrel and two endcap sections. Forward calorimeters extend the pseudorapidity coverage provided by the barrel and end cap detectors. The calorimeters provide measurements of the energies of electrons, photons, and hadronic jets, as well as of the directions of jets. Muons are measured in gas-ionization detectors embedded throughout the steel flux-return yoke outside the solenoid. A more detailed description of the CMS detector, together with a definition of the coordinate system used and the relevant kinematic variables, can be found in Ref. [98].

Events of interest are selected using a two-tiered trigger system. The first level, composed of custom hardware processors, uses information from the calorimeters and muon detectors to select events at a rate of around 100 kHz within a fixed latency of about 4 μs [99]. The second, or high-level, trigger consists of a farm of processors running a version of the full event reconstruction software optimized for fast processing, and reduces the event rate to around 1 kHz before data storage [100].

IV. EVENT RECONSTRUCTION AND MONTE CARLO SIMULATION

All analyses considered as an input to this combination share common event reconstruction methods that are summarized below together with a general description of

Monte Carlo (MC) simulated samples. Each analysis, however, targets a unique final state and different parts of kinematic phase space, and aims to maximize the background rejection. As a result, the details of the selection, such as those concerning object identification and isolation, can vary from analysis to analysis to ensure the best sensitivity for a given search. These details, in addition to the event selections, triggers, and MC simulated samples, are described in Refs. [71–76].

A. Common event reconstruction methods

The particle-flow (PF) algorithm [101] aims to reconstruct and identify each individual particle in an event, with an optimized combination of information from the various elements of the CMS detector. The energy of photons is obtained from the ECAL measurement. The energy of electrons is determined from a combination of the electron momentum at the primary interaction vertex as determined by the tracker, the energy of the corresponding ECAL cluster, and the energy sum of all bremsstrahlung photons spatially compatible with originating from the electron track. The energy of muons is obtained from the curvature of the corresponding track. The energy of charged hadrons is determined from a combination of their momentum measured in the tracker and the matching ECAL and HCAL energy deposits, corrected for the response function of the calorimeters to hadronic showers. Finally, the energy of neutral hadrons is obtained from the corresponding corrected ECAL and HCAL energies.

For each event, hadronic jets are clustered from PF candidates using the infrared- and collinear-safe anti- k_T algorithm [102,103]. The clustering is performed with distance parameter $R = 0.4$ (AK4 jets) to reconstruct jets designed to contain the fragmentation products of a single parton, and with $R = 0.8$ (AK8 jets) for jets originating from a multiparton system. Jet momentum is determined as the vectorial sum of the momenta of all reconstructed particles in the jet, and is found from simulation to be, on average, within 5%–10% of the true momentum over the whole p_T spectrum and detector acceptance. Besides the triggering event, pp interactions within the same or nearby bunch crossings (pileup) contribute tracks and calorimetric energy depositions to the jet momentum. To mitigate this effect, charged particles identified to be originating from pileup vertices are discarded, and an offset term is applied to correct for remaining contributions to the energy of the jet. Corrections derived from simulation are applied to match, on average, the measured response of jets to that of particle level jets. In situ measurements of the momentum balance in dijet, photon + jet, Z + jet, and multijet events are used to account for any residual differences in the jet energy scale between data and simulation [104]. The jet energy resolution amounts typically to 15–20% at 30 GeV, 10% at 100 GeV, and 5% at 1 TeV [104]. Additional selection criteria are applied to remove jets potentially

dominated by anomalous contributions from various sub-detector components or reconstruction failures.

The primary vertex is taken to be the vertex corresponding to the hardest scattering in the event, evaluated using tracking information alone, as described in Sec. 9.4.1 of Ref. [105].

The missing transverse momentum vector \vec{p}_T^{miss} is computed as the negative vector sum of the transverse momenta of all the PF candidates in an event, and its magnitude is denoted by p_T^{miss} [106]. The \vec{p}_T^{miss} is modified to account for corrections to the energy scale of the reconstructed jets in the event.

The identification of jets originating from b quarks (b tagging) is performed separately for AK4 and AK8 jets. The AK4 b jets are tagged with a version of the combined secondary vertex algorithm based on deep neural networks (DeepCSV [107]), and the analyses entering this combination utilize various working points. The medium working point, which is common among multiple analyses, corresponds to an efficiency of about 68% for a mistagging rate for light flavor quark and gluon jets of approximately 1%. The identification of AK8 jets containing two b quarks is performed with the deep-learning-based double- b tagging algorithm DeepdoubleBvL [108,109] with adversarial training [110] to decorrelate the neural network tagging score and the jet mass. AK8 jets are tagged as W , Z , or H bosons by the DeepAK8 algorithm [108,111].

Hadronically decaying tau lepton candidates (τ_h) are reconstructed from PF candidates with the “hadron-plus-strips” algorithm [112]. To reject the background originating from hadrons that are misreconstructed as τ_h , a boosted decision tree discriminant based on information from the reconstructed τ_h isolation, its measured lifetime, and the shape of the resulting jet is used [113]. A strict selection criterion is applied in this discriminant, resulting on an efficiency of 50% for selecting true τ_h decays and a less than 0.2% mistagging rate.

B. Monte Carlo simulation

Signal samples are generated with MadGraph 5_aMC@NLO (2.2.2 or newer) [114,115] at leading-order (LO) precision, including up to two additional partons in the matrix element calculations. The production cross sections are determined with approximate next-to-leading order (NLO) plus next-to-leading logarithmic (NLL) accuracy [95–97,116–120], and are used to normalize the signal samples. For all signal samples, the lowest NLSP mass considered is 100 GeV, while the highest varies between 1000 and 1500 GeV depending on the model. While the LSP mass is fixed at 1 GeV in the GMSB Higgsino model, it spans between 1 and 600 (650) GeV for the production of electroweakinos (sleptons). The mass points are generated with either 25 or 50 GeV steps in the uncompressed mass spectra scenarios, while for the compressed phase space a finer grid is used.

The background simulations rely on MadGraph 5_aMC@NLO (2.2.2 or newer), POWHEG (v1.0 or v2.0) [121–123], or MCFM7.0 [124–126], with calculations of either LO or NLO precision, all details depending on the process, as described in the individual published searches [71–76].

Showering, hadronization, and the underlying event description are carried out using the PYTHIA package 8.2 [127] (the specific version number depends on the considered sample). The CUETP8M1 underlying event tune [128] is used for the SM background and signal generation with 2016 data-taking conditions. For the 2017 and 2018 samples, the CP5 and CP2 tunes [129] are used for the SM background (NLO) and signal (LO) samples, respectively. Simulated samples generated at LO (NLO) with the CUETP8M1 tune use the parton distribution functions denoted by NNPDF3.0LO (NNPDF3.0NLO) [130], while those with the CP2 or CP5 tune use the NNPDF3.1LO (NNPDF3.1NNLO) [131] ones. For all Monte Carlo samples, simulated minimum bias interactions are superimposed on the generated events, with a number distribution that is adjusted to match the pileup distribution measured in data. For some analyses, because scans over numerous mass points are required for the signal models, the response of the detector is described using the CMS fast simulation program [132,133], which yields results that are generally consistent with those from the simulation based on GEANT4 [134] and have appropriate systematic uncertainties applied to cover differences.

All simulated events are reconstructed with the same programs as those used for collision data. Corrections are applied to simulated samples to account for differences between the trigger, b tagging, and lepton and photon efficiencies measured in data and the GEANT4 simulation. Additional differences arising from the use of fast simulation modeling, such as selection efficiencies and the modeling of p_T^{miss} , are corrected for and included in the systematic uncertainties.

V. INDIVIDUAL ANALYSES CONTRIBUTING TO THE COMBINATION

The searches included in the combination are briefly described in this section, together with a more detailed account of any update made to an analysis since its publication.

A. Search in final states with two or three soft leptons and p_T^{miss}

The “2/3 ℓ soft” search [73] selects events with two or three low- p_T light leptons. It targets the WZ topology of the wino-bino model with chargino-neutralino production in the compressed region, i.e., where the mass difference Δm between $\tilde{\chi}_1^0$ and the NLSP is small, such that the W and Z bosons are off-shell, and the observable decay products have low momentum. Events are divided into two search

TABLE I. “2/3 ℓ soft” search: definition of the lepton multiplicity and $p_T^{\text{miss,corr}}$ SRs. The boundaries are indicated in GeV. Events in the low- p_T^{miss} SR must additionally have $p_T^{\text{miss}} > 125$ GeV.

SR	Low- p_T^{miss} $p_T^{\text{miss,corr}}$	Med- p_T^{miss} $p_T^{\text{miss,corr}}$	High- p_T^{miss} $p_T^{\text{miss,corr}}$	Ultrahigh- p_T^{miss} $p_T^{\text{miss,corr}}$
2 ℓ soft	[125, 200]	[200, 240]	[240, 290]	>290
3 ℓ soft	[125, 200]		>200	

categories, “2 ℓ soft” and “3 ℓ soft.” Both require an e^+e^- or $\mu^+\mu^-$ pair, jets, and large p_T^{miss} . The presence of an additional electron or muon defines the “3 ℓ soft” category. The leptons are required to satisfy $p_T < 30$ GeV, with the minimum value of p_T being 3.5 (5.0) GeV for muons (electrons), except as noted in the following paragraph.

The variables used to discriminate signal from background are the dilepton mass $m_{\ell\ell}$, p_T^{miss} , and $p_T^{\text{miss,corr}}$; the latter is defined as the magnitude of the total \vec{p}_T^{miss} reconstructed excluding the muon transverse momentum vectors, as an approximation to the trigger-level p_T^{miss} quantity used during data-taking. Events in the two search categories are binned in $p_T^{\text{miss,corr}}$ as detailed in Table I, resulting in four (two) SRs in the “2 ℓ soft” (“3 ℓ soft”) category. Additionally, in the low- p_T^{miss} SRs all events must satisfy $p_T^{\text{miss}} > 125$ GeV, and only muon pairs are accepted because of the utilized triggers; the minimum value of p_T is increased to 5 GeV for these muons to ensure efficiency of the trigger. The trigger paths targeting the low- p_T^{miss} SRs were disabled during some parts of the data taking, resulting in the slightly lower integrated luminosity of 129 fb $^{-1}$. Each $p_T^{\text{miss,corr}}$ bin is further divided into regions of $m_{\ell\ell}$ with boundaries of 1, 4, 10, 20, 30, and 50 GeV, with the first bin removed in the low- p_T^{miss} category because of the trigger requirements. For the “2 ℓ soft” category $m_{\ell\ell}$ is the dilepton invariant mass $M(\ell\ell)$, whereas for the “3 ℓ soft” category it is the minimum of the invariant masses of the possible OSSF pairs, $M_{\text{OSSF}}^{\text{min}}(\ell\ell)$. In the following, $m_{\ell\ell}$ is used to denote the dilepton mass in either category.

Contributions from J/ψ and Υ mesons are removed by excluding events with $m_{\ell\ell}$ in the ranges 3.0–3.2 and 9.0–10.5 GeV, respectively. Additional kinematic requirements are applied to further reduce backgrounds. The largest backgrounds arise from Z/γ^* and $t\bar{t}$ production, as well as events with nonprompt leptons from mainly W + jets (2 ℓ) or $t\bar{t}$ (3 ℓ) production.

Two major updates are made to the search [73], designed with no prior knowledge of the distribution of data events in the updated SRs, and discussed in the following subsections. The first one is an improvement to the signal extraction, while the second introduces a new search for slepton pair production.

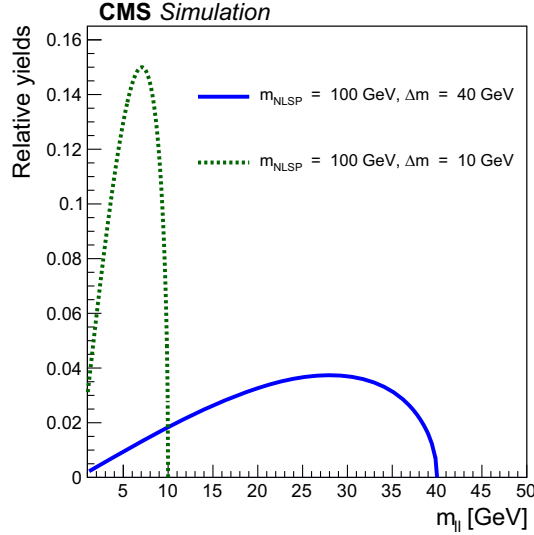


FIG. 5. “2/3 ℓ soft” search: dilepton mass spectrum for two mass hypotheses with the same NLSP mass (100 GeV) and different mass splittings Δm (40 or 10 GeV), both corresponding to analytical phase space only calculations. The distributions have a kinematic endpoint at the mass splitting.

1. Improved signal extraction: Parametric Δm binning

For signal, $m_{\ell\ell}$ corresponds to the mass of the off-shell Z-boson Z^* from the decay $\tilde{\chi}_2^0 \rightarrow \tilde{\chi}_1^0 Z^*$. The $m_{\ell\ell}$ spectrum has a kinematic end-point at Δm , and the shape depends on the sign of the product of the two smallest (in magnitude) eigenvalues of the neutralino mass matrix [135]. The dilepton mass spectra are corrected accordingly in Ref. [73], but for this combination we assume a flat phase space for the $\tilde{\chi}_2^0$ decay rate to ensure consistency among the input analyses. Two examples of the spectrum are shown in Fig. 5.

To better exploit the shape of the $m_{\ell\ell}$ distribution, we optimize the $m_{\ell\ell}$ binning for each Δm hypothesis, separately for each lepton category and p_T^{miss} bin. The procedure is iterative. The range $[1 \text{ GeV}, \Delta m]$ is first divided into four bins of equal signal quantiles. A fifth bin spans $[\Delta m, 50 \text{ GeV}]$, which is expected to be devoid of signal. Aside from resolution effects and statistical fluctuations, this construction leads to distributions of the events per bin that, for the bins below Δm , are uniform for signal, and depleted for background.

In the second step we check that none of the resulting bins introduces large statistical fluctuations of the expected SM background, taking into account both the relative importance of the various background processes and the statistical precision of their predictions. This is to avoid an artificial increase in the sensitivity. If the statistical fluctuations for any of the bins in $[1 \text{ GeV}, \Delta m]$ exceed those reported in Ref. [73], the number of bins in that range is reduced by one, and the binning is rederived. This process is repeated until a binning is found that satisfies this requirement, or results in the minimal two-bin case

$[1 \text{ GeV}, \Delta m]$, $[\Delta m, 50 \text{ GeV}]$. The CR binning and background estimation strategy remain the same as in Ref. [73], ensuring that there are no changes to how the CRs are correlated with the SRs.

For each of the nine Δm hypotheses considered in this search, six parametric binnings have been derived (one for each SR). Examples of the resulting post-fit SR distributions of $m_{\ell\ell}$ with parametric binnings (for signal mass points with $\Delta m = 20 \text{ GeV}$) are shown in Figs. 6 and 7 for the “2 ℓ soft” and “3 ℓ soft” search categories, respectively.

The expected sensitivity of the search is improved over the full parameter space considered in this analysis. The largest gains are obtained for mass splittings of $\Delta m < 20 \text{ GeV}$, where the expected sensitivity to the mass of $\tilde{\chi}_2^0$ is increased by 5–25 GeV, depending on Δm .

2. Slepton production in the compressed region

The production of a smuon or selectron pair for the case of a compressed SUSY spectrum has not been studied previously in a dedicated search by the CMS Collaboration. Here we analyze the events captured by the “2 ℓ soft” selection to search for this process, employing the parametric binning procedure described in Sec. VA 1 to optimize the sensitivity. In this case, to discriminate between signal and background we replace $m_{\ell\ell}$ with the kinematic variable $m_{T2}(k, k, \chi_{m_\chi})$ [136,137]. For a process producing two particles of equal mass M that each decay into an invisible daughter χ of mass m_χ and a light visible object k , we have

$$m_{T2}(k, k, \chi_{m_\chi}) = \min_{\vec{p}_T^{\text{miss}(1)} + \vec{p}_T^{\text{miss}(2)} = \vec{p}_T^{\text{miss}}} (\max[M_T^{(1)}(m_\chi), M_T^{(2)}(m_\chi)]). \quad (1)$$

The constraint enforces that the observed \vec{p}_T^{miss} is equal to the sum of $\vec{p}_T^{\text{miss}(i)}$ ($i = 1, 2$), two vectors in the transverse plane that represent the p_T vectors of the invisible objects. The $M_T^{(i)}$ are the transverse masses obtained by pairing the $\vec{p}_T^{\text{miss}(i)}$ with either of the two visible objects. The distribution in $m_{T2}(k, k, \chi_{m_\chi})$ extends between m_χ and M . Here the visible objects are the two low- p_T leptons, and we take m_χ to be 100 GeV, noting that the exact choice of m_χ is expected to have a negligible effect on the sensitivity of the search. In the following, we utilize the notation $m_{T2}(\ell, \ell, \chi_{100})$.

The analysis utilizes the same background estimation methods, CRs, and systematic uncertainties as Ref. [73], with the exclusion of the “3 ℓ soft” SRs. A separate parametric binning is chosen for each model point, $(m_{\tilde{\ell}}, \Delta m)$. An example of the resulting post-fit SR distributions of $m_{T2}(\ell, \ell, \chi_{100})$, for mass point $(m_{\tilde{\ell}} = 125 \text{ GeV}, m_{\tilde{\chi}_0} = 115 \text{ GeV})$, is shown in Fig. 8. The SM background normalizations are constrained in the same way as done for the search for charginos and neutralinos [73], including the $m_{\ell\ell}$ distribution in the CR.

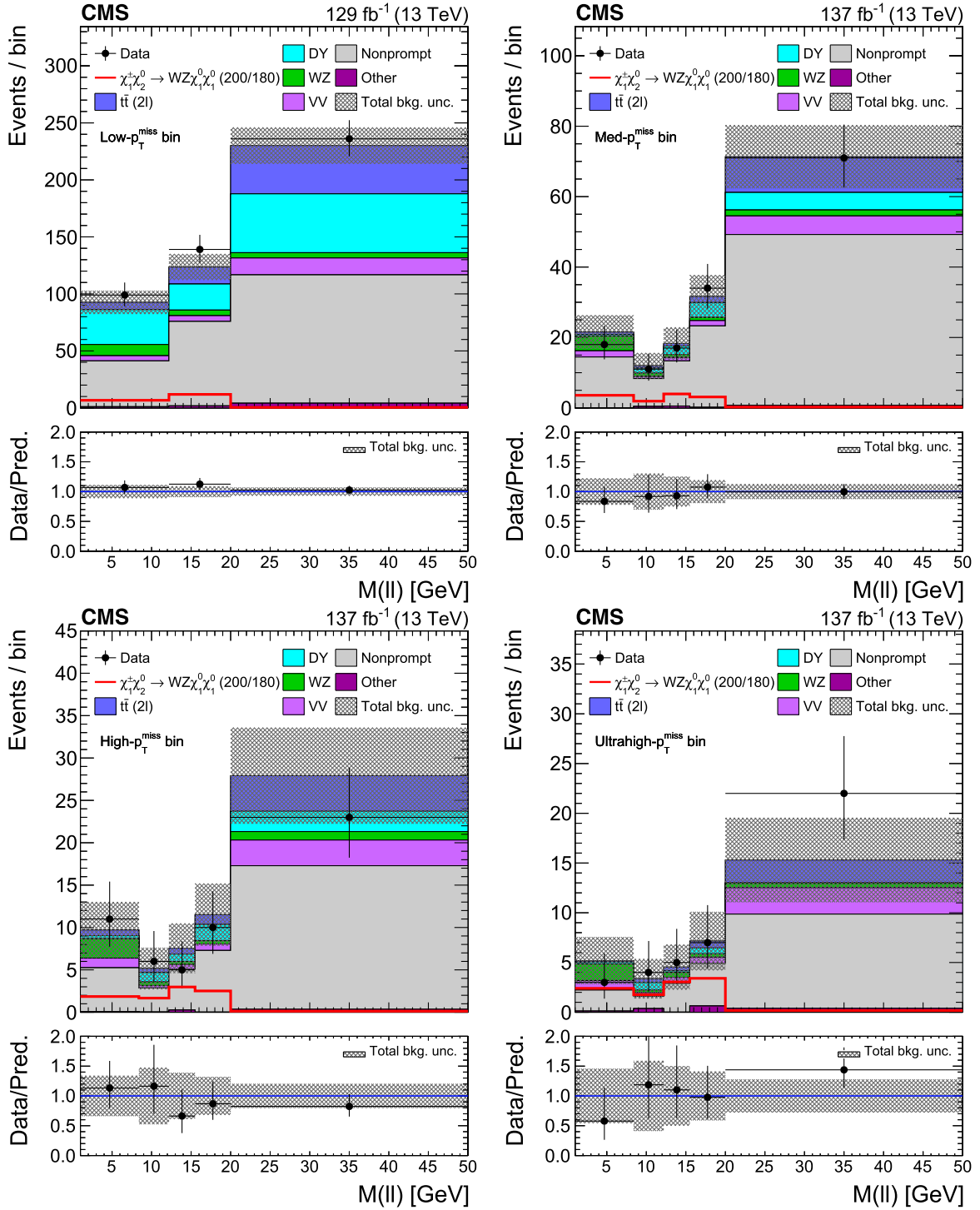


FIG. 6. “2/3 ℓ soft” search: post-fit distributions of the $M(\ell\ell)$ variable for the low- (upper left), medium- (upper right), high- (lower left), and ultrahigh- (lower right) p_T^{miss} bins in the “2 ℓ soft” signal region of Ref. [73]. These distributions are based on the parametric binnings derived for signal mass points with $\Delta m = 20$ GeV. The prefit signal distribution for $m_{\chi_1^\pm} = m_{\chi_2^0} = 200$ GeV, $m_{\chi_0} = 180$ GeV is overlaid for illustration. “Nonprompt” refers to the background contribution arising from nonprompt or misidentified leptons.

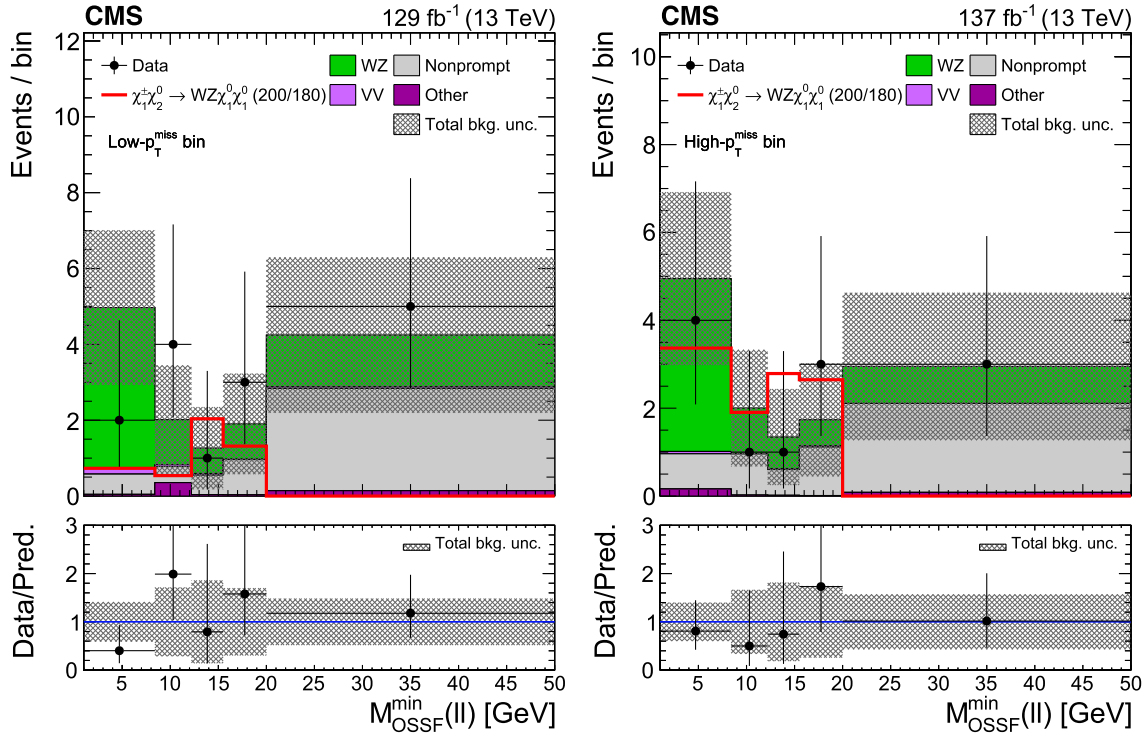


FIG. 7. “2/3 ℓ soft” search: post-fit distributions of the $M_{\text{OSSF}}^{\min}(\ell\ell)$ variable for the low- (left) and medium- (right) p_T^{miss} bins in the “3 ℓ soft” signal region of Ref. [73]. These distributions are based on the parametric binnings derived for signal mass points with $\Delta m = 20$ GeV. The prefitted signal distribution for $m_{\chi_1^\pm} = m_{\chi_2^0} = 200$ GeV, $m_{\chi_0} = 180$ GeV is overlaid for illustration. “Nonprompt” refers to the background contribution arising from nonprompt or misidentified leptons.

B. Searches in final states with an opposite-sign same-flavor lepton pair and p_T^{miss}

These searches [71] select events with lepton pairs e^+e^- or $\mu^+\mu^-$ and large p_T^{miss} . Of the SRs defined in Ref. [71], we include in the present combination those designated “EW on- Z ” and “Slepton.” The first targets the wino-bino and GMSB models, while the second targets the slepton-neutralino model, both in the uncompressed region of the model parameter space. Events in the two categories are required to have exactly two reconstructed OSSF leptons, with $p_T > 25(20)$ GeV for the leading (trailing)- p_T lepton. Threshold requirements are also imposed on the event p_T^{miss} and $m_{T2}(\ell, \ell, \chi_0)$, or $m_{T2}(\ell b, \ell b, \chi_0)$ for SRs with two b -tagged jets, to suppress SM backgrounds.

The main backgrounds in this final state are Drell-Yan lepton pairs with p_T^{miss} from mismeasured jet energies, $t\bar{t}$ production, and events with both a Z boson and prompt neutrinos, including $t\bar{t}Z$, $WZ \rightarrow 3\ell\nu$, and $ZZ \rightarrow 2\ell 2\nu$. They are estimated with CRs in the data.

1. On- Z search (“2 ℓ on- Z ”)

The “2 ℓ on- Z ” search focuses on cases in which the invariant mass $m_{\ell\ell}$ of the dilepton pair is consistent with the Z boson mass: $86 < m_{\ell\ell} < 96$ GeV. This targets the WZ , ZZ , and HZ topologies, where the Z boson (one of the Z bosons in the ZZ topology) is produced on-shell and

decays to two electrons or muons, while the other boson decays hadronically.

In addition to the two leptons, we require the presence of jets produced in the hadronic decay of the bosons. A total of three SRs in this category are considered, of which two target the WZ and ZZ topologies, and one is dedicated to the HZ topology. Events in the resolved WZ and ZZ regions are required to have at least two jets and no b -tagged jets. Events in the Lorentz-boosted region have < 2 AK4 jets and at least one AK8 jet satisfying mass and structure requirements. The HZ SR requires two b -tagged jets consistent with an $H \rightarrow b\bar{b}$ decay. The three SRs are then binned in p_T^{miss} .

2. Off- Z search (“2 ℓ nonresonant”)

The “2 ℓ nonresonant” SRs target nonresonant production of sleptons. In this case, the dilepton invariant mass must satisfy $20 < m_{\ell\ell} < 65$ GeV, or $m_{\ell\ell} > 120$ GeV. Two SRs (“Slepton”) are defined, those with and without jets in addition to the lepton pair. These SRs are further separated into bins in p_T^{miss} .

C. Search in final states with two same-sign leptons, or three or more leptons, and p_T^{miss}

The “2SS $\ell/\geq 3\ell$ ” search [74] focuses on final states with either two light same-sign leptons, or three or more

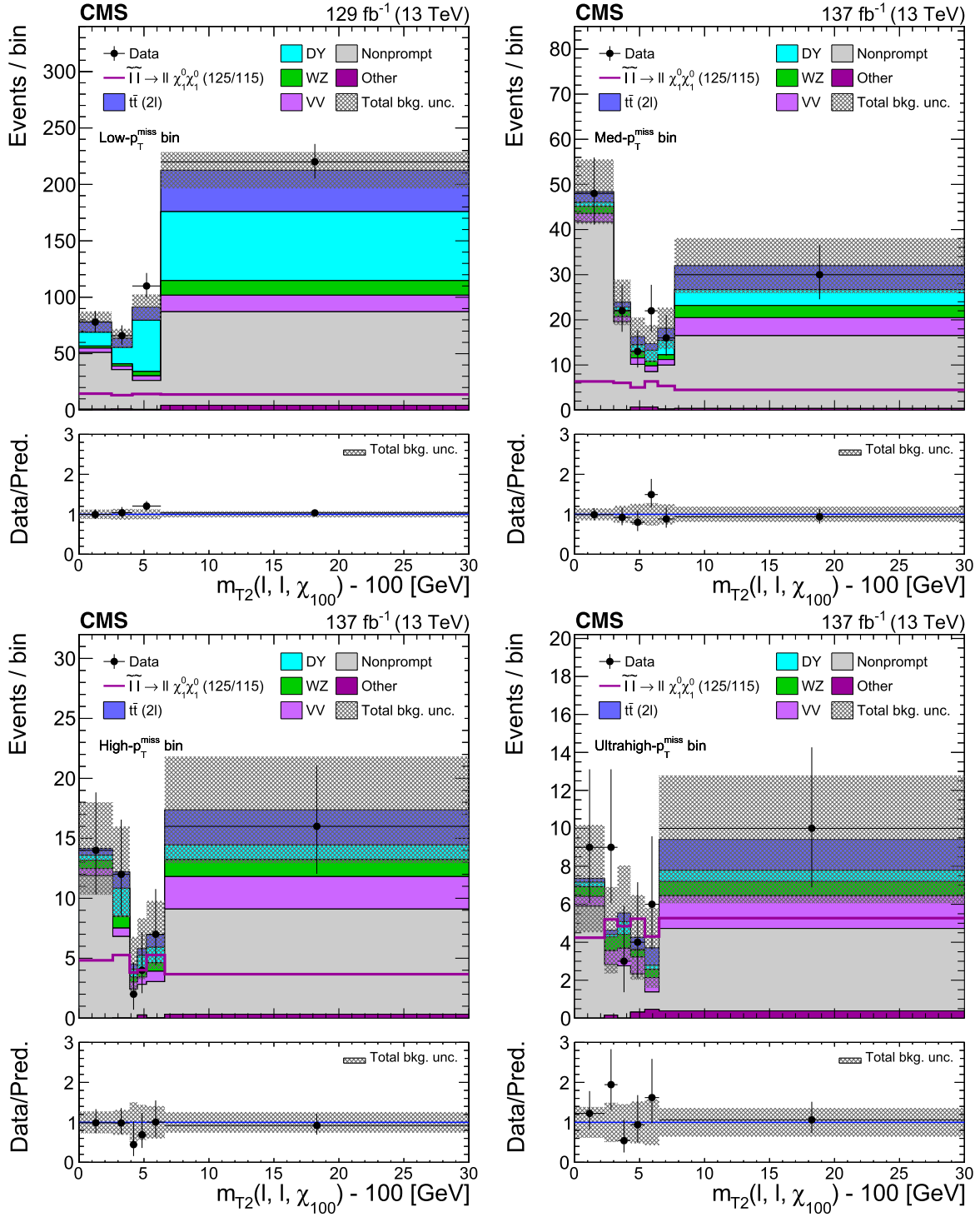


FIG. 8. “2/3 ℓ soft” search: postfit distributions of the $m_{T2}(\ell, \ell, \chi_{100})$ variable are shown for the low- (upper left), medium- (upper right), high- (lower left), and ultrahigh- (lower right) p_T^{miss} bins in the “2 ℓ soft” signal region of Ref. [73]. These distributions are based on the parametric binnings derived for the mass-point $m_{\tilde{\ell}} = 125$ GeV, $m_{\tilde{\chi}_0} = 115$ GeV, for which the pre-fit signal distribution is overlaid for illustration. Note that the signal distribution (purple line) is approximately flat across $m_{T2}(\ell, \ell, \chi_{100})$, by construction of the parametric binning procedure. The minimum value of $m_{T2}(\ell, \ell, \chi_{100})$, $m_{\chi} = 100$ GeV, is subtracted for the abscissa of the plot. “Nonprompt” refers to the background contribution arising from nonprompt or misidentified leptons.

leptons including τ_h , and p_T^{miss} . The analysis targets the WZ , WH , ZZ , HZ , and HH topologies.

The search is organized in a series of twelve exclusive categories that target the different decay modes of the W , Z , and H bosons. The categories are defined based on lepton multiplicity, flavor, and charge [74], summarized for purposes of this paper as follows:

- (i) Category SS: a pair of same-sign light leptons and no τ_h .
- (ii) Category A: three light leptons, including an OSSF lepton pair.
- (iii) Category B: three light leptons, with no OSSF lepton pairs.
- (iv) Categories C, D, E, and F: three leptons, at least one of which is a τ_h .
- (v) Categories G, H, I, J, and K: more than three leptons.

Within each category, several SRs are defined by requirements on multiple kinematical variables, including particle p_T , $m_{T2}(\ell, \ell, \chi_0)$, $m_{\ell\ell}$, and the scalar p_T sum H_T for all selected jets with $p_T > 30$ GeV, as detailed in Ref. [74]. For category A, an alternative approach based on parametric neural networks is used to build discriminant variables for the WZ model [74].

For the SS category, the main sources of background are nonprompt leptons or charge mismeasurements, estimated from control samples in data. Those for the other light-lepton categories A, B, G, and H result from WZ and ZZ production, and are estimated using MC simulation that is validated in low- p_T^{miss} CRs. For the remaining categories, those that contain τ_h candidates, the main backgrounds arise from Drell-Yan and $t\bar{t}$ production with associated nonprompt τ_h candidates. The predictions for these contributions are obtained directly from data using a loose-to-tight selection method [74].

Modifications to remove overlap with the “2/3 ℓ soft” analysis.

In Ref. [74], the requirements on the minimum p_T of electrons and muons vary between 10 and 25 GeV, chosen to ensure full trigger efficiency after the selection. Because of a small overlap between this and the “2/3 ℓ soft” analysis, for the present combination these threshold p_T values were raised to 30 GeV for the leading lepton in categories A and B. In this section we describe the changes in SR yields resulting from this modification.

The first consequence of the altered selection is a slight revision in the definitions of the CRs used for evaluation of

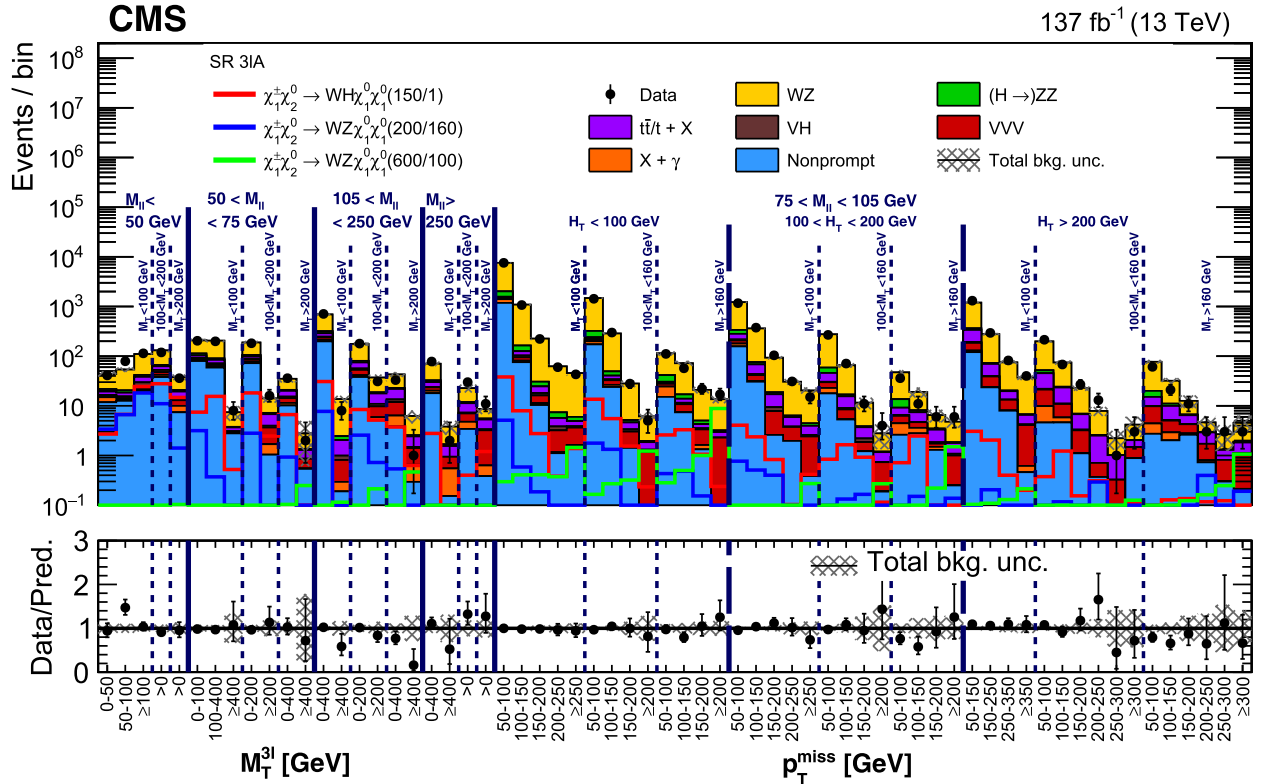


FIG. 9. “2SS $\ell/\geq 3\ell$ ” search: observed and expected event yields across the SRs in category A, events with three light leptons of which at least two form an OSSF pair, after the requirement that the leading-lepton p_T be greater than 30 GeV is applied. The pre-fit signal distributions for three mass-points are overlaid for illustration, and the considered mass hypothesis is indicated in the legend with notation $[m(\text{NLSP})/m(\text{LSP})]$; for example (150/1) stands for $m_{\tilde{\chi}_1^+} = m_{\tilde{\chi}_2^0} = 150$ GeV, $m_{\tilde{\chi}_0} = 1$ GeV. “Nonprompt” refers to the background contribution arising from nonprompt or misidentified leptons.

the backgrounds from WZ production and from asymmetric photon-to-electron conversions. The first of these CRs is included in all the analysis fits, while the second is used to validate the MC simulation of the conversion background. The level of agreement between the observed and expected yields in the CRs that was found in the previously published analysis is maintained. The effect of the tightened lepton p_T requirement on the WZ CR is nearly negligible; around 1% of the overall background events are lost. As photon-to-electron conversions tend to result in electrons of lower momenta, the effects of restricting the leading-lepton p_T are greater in the conversion CR: around 10% of the overall CR yield is lost.

The change in the minimum leading-lepton p_T also introduces slight variations in the signal extraction strategy, as not all SRs are affected equally by the tighter criteria. The SR definitions themselves are unchanged: those in category A are divided according to the value of $m_{\ell\ell}$ of the OSSF lepton pair into on- Z , with $75 < m_{\ell\ell} < 105$ GeV, and off- Z subcategories. Each of these subcategories is further divided into bins in p_T^{miss} , H_T , the transverse mass (M_T) of p_T^{miss} and the lepton not in the OSSF pair, and the transverse mass ($M_T^{3\ell}$) of the three leptons and p_T^{miss} . The exact definitions of the SRs of category A are shown by the labeling in Fig. 9, which gives the distribution of yields in those SRs with the altered leading-lepton p_T threshold.

The additional requirement causes a reduction in the yields of the overall SM backgrounds; for most SRs the effect on these yields is less than 1%, except for regions with low invariant mass ($m_{\ell\ell} < 75$ GeV) where the decrease in the background yields can be up to 7%. For the signal models the decrease in acceptance is strongly correlated with the model parameters. Signal models that target uncompressed scenarios are largely unaffected, while those that include compressed spectra have a reduction in overall yields of 5%–7%.

The evaluation of the neural network shapes for the WZ model of category A is kept unchanged after the additional leading-lepton p_T selection is applied.

In category B, the SR definition strategy is much simpler, as both the available event yields and number of studied models are smaller than in category A. In this case, the signal extraction strategy is based on a single variable, the minimum distance $\min \Delta R(\ell, \ell)$ between any two leptons. Figure 10 shows the expected and observed distributions of events in this category after the additional requirement is applied. The SM background contributions are reduced by roughly 5%, with the largest changes in the signal-depleted second and third bins. The signal efficiency is reduced by 1–2% overall.

The effect of the additional lepton p_T requirement on the analysis performance has been studied in terms of the expected upper limits for the GMSB model with degenerate Higgsinos (leading to the topologies HH , HZ , and ZZ),

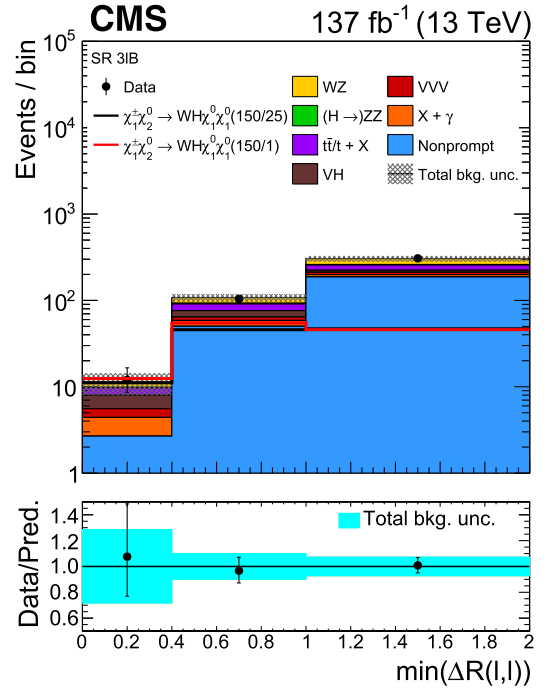


FIG. 10. “ $2SS\ell/\geq 3\ell$ ” search: observed and expected event yields across the SRs in category B, events with three light leptons and no OSSF pair, after the requirement that the leading-lepton p_T be greater than 30 GeV is applied. The prefit signal distributions for two mass-points are overlaid for illustration, and the considered mass hypothesis is indicated in the legend with notation $[m(\text{NLSP})/m(\text{LSP})]$; for example (150/1) stands for $m_{\tilde{\chi}_1^\pm} = m_{\tilde{\chi}_2^0} = 150$ GeV, $m_{\tilde{\chi}_0} = 1$ GeV. “Nonprompt” refers to the background contribution arising from nonprompt or misidentified leptons.

and for the wino-bino model with production of $\tilde{\chi}_1^\pm$ and $\tilde{\chi}_2^0$ (WZ , WH , and mixed-topology models). In most cases the upper limits are consistent at the 1% level before and after the additional requirement is applied. The only exceptions are the compressed scenarios in the WZ model, where decreases of 1–10% in expected sensitivity to the mass of NLSP are seen between mass splittings of $\Delta m = 70$ and 20 GeV. The effect translates to a loss of roughly 10 GeV in NLSP mass exclusion in the worst case scenario. In the combined analysis, this loss of sensitivity is compensated by the performance of the “ $2/3\ell$ soft” lepton analysis.

D. Search in final states with one lepton, two b jets, and p_T^{miss}

The “ $1\ell 2b$ ” search [72] targets the WH topology by focusing on events with one electron or muon ($p_T > 30$ GeV) produced in a W boson decay, two b -tagged jets from a Higgs boson decay, and large p_T^{miss} from the two LSPs and the neutrino. The search benefits from the large branching fraction for $H \rightarrow b\bar{b}$ (58%) [138] and the suppression of multijet background in the leptonic final state.

The two b -tagged jets are required to have an invariant mass consistent with that of the Higgs boson (90–150 GeV). The transverse mass of the lepton and p_T^{miss} is required to be larger than 150 GeV to remove events where the lepton and the p_T^{miss} both arise from a single leptonic W decay. In addition, events where the Higgs bosons are Lorentz boosted are selected by requiring a single large-radius jet ($R = 0.8$), identified by the DEEPAK8 algorithm [111]. To enhance the sensitivity, the selected events are sorted into SRs according to the presence or not of a boosted H -tagged jet, p_T^{miss} , and the number of AK4 jets.

The main backgrounds for the search arise from top quark production and W boson production. The contributions of these processes to the SR yields are estimated using observed yields in CRs scaled by transfer factors obtained from simulated samples. These extrapolations are studied extensively in validation regions orthogonal to the SRs in order to assess the systematic uncertainty in the background measurement.

E. Search in final states with four b jets and p_T^{miss}

The “4 b ” search [75] selects events with b -tagged hadronic jets, no charged leptons, and large p_T^{miss} , to target the HH topology through the decays $H \rightarrow b\bar{b}$. In each event, we consider either a resolved signature, in which the two b quarks of each H decay are contained in two separate AK4 jets, or a boosted signature, where the two b quarks are both contained in a single AK8 jet (“ bb -tagged jet”).

For the SRs of the resolved signature at least four (and to suppress combinatorial background no more than five) AK4 jets with $p_T > 30$ GeV are required. Separate SRs are defined for which three (3- b) or at least four (4- b) jets satisfy b -tagging criteria. The two H candidates are chosen by considering the four jets with the highest b tagging discriminator scores, forming all possible pairs of these jets, and selecting the pairing that minimizes the difference in the invariant masses of the two pairs. This difference is then required to be less than 40 GeV, and the average $\langle m_{bb} \rangle$ of the invariant masses of the two pairs is required to lie within the H mass peak region, $100 < \langle m_{bb} \rangle < 140$ GeV. An upper limit is imposed on the largest angular separation ΔR_{max} between pairs of the H daughter jets to remove lepton + jets tt events, the primary background to this search.

For the boosted signature, at least two AK8 jets with $p_T > 300$ GeV are required, with SRs having one (“1- bb ”) or at least two (“2- bb ”) of these satisfying bb tagging requirements. The H candidates are the two highest- p_T AK8 jets meeting these criteria. Each of these jets is required to have a mass, as computed by the “soft drop” algorithm [139,140], that lies in the H mass peak region, 60–260 GeV. The 1- bb CRs and SRs of the boosted signature are excluded from the Higgsino-bino interpretation to avoid overlap with the “Hadr. WX” search.

Both signatures’ SRs are binned in p_T^{miss} , while for the resolved signature an additional binning in ΔR_{max} further increases the sensitivity.

In addition to lepton + jets tt production, background contributions arise at higher p_T^{miss} from W or Z production in association with jets. The backgrounds from all sources are predicted using data CRs that require either exactly two b jets (resolved) or no $b\bar{b}$ jets (boosted), or an H candidate mass outside the defined H mass peak region.

F. Search in final states with multiple jets and p_T^{miss}

The “Hadr. WX” search [76] selects events with a pair of AK8 jets and large p_T^{miss} . The search targets the hadronically decaying WW , WZ , and WH signal topologies. We require at least 2 AK8 jets, $p_T^{\text{miss}} > 200$ GeV, $H_T > 300$ GeV, and no charged leptons. To reduce backgrounds with higher jet multiplicities, we further require at most 6 AK4 jets. (For signal, the requirement of two AK8 jets generally implies the presence of around four overlapping AK4 jets.) Taking advantage of the larger hadronic branching fraction of H and Z bosons, in particular to pairs of bottom quarks, the search is classified broadly into two SRs. The b -veto SR requires zero b -tagged jets, to be sensitive to the topologies WW , and WZ with the Z boson decaying to hadronic final states without b quarks. The b -tag SR requires at least one b -tagged jet, for the topologies WZ and WH with Z or H decaying to bb . The b -tag SR is further divided into one with a bb -tagged H candidate jet (WH) and one without (W). A third b -tag SR (H) [76] without a specific requirement on W candidate jets is excluded, together with the corresponding CR, from the Higgsino-bino interpretation to avoid overlap with the “4 b ” analysis.

The DEEPAK8 algorithm [111] is used to tag the decays of the W , Z , and H bosons. This algorithm provides multiple tagging scores that distinguish AK8 jets arising from different hadronic decay modes of the SM bosons and the top quark. The algorithm also provides two versions of neural networks with and without adversarial training [110] to decorrelate the neural network tagging score and the jet mass. The mass-decorrelated version of the DEEPAK8 W tagger (referred to as the V tagger) is used to tag hadronic decays of both W and Z bosons, while the DEEPAK8 W tagger without mass decorrelation (referred to as the W tagger) is used to tag decays of W bosons. The V tagger provides good efficiency for Z as well as W jets, while the dedicated W tagger has a lower misidentification rate. In the b -veto search region we require that at least one AK8 jet be tagged by the W tagger, and at least one other AK8 jet be tagged by the V tagger. The AK8 jet mass is required to be between 65 and 105 GeV. In the b -tag search region the W tagger and mass requirement are utilized for the AK8 jets from W bosons, while the AK8 jets from Z and H bosons are tagged using the DEEPAK8 bb tagger with mass decorrelation and with the jet mass requirement of 75–140 GeV.

TABLE II. Summary of the searches considered in the combination and the SRs that contribute to the interpretation of each signal model and topology. The following abbreviations appear in the table: For the “ 2ℓ on- Z ” analysis, “EW” refers to the resolved and boosted VZ SRs and the HZ SR. The row label “ 2ℓ nonres.” refers to the “ 2ℓ nonresonant” search, and in that row “Slepton” refers to the two dedicated slepton SRs, those requiring $N_{\text{jet}} = 0$ and $N_{\text{jet}} > 0$. For the “ $2SS\ell/\geq 3\ell$ ” search, “A(NN)” indicates SR A with the parametric neural network signal extraction. For the “Hadr. WX”, “ex H” means all SRs except the b -tag H SR.

Search	Wino-bino		GMSB			Higgsino-bino			Sleptons
	WZ	WH	ZZ	HZ	HH	WW	HH	WH	$\ell^+\ell^-$
$2/3\ell$ soft [73]	All								2ℓ soft
2ℓ on- Z [71]	EW		EW	EW					
2ℓ nonres. [71]									Slepton
$2SS\ell/\geq 3\ell$ [74]	SS, A(NN)	SS, A-F	All	All	All			SS, A-F	
$1\ell 2b$ [72]		All						All	
$4b$ [75]					All		$3-b, 4-b, 2-bb$		
Hadr. WX [76]	All	All				ex H		ex H	

The main backgrounds in this search include $W + \text{jets}$, $Z + \text{jets}$, and $t\bar{t}$ processes. These backgrounds are estimated with techniques based on CRs in data that are disjoint from the corresponding SRs. The CRs are defined by inverting the tagging requirements for the AK8 jets or by requiring one charged electron or muon candidate. Transfer factors from the CRs to the SRs are derived from simulation and multiplied by the CR yields to obtain the estimated background yields in the SRs.

VI. COMBINATION STRATEGY

A simultaneous maximum likelihood fit to the signal and control regions of the searches described above is made for each signal model, as detailed in Sec. VIII. Table II shows which SRs are used for each model and topology. It should be noted that not all analyses target the same signal parameter space. For example, the “ $2/3\ell$ soft” lepton analysis has sensitivity for compressed signals due to the low- p_T leptons, while the rest target the mostly uncompressed signals.

The SRs and CRs are those defined in the original publications, except as noted in Sec. V. The modifications made to avoid sample overlap are briefly summarized here. For the “ $2SS\ell/\geq 3\ell$ ” analysis a small change was made to the leading-lepton p_T selection in categories A and B to avoid overlaps with the “ $2/3\ell$ soft” search. The “ 3ℓ ” WZ CR of the “ $2/3\ell$ soft” search was removed to avoid overlap with the aforementioned categories of the “ $2SS\ell/\geq 3\ell$ ” analysis when these searches are combined. To provide a constraint on the background contribution for the “ $2/3\ell$ soft” lepton search in the combined fit, the WZ backgrounds of the two analyses are correlated by utilizing a common nuisance parameter in the fit, constrained by a region of the “ $2SS\ell/\geq 3\ell$ ” analysis. For the Higgsino-bino combination, to avoid overlap between the “Hadr. WX” and “ $4b$ ” searches, the b -tag H SRs and CRs of the “Hadr. WX” analysis and the single bb -tag SRs and CRs of the boosted “ $4b$ ” sample are removed.

VII. SYSTEMATIC UNCERTAINTIES

Systematic uncertainties in each of the input analyses are given in the respective publications [71–76]. The sources and their level of correlation across the analyses are shown in Table III. Some analyses have additional uncertainties beyond these, which are analysis-specific and treated as uncorrelated.

TABLE III. Sources of systematic uncertainties and the treatment of their correlations between analyses. Exceptions to the notations in the last column are: for the “SM background normalization” row, the WZ normalization is correlated between the “ $2SS\ell/\geq 3\ell$ ” [74] and “ $2/3\ell$ soft” [73] searches, and for the “lepton efficiency” row the two contributing searches, “ $2/3\ell$ soft” [73] and “ 2ℓ nonresonant” [71], are uncorrelated because they cover disjoint regions of the model parameter space.

Source	Correlated?
General	
MC sample size	No
SM background normalization	No
Integrated luminosity	Yes
Trigger efficiency	Partially
Pileup	Yes
Trigger timing	Yes
Objects and signal modeling	
Lepton efficiency	Yes
Jet energy resolution	Yes
Jet energy scale	Yes
b (mis)tagging efficiency	Yes
AK8 bb tagging efficiency	Yes
AK8 jet mass resolution	Yes
μ_R and μ_F	Partially
ISR modeling	Yes
Attributable to the CMS fast simulation	
p_T^{miss} modeling	Yes
b (mis)tagging	Yes
AK8 bb tagging	Yes
AK8 bb mass	Yes

The signal yield predictions are affected by the experimental calibration uncertainties listed in Table III. Uncertainties are also computed for theoretical and experimental inputs to the simulations, specifically the renormalization and factorization scales μ_R and μ_F [141], and corrections to the treatment of initial-state radiation (ISR). Most uncertainties affecting the signal prediction are treated as fully correlated among the analyses. The uncertainty in the modeling of the trigger efficiency is correlated between individual analyses that share primary high-level trigger paths. The uncertainty labeled as “trigger timing” relates to correction factors that were applied to account for a gradual shift in the timing of the trigger information from the ECAL toward early values, present during the 2016 and 2017 data-taking periods. All analyses include the statistical uncertainty of the simulated signal samples, which is taken as uncorrelated.

The dominant uncertainties in the background predictions are generally not correlated among analyses, as they tend to be

either statistical in nature or inherent in the methods themselves. All systematic uncertainties associated with the normalization of SM backgrounds are taken to be uncorrelated, with the exception of the WZ normalization for the “ $2SS\ell/\geq 3\ell$ ” [74] and the “ $2/3\ell$ soft” [73] searches.

VIII. RESULTS AND INTERPRETATION

The observed SR yields are incorporated into an ML fit, along with the predicted yields pertinent to a given model, for each point in the model parameter space considered. The fit is implemented with the statistical framework described in Ref. [142], which builds the likelihood as a product of Poisson probability density functions of the observed yields in all bins of all SRs. The expectation in each bin is defined as the sum of background and signal contributions, with the signal contribution scaled by a strength parameter μ that is free in the fit. The observed data yields in control regions are incorporated either by

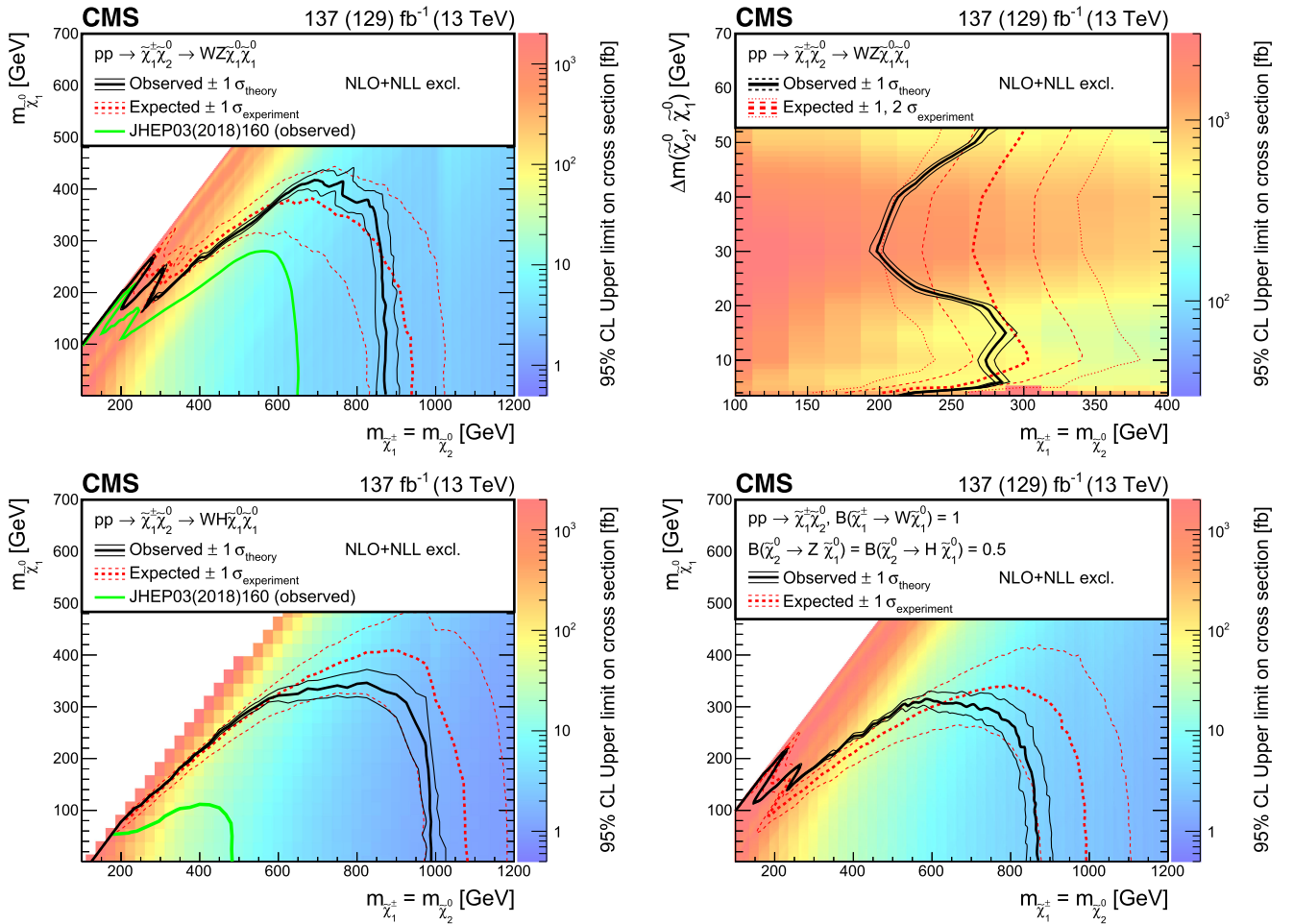


FIG. 11. Wino-bino model: cross section limits with expected and observed exclusion boundaries in the model parameter space in the WZ topology for the full parameter space (upper left) as well as the compressed region (upper right), the WH topology (lower left), and the mixed topology with 50% branching fraction to WZ and WH (lower right). All masses below the contours are excluded, except in the case of the upper-right plot where the area on the left of the contour is excluded. For some signal regions the analysis was based on a subset of the data, corresponding to the integrated luminosity of 129 fb^{-1} .

inclusion of the CRs in the likelihood or through parametrization using gamma functions. Systematic uncertainties are taken as nuisance parameters in the fit, and are implemented using log-normal functions, whose widths reflect the size of the systematic uncertainty, or as Gaussian shape constraints based on the relevant distributions.

No significant deviations from the SM background are observed, consistent with the findings of the input searches.

Small tensions between the data and background seen in the original searches are generally reduced or are unchanged. Cross section upper limits at 95% confidence level (C.L.) as a function of the SUSY particle masses are set using a modified frequentist approach, employing the CL_s criterion and an asymptotic formulation [142–145].

The following paragraphs present the cross section limits as functions of one or two model parameters, together with

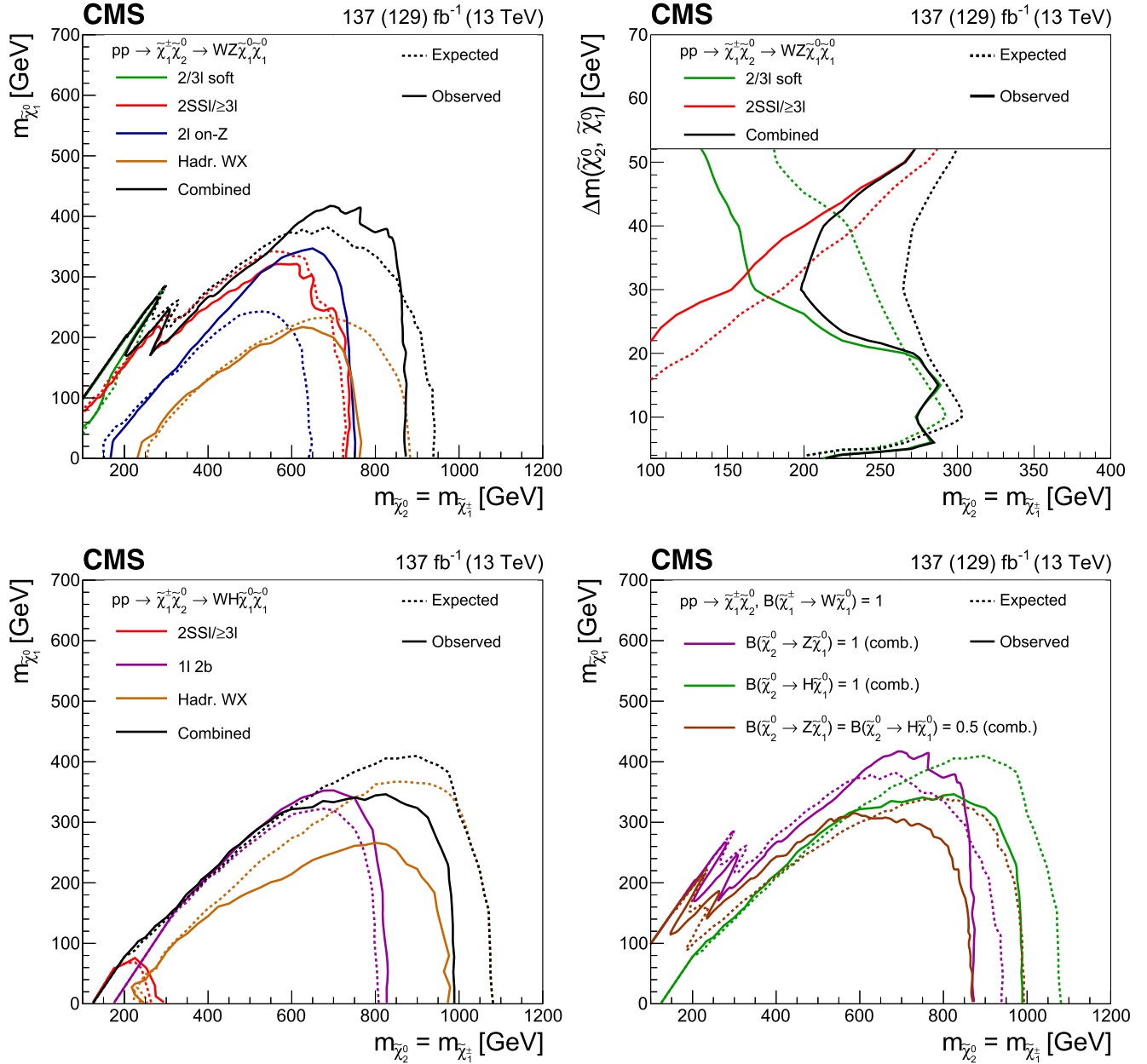


FIG. 12. Wino-bino model: exclusion contours from the individual analyses targeting the WZ topology for the full parameter space (upper left), the corresponding compressed region (upper right), and the WH topology (lower left). The combined contours for these two topologies are also shown. The combined contours for these and the mixed topology are overlaid in the lower-right plot. The decay modes assumed for each contour are given in the legends. All masses below the contours are excluded, except in the case of the upper-right plot where the area on the left of the contour is excluded. For some signal regions the analysis was based on a subset of the data, corresponding to the integrated luminosity of 129 fb⁻¹.

exclusion limits given by the $\mu = 1$ contours. For visualization of the results, linear interpolation is employed to account for the limited granularity of the available signal samples.

The cross section upper limits and mass-limit contours for the wino-bino model with chargino-neutralino production (Fig. 1) are shown in Fig. 11. The contributions of the input analyses to the limit curves in comparison with those from the combination appear in Fig. 12, along with the combined mass plane limit contours for three values of the $H\tilde{\chi}_1^0/Z\tilde{\chi}_1^0$ branching ratio of the $\tilde{\chi}_2^0$ decay.

The distributions in Fig. 12 show that the excluded parameter space is expanded by the combination compared with that from the input analyses, rather substantially in the case of the WZ topology in the uncompressed region (Fig. 12 upper left). For that case the combined data exclude NLSP masses below 875 GeV for a light LSP, and LSP masses below 420 for a 700 GeV NLSP, gains of about 125 and 110 GeV, respectively. In the compressed region, excesses observed in the combined data for the WZ topology reduce the excluded space relative to the expected one by ≈ 2 standard deviations in the region of Δm around 30–40 GeV. The upper-right plot in Fig. 12 shows that this falls in the crossover region where the exclusion power shifts between the two contributing analyses, “ $2/3\ell$ soft” and “ $2SS\ell/\geq 3\ell$.” The less restrictive observed than expected exclusion in the region of large NLSP and LSP masses for the WH and mixed topologies is driven by ≈ 1 standard deviation excesses in several p_T^{miss} bins of the WH SR in the “Hadr. WX” analysis, as demonstrated by the curves in Fig. 12, lower left.

For the GMSB model (Fig. 2) with production of degenerate Higgsinos decaying to the goldstino G (neutralino-neutralino production), the cross section upper limits and exclusion curves are shown in Fig. 13, for the topologies ZZ , HH , and the mixture of these with HZ assuming $\mathcal{B}(\tilde{\chi}_1^0 \rightarrow Z\tilde{G}) = \mathcal{B}(\tilde{\chi}_1^0 \rightarrow H\tilde{G}) = 50\%$. For the mixed topology, we also provide, in Fig. 14, exclusion limits spanning the full range of branching fractions into an H and Z boson. Mass values for $\tilde{\chi}_1^0$ less than 840 GeV are excluded for ZZ , < 1025 GeV for the HH topology, and < 760 GeV for the 50% mixed topology. The impact of the combination is substantial for the mixed topology, increasing the excluded region by about 100 GeV. The ZZ and mixed topologies show better than expected exclusion, whereas the HH topology shows the impact of a one-bin excess from the “4b” analysis, a 1–2 standard deviation effect for $300 < m_{\tilde{\chi}_1^0} < 600$ GeV.

The limits for the Higgsino-bino interpretation (Fig. 3), which assume mass-degenerate Higgsino-like $\tilde{\chi}_2^0$, $\tilde{\chi}_3^0$, and $\tilde{\chi}_1^\pm$ that decay to a binolike $\tilde{\chi}_1^0$ and an SM boson, are shown in Fig. 15. Values of $m_{\tilde{\chi}_1^\pm} = m_{\tilde{\chi}_2^0}$ between 225 and 800 GeV are excluded for $\tilde{\chi}_1^0$ masses below 50 GeV. As noted, this interpretation was not addressed in the previous analyses.

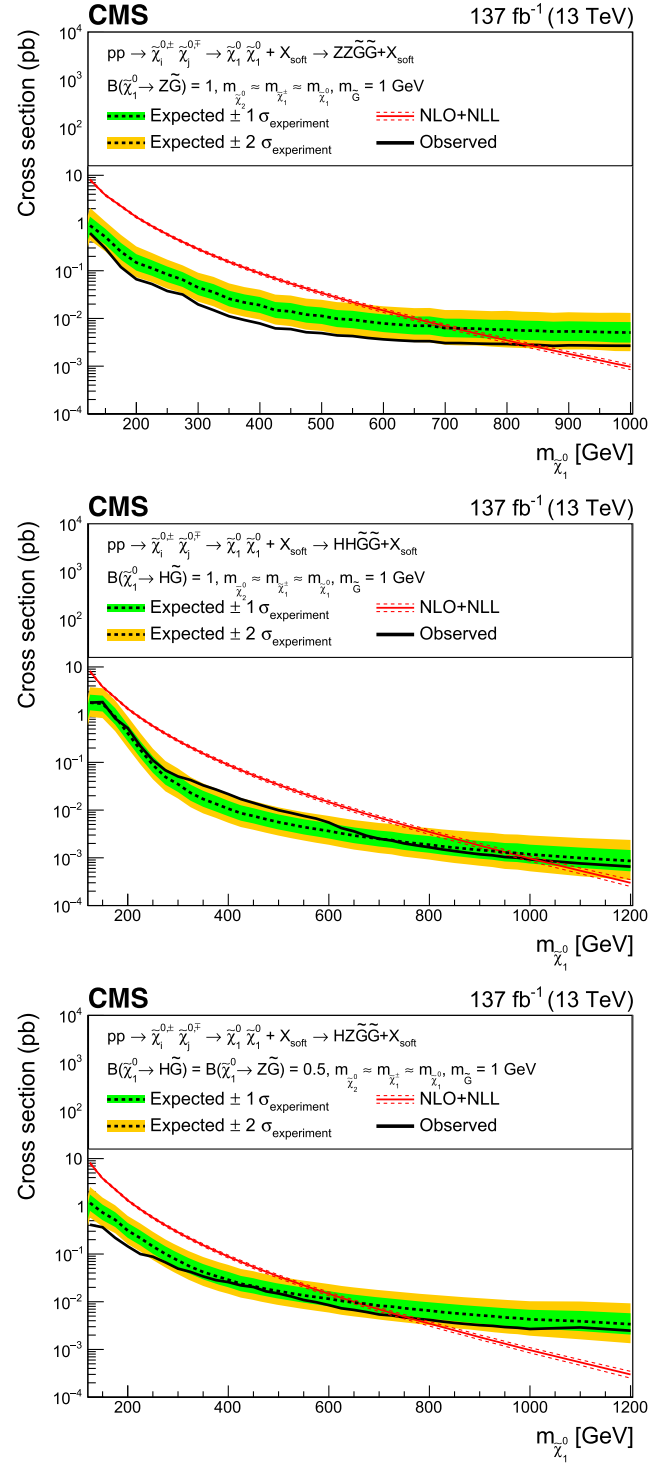


FIG. 13. GMSB model: expected and observed exclusion limits for the ZZ topology (upper), the HH topology (middle), and the mixed topology with 50% branching fraction to H and Z (lower). All masses on the left of the crossing between the exclusion limits and theory prediction are excluded.

The limits for slepton pair production under the slepton-neutralino model (Fig. 4) are shown in Fig. 16. The left-hand plot shows the combined limit over the $(m_\ell, m_{\tilde{\chi}_1^0})$

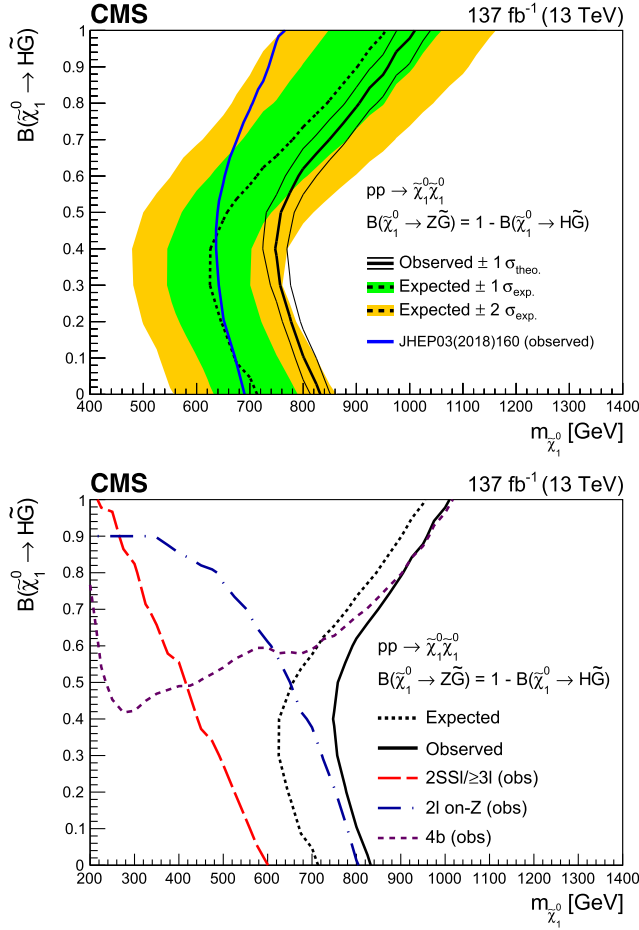


FIG. 14. GMSB model: NLSP mass exclusion limit as a function of the branching fraction to the H boson. Upper: expected and observed limits for the combination of the searches, shown together with the observed limits of the combination [53] based on the 2016 CMS data. Lower: expected and observed exclusion limits for the combination in comparison with those of the input searches. All masses on the left of the contours are excluded.

plane, while the right-hand plot gives an expanded view of the compressed region. In this region the “ $2/3\ell$ soft” search is able to exclude values of slepton masses up to 215 GeV at $\Delta m = 5$ GeV, complementing the results in the uncompressed region of the model parameter space where the observed exclusion reaches the slepton mass of about 700 GeV.

IX. SUMMARY

A number of previously reported searches for supersymmetry (SUSY) in different final states from proton-proton collisions at $\sqrt{s} = 13$ TeV have been reoptimized and combined. The data were recorded with the CMS detector at the LHC and correspond to an integrated luminosity of up to 137 fb^{-1} . These data are used to test the predictions of a variety of simplified SUSY models that involve the electroweak production of the superpartners of

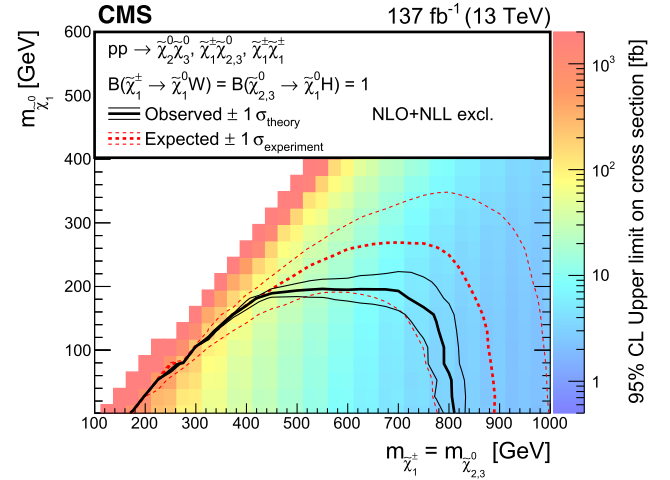


FIG. 15. Higgsino-bino model: cross section upper limit in the mass plane of the model, and the expected and observed exclusion limits. The model assumes mass-degenerate Higgsino-like $\tilde{\chi}_2^0, \tilde{\chi}_3^0$, and $\tilde{\chi}_1^\pm$ that decay to a binolike $\tilde{\chi}_1^0$ and an SM boson. All masses below the contours are excluded.

electroweak gauge or Higgs bosons. No significant deviation from the standard model expectation has been observed, and limits are set on the production of winolike chargino-neutralino pairs, Higgsino-like neutralino pair production in a gauge-mediated SUSY breaking inspired scenario, a Higgsino-bino interpretation, and slepton pair production.

In the case of winolike chargino-neutralino production, for a $\tilde{\chi}_1^0$, the lightest SUSY particle in this model, with mass $m_{\tilde{\chi}_1^\pm} < 50$ GeV, the combined result gives an observed (expected) limit on $m_{\tilde{\chi}_1^\pm}$ of about 875 (950) GeV for the WZ topology, 990 (1075) GeV for the WH topology, and 875 (1000) GeV for a mixed topology, extending the previous CMS combination [53] (based on a 2016 dataset corresponding to 36 fb^{-1}), by 225, 510, and 340 GeV, respectively, for the three topologies.

For Higgsino-like neutralino pair production, the mass exclusion limit is a function of the branching ratio between the H and Z channels; the expected limit ranges between about 620 and 950 GeV, the smaller value occurring for $B(\tilde{\chi}_1^0 \rightarrow H\tilde{G}) \approx 0.4$. For this value of the branching fraction, the observed limit results in the exclusion of masses below 750 GeV, and extends the previous result [53] by 100 GeV. The observed limit reaches nearly 1025 GeV at $B(\tilde{\chi}_1^0 \rightarrow H\tilde{G}) = 1$, to be compared with 750 GeV reported in Ref. [53].

A Higgsino-bino model that assumes mass degenerate Higgsino-like $\tilde{\chi}_2^0, \tilde{\chi}_3^0$, and $\tilde{\chi}_1^\pm$ decaying to a binolike $\tilde{\chi}_1^0$ and a standard model boson is excluded for $m_{\tilde{\chi}_1^\pm} = m_{\tilde{\chi}_2^0}$ between 225 and 800 GeV for $m_{\tilde{\chi}_1^0} < 50$ GeV.

For direct production of the superpartners of electrons and muons (sleptons), this combined search yields an

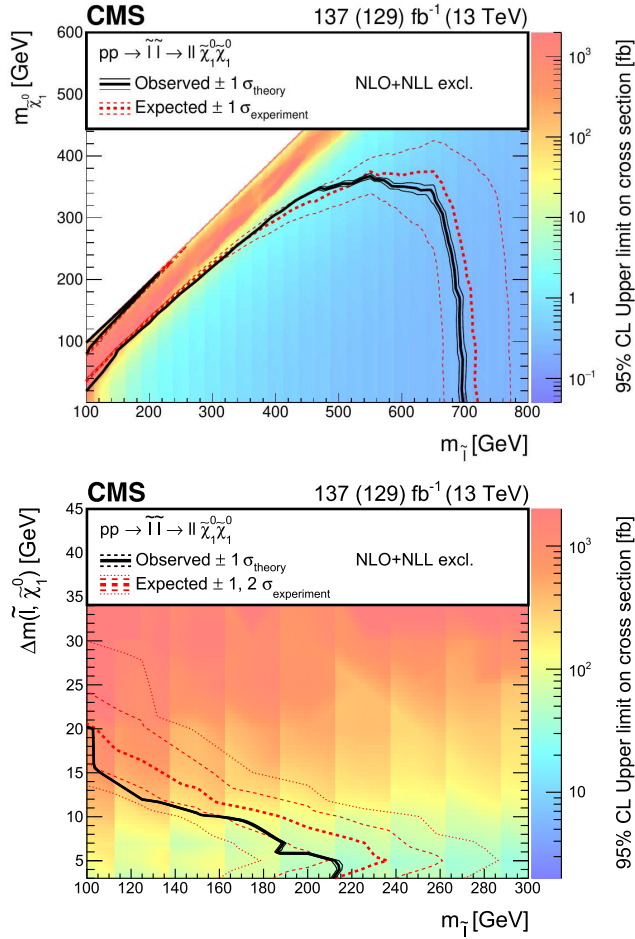


FIG. 16. Slepton-neutralino model: mass plane cross section upper limit with observed and expected exclusion limits. Upper: the full mass plane from the combination. Lower: the compressed region, obtained by the “2/3 ℓ soft” search. For some signal regions the analysis was based on a subset of the data, corresponding to the integrated luminosity of 129 fb $^{-1}$. All masses below the contours are excluded, except in the case of the right figure where the area on the left of the contour is excluded.

observed (expected) exclusion in the slepton mass of about 130–700 (110–720) GeV, for $m_{\tilde{\chi}_1^0} < 50$ GeV. In the compressed-spectrum region, a dedicated search first reported here excludes slepton masses above 215 GeV for a 5 GeV difference between the slepton and $\tilde{\chi}_1^0$ masses.

In general for the models considered in this combination, winolike chargino masses are excluded up to 990 GeV, while Higgsino-like neutralino masses are excluded up to 1025 GeV. The improvement is between 100–510 GeV with respect to the previous exclusion limits [53], whereas the excluded model parameter space is expanded by as much as 125 GeV, depending on the model, with respect to the best of the component searches. The compressed parameter space of the slepton production model is explored here for the first time by CMS.

ACKNOWLEDGMENTS

We congratulate our colleagues in the CERN accelerator departments for the excellent performance of the LHC and thank the technical and administrative staffs at CERN and at other CMS institutes for their contributions to the success of the CMS effort. In addition, we gratefully acknowledge the computing centers and personnel of the Worldwide LHC Computing Grid and other centers for delivering so effectively the computing infrastructure essential to our analyses. Finally, we acknowledge the enduring support for the construction and operation of the LHC, the CMS detector, and the supporting computing infrastructure provided by the following funding agencies: SC (Armenia), BMBWF and FWF (Austria); FNRS and FWO (Belgium); CNPq, CAPES, FAPERJ, FAPERGS, and FAPESP (Brazil); MES and BNSF (Bulgaria); CERN; CAS, MoST, and NSFC (China); Minciencias (Colombia); MSES and CSF (Croatia); RIF (Cyprus); SENESCYT (Ecuador); ERC PRG, RVTT3 and TK202 (Estonia); Academy of Finland, MEC, and HIP (Finland); CEA and CNRS/IN2P3 (France); SRNSF (Georgia); BMBF, DFG, and HGF (Germany); GSRI (Greece); NKFIH (Hungary); DAE and DST (India); IPM (Iran); SFI (Ireland); INFN (Italy); MSIP and NRF (Republic of Korea); MES (Latvia); LAS (Lithuania); MOE and UM (Malaysia); BUAP, CINVESTAV, CONACYT, LNS, SEP, and UASLP-FAI (Mexico); MOS (Montenegro); MBIE (New Zealand); PAEC (Pakistan); MES and NSC (Poland); FCT (Portugal); MESTD (Serbia); MCIN/AEI and PCTI (Spain); MOSTR (Sri Lanka); Swiss Funding Agencies (Switzerland); MST (Taipei); MHESI and NSTDA (Thailand); TUBITAK and TENMAK (Turkey); NASU (Ukraine); STFC (United Kingdom); DOE and NSF (USA). Individuals have received support from the Marie-Curie program and the European Research Council and Horizon 2020 Grant, Contracts No. 675440, No. 724704, No. 752730, No. 758316, No. 765710, No. 824093, and COST Action CA16108 (European Union); the Leventis Foundation; the Alfred P. Sloan Foundation; the Alexander von Humboldt Foundation; the Science Committee, Project No. 22r1-037 (Armenia); the Belgian Federal Science Policy Office; the Fonds pour la Formation à la Recherche dans l’Industrie et dans l’Agriculture (FRIA-Belgium); the Agentschap voor Innovatie door Wetenschap en Technologie (IWT-Belgium); the F.R.S.-FNRS and FWO (Belgium) under the “Excellence of Science—EOS”—be.h Project No. 30820817; the Beijing Municipal Science & Technology Commission, No. Z191100007219010 and Fundamental Research Funds for the Central Universities (China); the Ministry of Education, Youth and Sports (MEYS) of the Czech Republic; the Shota Rustaveli National Science Foundation, grant No. FR-22-985 (Georgia); the Deutsche Forschungsgemeinschaft (DFG), under Germany’s Excellence Strategy—EXC 2121

“Quantum Universe”—390833306, and under project number 400140256—GRK2497; the Hellenic Foundation for Research and Innovation (HFRI), Project Number 2288 (Greece); the Hungarian Academy of Sciences, the New National Excellence Program—ÚNKP, the NKFIH research grants No. K 124845, No. K 124850, No. K 128713, No. K 128786, No. K 129058, No. K 131991, No. K 133046, No. K 138136, No. K 143460, No. K 143477, No. 2020-2.2.1-ED-2021-00181, and No. TKP2021-NKTA-64 (Hungary); the Council of Science and Industrial Research, India; ICSC—National Research Center for High Performance Computing, Big Data and Quantum Computing, funded by the NextGenerationEU program (Italy); the Latvian Council of Science; the Ministry of Education and Science, Project No. 2022/WK/14, and the National Science Center, contracts No. Opus 2021/41/B/ST2/01369 and No. 2021/43/B/

ST2/01552 (Poland); the Fundação para a Ciência e a Tecnologia, grant No. CEECIND/01334/2018 (Portugal); the National Priorities Research Program by Qatar National Research Fund; MCIN/AEI/10.13039/501100011033, ERDF “a way of making Europe”, and the Programa Estatal de Fomento de la Investigación Científica y Técnica de Excelencia María de Maeztu, Grant No. MDM-2017-0765 and Programa Severo Ochoa del Principado de Asturias (Spain); the Chulalongkorn Academic into Its 2nd Century Project Advancement Project, and the National Science, Research and Innovation Fund via the Program Management Unit for Human Resources & Institutional Development, Research and Innovation, Grant No. B37G660013 (Thailand); the Kavli Foundation; the Nvidia Corporation; the SuperMicro Corporation; the Welch Foundation, contract No. C-1845; and the Weston Havens Foundation (USA).

-
- [1] J. Wess and B. Zumino, Supergauge transformations in four dimensions, *Nucl. Phys.* **B70**, 39 (1974).
 - [2] H. P. Nilles, Supersymmetry, supergravity and particle physics, *Phys. Rep.* **110**, 1 (1984).
 - [3] H. E. Haber and G. L. Kane, The search for supersymmetry: Probing physics beyond the standard model, *Phys. Rep.* **117**, 75 (1985).
 - [4] R. Barbieri, S. Ferrara, and C. A. Savoy, Gauge models with spontaneously broken local supersymmetry, *Phys. Lett.* **119B**, 343 (1982).
 - [5] S. Dawson, E. Eichten, and C. Quigg, Search for supersymmetric particles in hadron-hadron collisions, *Phys. Rev. D* **31**, 1581 (1985).
 - [6] S. Dimopoulos and G. F. Giudice, Naturalness constraints in supersymmetric theories with nonuniversal soft terms, *Phys. Lett. B* **357**, 573 (1995).
 - [7] R. Barbieri and D. Pappadopulo, S-particles at their naturalness limits, *J. High Energy Phys.* **10** (2009) 061.
 - [8] M. Papucci, J. T. Ruderman, and A. Weiler, Natural SUSY endures, *J. High Energy Phys.* **09** (2012) 035.
 - [9] A. J. Buras, J. Ellis, M. K. Gaillard, and D. V. Nanopoulos, Aspects of the grand unification of strong, weak and electromagnetic interactions, *Nucl. Phys.* **B135**, 66 (1978).
 - [10] G. R. Farrar and P. Fayet, Phenomenology of the production, decay, and detection of new hadronic states associated with supersymmetry, *Phys. Lett.* **76B**, 575 (1978).
 - [11] H. Goldberg, Constraint on the photino mass from cosmology, *Phys. Rev. Lett.* **50**, 1419 (1983); **103**, 099905(E) (2009).
 - [12] J. R. Ellis, J. S. Hagelin, D. V. Nanopoulos, K. A. Olive, and M. Srednicki, Supersymmetric relics from the big bang, *Nucl. Phys.* **B238**, 453 (1984).
 - [13] P. Fayet and S. Ferrara, Supersymmetry, *Phys. Rep.* **32**, 249 (1977).
 - [14] S. P. Martin, A supersymmetry primer, *Adv. Ser. Dir. High Energy Phys.* **21**, 1 (2010).
 - [15] S. Dimopoulos, M. Dine, S. Raby, and S. D. Thomas, Experimental signatures of low-energy gauge mediated supersymmetry breaking, *Phys. Rev. Lett.* **76**, 3494 (1996).
 - [16] K. T. Matchev and S. D. Thomas, Higgs and Z boson signatures of supersymmetry, *Phys. Rev. D* **62**, 077702 (2000).
 - [17] ATLAS Collaboration, Search for supersymmetry in events with photons, bottom quarks, and missing transverse momentum in proton-proton collisions at a centre-of-mass energy of 7 TeV with the ATLAS detector, *Phys. Lett. B* **719**, 261 (2013).
 - [18] ATLAS Collaboration, Search for direct pair production of a chargino and a neutralino decaying to the 125 GeV Higgs boson in $\sqrt{s} = 8$ TeV pp collisions with the ATLAS detector, *Eur. Phys. J. C* **75**, 208 (2015).
 - [19] ATLAS Collaboration, Search for the electroweak production of supersymmetric particles in $\sqrt{s} = 8$ TeV pp collisions with the ATLAS detector, *Phys. Rev. D* **93**, 052002 (2016).
 - [20] ATLAS Collaboration, Search for supersymmetry in final states with two same-sign or three leptons and jets using 36 fb⁻¹ of $\sqrt{s} = 13$ TeV pp collision data with the ATLAS detector, *J. High Energy Phys.* **09** (2017) 084; **08** (2019) 121(E).
 - [21] ATLAS Collaboration, Search for new phenomena with large jet multiplicities and missing transverse momentum using large-radius jets and flavour-tagging at ATLAS in 13 TeV pp collisions, *J. High Energy Phys.* **12** (2017) 034.
 - [22] ATLAS Collaboration, Search for the direct production of charginos and neutralinos in final states with tau leptons in $\sqrt{s} = 13$ TeV pp collisions with the ATLAS detector, *Eur. Phys. J. C* **78**, 154 (2018).

- [23] ATLAS Collaboration, Search for electroweak production of supersymmetric states in scenarios with compressed mass spectra at $\sqrt{s} = 13$ TeV with the ATLAS detector, *Phys. Rev. D* **97**, 052010 (2018).
- [24] ATLAS Collaboration, Search for photonic signatures of gauge-mediated supersymmetry in 13 TeV pp collisions with the ATLAS detector, *Phys. Rev. D* **97**, 092006 (2018).
- [25] ATLAS Collaboration, Search for supersymmetry in events with four or more leptons in $\sqrt{s} = 13$ TeV pp collisions with ATLAS, *Phys. Rev. D* **98**, 032009 (2018).
- [26] ATLAS Collaboration, Search for electroweak production of supersymmetric particles in final states with two or three leptons at $\sqrt{s} = 13$ TeV with the ATLAS detector, *Eur. Phys. J. C* **78**, 995 (2018).
- [27] ATLAS Collaboration, Search for chargino-neutralino production using recursive jigsaw reconstruction in final states with two or three charged leptons in proton-proton collisions at $\sqrt{s} = 13$ TeV with the ATLAS detector, *Phys. Rev. D* **98**, 092012 (2018).
- [28] ATLAS Collaboration, Search for pair production of Higgsinos in final states with at least three b -tagged jets in $\sqrt{s} = 13$ TeV pp collisions using the ATLAS detector, *Phys. Rev. D* **98**, 092002 (2018).
- [29] ATLAS Collaboration, Search for chargino and neutralino production in final states with a Higgs boson and missing transverse momentum at $\sqrt{s} = 13$ TeV with the ATLAS detector, *Phys. Rev. D* **100**, 012006 (2019).
- [30] ATLAS Collaboration, Searches for electroweak production of supersymmetric particles with compressed mass spectra in $\sqrt{s} = 13$ TeV pp collisions with the ATLAS detector, *Phys. Rev. D* **101**, 052005 (2020).
- [31] ATLAS Collaboration, Search for chargino-neutralino production with mass splittings near the electroweak scale in three-lepton final states in $\sqrt{s} = 13$ TeV pp collisions with the ATLAS detector, *Phys. Rev. D* **101**, 072001 (2020).
- [32] ATLAS Collaboration, Search for direct production of electroweakinos in final states with missing transverse momentum and a Higgs boson decaying into photons in pp collisions at $\sqrt{s} = 13$ TeV with the ATLAS detector, *J. High Energy Phys.* **10** (2020) 005.
- [33] ATLAS Collaboration, Search for direct production of electroweakinos in final states with one lepton, missing transverse momentum and a Higgs boson decaying into two b -jets in pp collisions at $\sqrt{s} = 13$ TeV with the ATLAS detector, *Eur. Phys. J. C* **80**, 691 (2020).
- [34] ATLAS Collaboration, Search for direct stau production in events with two hadronic τ -leptons in $\sqrt{s} = 13$ TeV pp collisions with the ATLAS detector, *Phys. Rev. D* **101**, 032009 (2020).
- [35] ATLAS Collaboration, Search for electroweak production of charginos and sleptons decaying into final states with two leptons and missing transverse momentum in $\sqrt{s} = 13$ TeV pp collisions using the ATLAS detector, *Eur. Phys. J. C* **80**, 123 (2020).
- [36] ATLAS Collaboration, Search for supersymmetry in events with four or more charged leptons in 139 fb⁻¹ of $\sqrt{s} = 13$ TeV pp collisions with the ATLAS detector, *J. High Energy Phys.* **07** (2021) 167.
- [37] ATLAS Collaboration, Search for chargino-neutralino pair production in final states with three leptons and missing transverse momentum in $\sqrt{s} = 13$ TeV pp collisions with the ATLAS detector, *Eur. Phys. J. C* **81**, 1118 (2021).
- [38] ATLAS Collaboration, Search for charginos and neutralinos in final states with two boosted hadronically decaying bosons and missing transverse momentum in pp collisions at $\sqrt{s} = 13$ TeV with the ATLAS detector, *Phys. Rev. D* **104**, 112010 (2021).
- [39] ATLAS Collaboration, Searches for new phenomena in events with two leptons, jets, and missing transverse momentum in 139 fb⁻¹ of $\sqrt{s} = 13$ TeV pp collisions with the ATLAS detector, *Eur. Phys. J. C* **83**, 515 (2023).
- [40] ATLAS Collaboration, Search for direct pair production of sleptons and charginos decaying to two leptons and neutralinos with mass splittings near the W-boson mass in $\sqrt{s} = 13$ TeV pp collisions with the ATLAS detector, *J. High Energy Phys.* **06** (2023) 031.
- [41] ATLAS Collaboration, Search for direct production of winos and Higgsinos in events with two same-charge leptons or three leptons in pp collision data at $\sqrt{s} = 13$ TeV with the ATLAS detector, *J. High Energy Phys.* **11** (2023) 150.
- [42] ATLAS Collaboration, Search for direct production of electroweakinos in final states with one lepton, jets and missing transverse momentum in pp collisions at $\sqrt{s} = 13$ TeV with the ATLAS detector, *J. High Energy Phys.* **12** (2023) 167.
- [43] ATLAS Collaboration, Search for pair production of Higgsinos in events with two Higgs bosons and missing transverse momentum in $\sqrt{s} = 13$ TeV pp collisions at the ATLAS experiment, [arXiv:2401.14922](https://arxiv.org/abs/2401.14922) [*Phys. Rev. D* (to be published)].
- [44] ATLAS Collaboration, A statistical combination of ATLAS Run 2 searches for charginos and neutralinos at the LHC, [arXiv:2402.08347](https://arxiv.org/abs/2402.08347) [*Phys. Rev. Lett.* (to be published)].
- [45] CMS Collaboration, Searches for electroweak production of charginos, neutralinos, and sleptons decaying to leptons and W, Z, and Higgs bosons in pp collisions at 8 TeV, *Eur. Phys. J. C* **74**, 3036 (2014).
- [46] CMS Collaboration, Search for top squark and Higgsino production using diphoton Higgs boson decays, *Phys. Rev. Lett.* **112**, 161802 (2014).
- [47] CMS Collaboration, Searches for electroweak neutralino and chargino production in channels with Higgs, Z, and W bosons in pp collisions at 8 TeV, *Phys. Rev. D* **90**, 092007 (2014).
- [48] CMS Collaboration, Search for physics beyond the standard model in events with two leptons of same sign, missing transverse momentum, and jets in proton-proton collisions at $\sqrt{s} = 13$ TeV, *Eur. Phys. J. C* **77**, 578 (2017).
- [49] CMS Collaboration, Search for electroweak production of charginos and neutralinos in WH events in proton-proton collisions at $\sqrt{s} = 13$ TeV, *J. High Energy Phys.* **11** (2017) 029.
- [50] CMS Collaboration, Search for supersymmetry in events with at least one photon, missing transverse momentum, and large transverse event activity in proton-proton

- collisions at $\sqrt{s} = 13$ TeV, *J. High Energy Phys.* **12** (2017) 142.
- [51] CMS Collaboration, Search for supersymmetry with Higgs boson to diphoton decays using the razor variables at $\sqrt{s} = 13$ TeV, *Phys. Lett. B* **779**, 166 (2018).
- [52] CMS Collaboration, Search for Higgsino pair production in pp collisions at $\sqrt{s} = 13$ TeV in final states with large missing transverse momentum and two Higgs bosons decaying via $H \rightarrow b\bar{b}$, *Phys. Rev. D* **97**, 032007 (2018).
- [53] CMS Collaboration, Combined search for electroweak production of charginos and neutralinos in proton-proton collisions at $\sqrt{s} = 13$ TeV, *J. High Energy Phys.* **03** (2018) 160.
- [54] CMS Collaboration, Search for new phenomena in final states with two opposite-charge, same-flavor leptons, jets, and missing transverse momentum in pp collisions at $\sqrt{s} = 13$ TeV, *J. High Energy Phys.* **03** (2018) 076.
- [55] CMS Collaboration, Search for supersymmetry in events with one lepton and multiple jets exploiting the angular correlation between the lepton and the missing transverse momentum in proton-proton collisions at $\sqrt{s} = 13$ TeV, *Phys. Lett. B* **780**, 384 (2018).
- [56] CMS Collaboration, Search for supersymmetry in events with at least three electrons or muons, jets, and missing transverse momentum in proton-proton collisions at $\sqrt{s} = 13$ TeV, *J. High Energy Phys.* **02** (2018) 067.
- [57] CMS Collaboration, Search for gauge-mediated supersymmetry in events with at least one photon and missing transverse momentum in pp collisions at $\sqrt{s} = 13$ TeV, *Phys. Lett. B* **780**, 118 (2018).
- [58] CMS Collaboration, Search for physics beyond the standard model in events with high-momentum Higgs bosons and missing transverse momentum in proton-proton collisions at 13 TeV, *Phys. Rev. Lett.* **120**, 241801 (2018).
- [59] CMS Collaboration, Search for electroweak production of charginos and neutralinos in multilepton final states in proton-proton collisions at $\sqrt{s} = 13$ TeV, *J. High Energy Phys.* **03** (2018) 166.
- [60] CMS Collaboration, Search for new physics in events with two soft oppositely charged leptons and missing transverse momentum in proton-proton collisions at $\sqrt{s} = 13$ TeV, *Phys. Lett. B* **782**, 440 (2018).
- [61] CMS Collaboration, Searches for pair production of charginos and top squarks in final states with two oppositely charged leptons in proton-proton collisions at $\sqrt{s} = 13$ TeV, *J. High Energy Phys.* **11** (2018) 079.
- [62] CMS Collaboration, Search for supersymmetry in events with a photon, a lepton, and missing transverse momentum in proton-proton collisions at $\sqrt{s} = 13$ TeV, *J. High Energy Phys.* **01** (2019) 154.
- [63] CMS Collaboration, Search for supersymmetry in events with a photon, jets, b -jets, and missing transverse momentum in proton-proton collisions at 13 TeV, *Eur. Phys. J. C* **79**, 444 (2019).
- [64] CMS Collaboration, Search for supersymmetry with a compressed mass spectrum in the vector boson fusion topology with 1-lepton and 0-lepton final states in proton-proton collisions at $\sqrt{s} = 13$ TeV, *J. High Energy Phys.* **08** (2019) 150.
- [65] CMS Collaboration, Search for supersymmetry in final states with photons and missing transverse momentum in proton-proton collisions at 13 TeV, *J. High Energy Phys.* **06** (2019) 143.
- [66] CMS Collaboration, Combined search for supersymmetry with photons in proton-proton collisions at $\sqrt{s} = 13$ TeV, *Phys. Lett. B* **801**, 135183 (2020).
- [67] CMS Collaboration, Search for supersymmetry using Higgs boson to diphoton decays at $\sqrt{s} = 13$ TeV, *J. High Energy Phys.* **11** (2019) 109.
- [68] CMS Collaboration, Searches for physics beyond the standard model with the M_{T2} variable in hadronic final states with and without disappearing tracks in proton-proton collisions at $\sqrt{s} = 13$ TeV, *Eur. Phys. J. C* **80**, 3 (2020).
- [69] CMS Collaboration, Search for supersymmetry with a compressed mass spectrum in events with a soft τ lepton, a highly energetic jet, and large missing transverse momentum in proton-proton collisions at $\sqrt{s} = 13$ TeV, *Phys. Rev. Lett.* **124**, 041803 (2020).
- [70] CMS Collaboration, Search for direct pair production of supersymmetric partners to the τ lepton in proton-proton collisions at $\sqrt{s} = 13$ TeV, *Eur. Phys. J. C* **80**, 189 (2020).
- [71] CMS Collaboration, Search for supersymmetry in final states with two oppositely charged same-flavor leptons and missing transverse momentum in proton-proton collisions at $\sqrt{s} = 13$ TeV, *J. High Energy Phys.* **04** (2021) 123.
- [72] CMS Collaboration, Search for chargino-neutralino production in events with Higgs and W bosons using 137 fb $^{-1}$ of proton-proton collisions at $\sqrt{s} = 13$ TeV, *J. High Energy Phys.* **10** (2021) 045.
- [73] CMS Collaboration, Search for supersymmetry in final states with two or three soft leptons and missing transverse momentum in proton-proton collisions at $\sqrt{s} = 13$ TeV, *J. High Energy Phys.* **04** (2022) 091.
- [74] CMS Collaboration, Search for electroweak production of charginos and neutralinos in proton-proton collisions at $\sqrt{s} = 13$ TeV, *J. High Energy Phys.* **04** (2022) 147.
- [75] CMS Collaboration, Search for Higgsinos decaying to two Higgs bosons and missing transverse momentum in proton-proton collisions at $\sqrt{s} = 13$ TeV, *J. High Energy Phys.* **05** (2022) 014.
- [76] CMS Collaboration, Search for electroweak production of charginos and neutralinos at $\sqrt{s} = 13$ TeV in final states containing hadronic decays of WW , WZ , or WH and missing transverse momentum, *Phys. Lett. B* **842**, 137460 (2023).
- [77] CMS Collaboration, Search for new physics in multijet events with at least one photon and large missing transverse momentum in proton-proton collisions at 13 TeV, *J. High Energy Phys.* **10** (2023) 046.
- [78] N. Arkani-Hamed, P. Schuster, N. Toro, J. Thaler, L.-T. Wang, B. Knuteson, and S. Mrenna, MARMOSET: The path from LHC data to the new standard model via on-shell effective theories, [arXiv:hep-ph/0703088](https://arxiv.org/abs/hep-ph/0703088).
- [79] J. Alwall, P. C. Schuster, and N. Toro, Simplified models for a first characterization of new physics at the LHC, *Phys. Rev. D* **79**, 075020 (2009).

- [80] J. Alwall, M.-P. Le, M. Lisanti, and J. G. Wacker, Model-independent jets plus missing energy searches, *Phys. Rev. D* **79**, 015005 (2009).
- [81] D. Alves, N. Arkani-Hamed, S. Arora, Y. Bai, M. Baumgart, J. Berger, M. Buckley, B. Butler, S. Chang, H.-C. Cheng, C. Cheung, R. S. Chivukula, W. S. Cho, R. Cotta, M. D'Alfonso *et al.*, Simplified models for LHC new physics searches, *J. Phys. G* **39**, 105005 (2012).
- [82] CMS Collaboration, HEPData record for this analysis, [10.17182/hepdata.145859](https://hepdata.cern.ch/archive/10.17182/hepdata.145859) (2024).
- [83] A. Canepa, T. Han, and X. Wang, The search for electroweakinos, *Annu. Rev. Nucl. Part. Sci.* **70**, 425 (2020).
- [84] J. L. Feng, K. T. Matchev, and T. Moroi, Focus points and naturalness in supersymmetry, *Phys. Rev. D* **61**, 075005 (2000).
- [85] L. J. Hall, D. Pinner, and J. T. Ruderman, A natural SUSY Higgs near 126 GeV, *J. High Energy Phys.* **04** (2012) 131.
- [86] H. Baer, V. Barger, P. Huang, A. Mustafayev, and X. Tata, Radiative natural SUSY with a 125 GeV Higgs boson, *Phys. Rev. Lett.* **109**, 161802 (2012).
- [87] M. Dine and W. Fischler, A phenomenological model of particle physics based on supersymmetry, *Phys. Lett.* **110B**, 227 (1982).
- [88] C. R. Nappi and B. A. Ovrut, Supersymmetric extension of the $SU(3) \times SU(2) \times U(1)$ model, *Phys. Lett.* **113B**, 175 (1982).
- [89] L. Alvarez-Gaume, M. Claudson, and M. B. Wise, Low-energy supersymmetry, *Nucl. Phys.* **B207**, 96 (1982).
- [90] M. Dine and A. E. Nelson, Dynamical supersymmetry breaking at low-energies, *Phys. Rev. D* **48**, 1277 (1993).
- [91] M. Dine, A. E. Nelson, and Y. Shirman, Low-energy dynamical supersymmetry breaking simplified, *Phys. Rev. D* **51**, 1362 (1995).
- [92] M. Dine, A. E. Nelson, Y. Nir, and Y. Shirman, New tools for low-energy dynamical supersymmetry breaking, *Phys. Rev. D* **53**, 2658 (1996).
- [93] G. F. Giudice and R. Rattazzi, Theories with gauge mediated supersymmetry breaking, *Phys. Rep.* **322**, 419 (1999).
- [94] H. Baer, V. Barger, P. Huang, D. Mickelson, M. Padeffke-Kirkland, and X. Tata, Natural SUSY with a bino- or wino-like LSP, *Phys. Rev. D* **91**, 075005 (2015).
- [95] G. Bozzi, B. Fuks, and M. Klasen, Threshold resummation for slepton-pair production at hadron colliders, *Nucl. Phys.* **B777**, 157 (2007).
- [96] B. Fuks, M. Klasen, D. R. Lamprea, and M. Rothering, Revisiting slepton pair production at the Large Hadron Collider, *J. High Energy Phys.* **01** (2014) 168.
- [97] J. Fiaschi and M. Klasen, Slepton pair production at the LHC in NLO + NLL with resummation-improved parton densities, *J. High Energy Phys.* **03** (2018) 094.
- [98] CMS Collaboration, The CMS experiment at the CERN LHC, *J. Instrum.* **3**, S08004 (2008).
- [99] CMS Collaboration, Performance of the CMS Level-1 trigger in proton-proton collisions at $\sqrt{s} = 13$ TeV, *J. Instrum.* **15**, P10017 (2020).
- [100] CMS Collaboration, The CMS trigger system, *J. Instrum.* **12**, P01020 (2017).
- [101] CMS Collaboration, Particle-flow reconstruction and global event description with the CMS detector, *J. Instrum.* **12**, P10003 (2017).
- [102] M. Cacciari, G. P. Salam, and G. Soyez, The anti- k_T jet clustering algorithm, *J. High Energy Phys.* **04** (2008) 063.
- [103] M. Cacciari, G. P. Salam, and G. Soyez, FastJet user manual, *Eur. Phys. J. C* **72**, 1896 (2012).
- [104] CMS Collaboration, Jet energy scale and resolution in the CMS experiment in pp collisions at 8 TeV, *J. Instrum.* **12**, P02014 (2017).
- [105] CMS Collaboration, Technical proposal for the Phase-II upgrade of the Compact Muon Solenoid, CMS Technical Proposal Reports No. CERN-LHCC-2015-010, No. CMS-TDR-15-02, 2015, <http://cds.cern.ch/record/2020886>.
- [106] CMS Collaboration, Performance of missing transverse momentum reconstruction in proton-proton collisions at $\sqrt{s} = 13$ TeV using the CMS detector, *J. Instrum.* **14**, P07004 (2019).
- [107] CMS Collaboration, Identification of heavy-flavour jets with the CMS detector in pp collisions at 13 TeV, *J. Instrum.* **13**, P05011 (2018).
- [108] CMS Collaboration, Performance of heavy-flavour jet identification in boosted topologies in proton-proton collisions at $\sqrt{s} = 13$ TeV, CMS Physics Analysis Summary Report No. CMS-PAS-BTV-22-001, 2023, <http://cds.cern.ch/record/2866276>.
- [109] CMS Collaboration, Performance of deep tagging algorithms for boosted double quark jet topology in proton-proton collisions at 13 TeV with the phase-0 CMS detector, CMS Detector Performance Note Report No. CMS-DP-2018-046, 2018, <http://cds.cern.ch/record/2630438?ln=en>.
- [110] G. Louppe, M. Kagan, and K. Cranmer, Learning to pivot with adversarial networks, in *Advances in Neural Information Processing Systems*, v. 30 (2017), p. 981, <https://www.proceedings.com/39083.html>.
- [111] CMS Collaboration, Identification of heavy, energetic, hadronically decaying particles using machine-learning techniques, *J. Instrum.* **15**, P06005 (2020).
- [112] CMS Collaboration, Reconstruction and identification of τ lepton decays to hadrons and ν_τ at CMS, *J. Instrum.* **11**, P01019 (2016).
- [113] CMS Collaboration, Performance of reconstruction and identification of τ leptons decaying to hadrons and ν_τ in pp collisions at $\sqrt{s} = 13$ TeV, *J. Instrum.* **13**, P10005 (2018).
- [114] J. Alwall, R. Frederix, S. Frixione, V. Hirschi, F. Maltoni, O. Mattelaer, H.-S. Shao, T. Stelzer, P. Torrielli, and M. Zaro, The automated computation of tree-level and next-to-leading order differential cross sections, and their matching to parton shower simulations, *J. High Energy Phys.* **07** (2014) 079.
- [115] R. Frederix and S. Frixione, Merging meets matching in MC@NLO, *J. High Energy Phys.* **12** (2012) 061.
- [116] W. Beenakker, M. Klasen, M. Krämer, T. Plehn, M. Spira, and P. M. Zerwas, Production of charginos, neutralinos, and sleptons at hadron colliders, *Phys. Rev. Lett.* **83**, 3780 (1999); **100**, 029901(E) (2008).
- [117] J. Debove, B. Fuks, and M. Klasen, Threshold resummation for gaugino pair production at hadron colliders, *Nucl. Phys.* **B842**, 51 (2011).
- [118] B. Fuks, M. Klasen, D. R. Lamprea, and M. Rothering, Gaugino production in proton-proton collisions at a center-of-mass energy of 8 TeV, *J. High Energy Phys.* **10** (2012) 081.
- [119] B. Fuks, M. Klasen, D. R. Lamprea, and M. Rothering, Precision predictions for electroweak superpartner

- production at hadron colliders with RESUMMINO, *Eur. Phys. J. C* **73**, 2480 (2013).
- [120] J. Fiaschi and M. Klasen, Neutralino-chargino pair production at NLO + NLL with resummation-improved parton density functions for LHC Run II, *Phys. Rev. D* **98**, 055014 (2018).
- [121] P. Nason, A new method for combining NLO QCD with shower Monte Carlo algorithms, *J. High Energy Phys.* **11** (2004) 040.
- [122] S. Frixione, P. Nason, and C. Oleari, Matching NLO QCD computations with parton shower simulations: The POWHEG method, *J. High Energy Phys.* **11** (2007) 070.
- [123] S. Alioli, P. Nason, C. Oleari, and E. Re, NLO single-top production matched with shower in POWHEG: s - and t -channel contributions, *J. High Energy Phys.* **09** (2009) 111; **02** (2010) 011(E).
- [124] J. M. Campbell and R. K. Ellis, An update on vector boson pair production at hadron colliders, *Phys. Rev. D* **60**, 113006 (1999).
- [125] J. M. Campbell, R. K. Ellis, and C. Williams, Vector boson pair production at the LHC, *J. High Energy Phys.* **07** (2011) 018.
- [126] J. M. Campbell, R. K. Ellis, and W. T. Giele, A multi-threaded version of MCFM, *Eur. Phys. J. C* **75**, 246 (2015).
- [127] T. Sjöstrand, S. Ask, J. R. Christiansen, R. Corke, N. Desai, P. Ilten, S. Mrenna, S. Prestel, C. O. Rasmussen, and P. Z. Skands, An introduction to PYTHIA8.2, *Comput. Phys. Commun.* **191**, 159 (2015).
- [128] CMS Collaboration, Event generator tunes obtained from underlying event and multiparton scattering measurements, *Eur. Phys. J. C* **76**, 155 (2016).
- [129] CMS Collaboration, Extraction and validation of a new set of CMS PYTHIA8 tunes from underlying-event measurements, *Eur. Phys. J. C* **80**, 4 (2020).
- [130] R. D. Ball *et al.* (NNPDF Collaboration), Parton distributions for the LHC Run II, *J. High Energy Phys.* **04** (2015) 040.
- [131] R. D. Ball *et al.* (NNPDF Collaboration), Parton distributions from high-precision collider data, *Eur. Phys. J. C* **77**, 663 (2017).
- [132] S. Abdullin, P. Azzi, F. Beaudette, P. Janot, and A. Perrotta, The fast simulation of the CMS detector at LHC, *J. Phys. Conf. Ser.* **331**, 032049 (2011).
- [133] A. Giammanco, The fast simulation of the CMS experiment, *J. Phys. Conf. Ser.* **513**, 022012 (2014).
- [134] S. Agostinelli *et al.* (GEANT4 Collaboration), GEANT4—a simulation toolkit, *Nucl. Instrum. Methods Phys. Res., Sect. A* **506**, 250 (2003).
- [135] U. De Sanctis, T. Lari, S. Montesano, and C. Troncon, Perspectives for the detection and measurement of supersymmetry in the focus point region of mSUGRA models with the ATLAS detector at LHC, *Eur. Phys. J. C* **52**, 743 (2007).
- [136] C. G. Lester and D. J. Summers, Measuring masses of semiinvisibly decaying particles pair produced at hadron colliders, *Phys. Lett. B* **463**, 99 (1999).
- [137] A. Barr, C. Lester, and P. Stephens, m(T2): The truth behind the glamour, *J. Phys. G* **29**, 2343 (2003).
- [138] Particle Data Group, Review of particle physics, *Prog. Theor. Exp. Phys.* **2022**, 083C01 (2022).
- [139] A. J. Larkoski, S. Marzani, G. Soyez, and J. Thaler, Soft drop, *J. High Energy Phys.* **05** (2014) 146.
- [140] M. Dasgupta, A. Fregoso, S. Marzani, and G. P. Salam, Towards an understanding of jet substructure, *J. High Energy Phys.* **09** (2013) 029.
- [141] A. Kalogeropoulos and J. Alwall, The SysCalc code: A tool to derive theoretical systematic uncertainties, [arXiv:1801.08401](https://arxiv.org/abs/1801.08401).
- [142] ATLAS and CMS Collaborations, LHC Higgs Combination Group, Procedure for the LHC Higgs boson search combination in Summer 2011, Technical Reports No. CMS-NOTE-2011-005, No. ATL-PHYS-PUB-2011-11, 2011, <http://cds.cern.ch/record/1379837>.
- [143] T. Junk, Confidence level computation for combining searches with small statistics, *Nucl. Instrum. Methods Phys. Res., Sect. A* **434**, 435 (1999).
- [144] A. L. Read, Presentation of search results: The CL_s technique, *J. Phys. G* **28**, 2693 (2002).
- [145] G. Cowan, K. Cranmer, E. Gross, and O. Vitells, Asymptotic formulae for likelihood-based tests of new physics, *Eur. Phys. J. C* **71**, 1554 (2011); **73**, 2501(E) (2013).

A. Hayrapetyan,¹ A. Tumasyan^{1,b} W. Adam² J. W. Andrejkovic,² T. Bergauer² S. Chatterjee² K. Damanakis² M. Dragicovic² A. Escalante Del Valle² P. S. Hussain² M. Jeitler^{2,c} N. Krammer² D. Liko² I. Mikulec² J. Schieck^{2,c} R. Schöfbeck² D. Schwarz² M. Sonawane² S. Templ² W. Waltenberger² C.-E. Wulz^{2,c} M. R. Darwish^{3,d} T. Janssen³ P. Van Mechelen³ E. S. Bols⁴ J. D'Hondt⁴ S. Dansana⁴ A. De Moor⁴ M. Delcourt⁴ H. El Faham⁴ S. Lowette⁴ I. Makarenko⁴ D. Müller⁴ A. R. Sahasransu⁴ S. Tavernier⁴ M. Tytgat^{4,e} S. Van Putte⁴ D. Vannerom⁴ B. Clerbaux⁵ G. De Lentdecker⁵ L. Favart⁵ D. Hohov⁵ J. Jaramillo⁵ A. Khalilzadeh⁵ K. Lee⁵ M. Mahdavihorrani⁵ A. Malara⁵ S. Paredes⁵ L. Pétré⁵ N. Postiau⁵ L. Thomas⁵ M. Vanden Bemden⁵ C. Vander Velde⁵ P. Vanlaer⁵ M. De Coen⁶ D. Dobur⁶ Y. Hong⁶ J. Knolle⁶ L. Lambrecht⁶ G. Mestdach⁶ C. Rendón⁶ A. Samalan⁶ K. Skovpen⁶ N. Van Den Bossche⁶ L. Wezenbeek⁶ A. Benecke⁷ G. Bruno⁷ C. Caputo⁷ C. Delaere⁷ I. S. Donertas⁷ A. Giammanco⁷ K. Jaffel⁷ Sa. Jain⁷ V. Lemaître⁷ J. Lidrych⁷ P. Mastrapasqua⁷ K. Mondal⁷ T. T. Tran⁷ S. Wertz⁷ G. A. Alves⁸ E. Coelho⁸ C. Hensel⁸ T. Menezes De Oliveira⁸ A. Moraes⁸ P. Rebello Teles⁸ M. Soeiro⁸ W. L. Aldá Júnior⁹ M. Alves Gallo Pereira⁹ M. Barroso Ferreira Filho⁹ H. Brandao Malbouisson⁹ W. Carvalho⁹

J. Chinellato,^{9,f} E. M. Da Costa⁹ G. G. Da Silveira^{9,g} D. De Jesus Damiao⁹ S. Fonseca De Souza⁹ J. Martins^{9,h} C. Mora Herrera⁹ K. Mota Amarilo⁹ L. Mundim⁹ H. Nogima⁹ A. Santoro⁹ A. Sznajder⁹ M. Thiel⁹ A. Vilela Pereira⁹ C. A. Bernardes^{10,g} L. Calligaris¹⁰ T. R. Fernandez Perez Tomei¹⁰ E. M. Gregores¹⁰ P. G. Mercadante¹⁰ S. F. Novaes¹⁰ B. Orzari¹⁰ Sandra S. Padula¹⁰ A. Aleksandrov¹¹ G. Antchev¹¹ R. Hadjiiska¹¹ P. Iaydjiev¹¹ M. Misheva¹¹ M. Shopova¹¹ G. Sultanov¹¹ A. Dimitrov¹² L. Litov¹² B. Pavlov¹² P. Petkov¹² A. Petrov¹² E. Shumka¹² S. Keshri¹³ S. Thakur¹³ T. Cheng¹⁴ Q. Guo¹⁴ T. Javai¹⁴ M. Mittal¹⁴ L. Yuan¹⁴ G. Bauer,^{15,i,j} Z. Hu¹⁵ J. Liu¹⁵ K. Yi^{15,i,k} G. M. Chen^{16,l} H. S. Chen^{16,l} M. Chen^{16,l} F. Iemmi¹⁶ C. H. Jiang¹⁶ A. Kapoor^{16,m} H. Liao¹⁶ Z.-A. Liu^{16,n} F. Monti¹⁶ M. A. Shahzad,^{16,l} R. Sharma^{16,o} J. N. Song,^{16,n} J. Tao¹⁶ C. Wang,^{16,l} J. Wang¹⁶ Z. Wang,^{16,l} H. Zhang¹⁶ A. Agapitos¹⁷ Y. Ban¹⁷ A. Levin¹⁷ C. Li¹⁷ Q. Li¹⁷ Y. Mao¹⁷ S. J. Qian¹⁷ X. Sun¹⁷ D. Wang¹⁷ H. Yang¹⁷ L. Zhang¹⁷ C. Zhou¹⁷ Z. You¹⁸ N. Lu¹⁹ X. Gao^{20,p} D. Leggat,²⁰ H. Okawa²⁰ Y. Zhang²⁰ Z. Lin²¹ C. Lu²¹ M. Xiao²¹ C. Avila²² D. A. Barbosa Trujillo,²² A. Cabrera²² C. Florez²² J. Fraga²² J. A. Reyes Vega,²² J. Mejia Guisao²³ F. Ramirez²³ M. Rodriguez²³ J. D. Ruiz Alvarez²³ D. Giljanovic²⁴ N. Godinovic²⁴ D. Lelas²⁴ A. Sculac²⁴ M. Kovac²⁵ T. Sculac²⁵ P. Bargassa²⁶ V. Brigljevic²⁶ B. K. Chitroda²⁶ D. Ferencek²⁶ S. Mishra²⁶ A. Starodumov^{26,q} T. Susa²⁶ A. Attikis²⁷ K. Christoforou²⁷ S. Konstantinou²⁷ J. Mousa²⁷ C. Nicolaou,²⁷ F. Ptochos²⁷ P. A. Razis²⁷ H. Rykaczewski,²⁷ H. Saka²⁷ A. Stepennov²⁷ M. Finger²⁸ M. Finger Jr.²⁸ A. Kveton²⁸ E. Ayala²⁹ E. Carrera Jarrin³⁰ H. Abdalla^{31,r} Y. Assran,^{31,s,t} A. Lotfy³² M. A. Mahmoud³² R. K. Dewanjee^{33,u} K. Ehataht³³ M. Kadastik,³³ T. Lange³³ S. Nandan³³ C. Nielsen³³ J. Pata³³ M. Raidal³³ L. Tani³³ C. Veelken³³ H. Kirschenmann³⁴ K. Osterberg³⁴ M. Voutilainen³⁴ S. Bharthuar³⁵ E. Brücken³⁵ F. Garcia³⁵ J. Havukainen³⁵ K. T. S. Kallonen³⁵ M. S. Kim³⁵ R. Kinnunen³⁵ T. Lampén³⁵ K. Lassila-Perini³⁵ S. Lehti³⁵ T. Lindén³⁵ M. Lotti³⁵ L. Martikainen³⁵ M. Myllymäki³⁵ M. m. Rantanen³⁵ H. Siikonen³⁵ E. Tuominen³⁵ J. Tuominiemi³⁵ P. Luukka³⁶ H. Petrow³⁶ T. Tuuva,^{36,a} M. Besancon³⁷ F. Couderc³⁷ M. Dejardin³⁷ D. Denegri,³⁷ J. L. Faure,³⁷ F. Ferri³⁷ S. Ganjour³⁷ P. Gras³⁷ G. Hamel de Monchenault³⁷ V. Lohezic³⁷ J. Malcles³⁷ J. Rander,³⁷ A. Rosowsky³⁷ M. Ö. Sahin³⁷ A. Savoy-Navarro^{37,v} P. Simkina³⁷ M. Titov³⁷ M. Tornago³⁷ C. Baldenegro Barrera³⁸ F. Beaudette³⁸ A. Buchot Perraguin³⁸ P. Busson³⁸ A. Cappati³⁸ C. Charlot³⁸ F. Damas³⁸ O. Davignon³⁸ A. De Wit³⁸ G. Falmagne³⁸ B. A. Fontana Santos Alves³⁸ S. Ghosh³⁸ A. Gilbert³⁸ R. Granier de Cassagnac³⁸ A. Hakimi³⁸ B. Harikrishnan³⁸ L. Kalipoliti³⁸ G. Liu³⁸ J. Motta³⁸ M. Nguyen³⁸ C. Ochando³⁸ L. Portales³⁸ R. Salerno³⁸ U. Sarkar³⁸ J. B. Sauvan³⁸ Y. Sirois³⁸ A. Tarabini³⁸ E. Vernazza³⁸ A. Zabi³⁸ A. Zghiche³⁸ J.-L. Agram^{39,w} J. Andrea³⁹ D. Apparu³⁹ D. Bloch³⁹ J.-M. Brom³⁹ E. C. Chabert³⁹ C. Collard³⁹ S. Falke³⁹ U. Goerlach³⁹ C. Grimault³⁹ R. Haeberle³⁹ A.-C. Le Bihan³⁹ G. Saha³⁹ M. A. Sessini³⁹ P. Van Hove³⁹ S. Beauceron⁴⁰ B. Blancon⁴⁰ G. Boudoul⁴⁰ N. Chanon⁴⁰ J. Choi⁴⁰ D. Contardo⁴⁰ P. Depasse⁴⁰ C. Dozen^{40,x} H. El Mamouni,⁴⁰ J. Fay⁴⁰ S. Gascon⁴⁰ M. Gouzevitch⁴⁰ C. Greenberg,⁴⁰ G. Grenier⁴⁰ B. Ille⁴⁰ I. B. Laktineh,⁴⁰ M. Lethuillier⁴⁰ L. Mirabito⁴⁰ S. Perries⁴⁰ A. Purohit⁴⁰ M. Vander Donckt⁴⁰ P. Verdier⁴⁰ J. Xiao⁴⁰ A. Khvedelidze^{41,q} I. Lomidze⁴¹ Z. Tsamalaidze^{41,q} V. Botta⁴² L. Feld⁴² K. Klein⁴² M. Lipinski⁴² D. Meuser⁴² A. Pauls⁴² N. Röwert⁴² M. Teroerde⁴² S. Diekmann⁴³ A. Dodonova⁴³ N. Eich⁴³ D. Eliseev⁴³ F. Engelke⁴³ M. Erdmann⁴³ P. Fackeldey⁴³ B. Fischer⁴³ T. Hebbeker⁴³ K. Hoepfner⁴³ F. Ivone⁴³ A. Jung⁴³ M. y. Lee⁴³ L. Mastrolorenzo⁴³ M. Merschmeyer⁴³ A. Meyer⁴³ S. Mukherjee⁴³ D. Noll⁴³ A. Novak⁴³ F. Nowotny⁴³ A. Pozdnyakov⁴³ Y. Rath⁴³ W. Redjeb⁴³ F. Rehm⁴³ H. Reithler⁴³ V. Sarkisovi⁴³ A. Schmidt⁴³ A. Sharma⁴³ J. L. Spah⁴³ A. Stein⁴³ F. Torres Da Silva De Araujo^{43,y} L. Vigilante⁴³ S. Wiedenbeck⁴³ S. Zaleski⁴³ C. Dziwok⁴⁴ G. Flügge⁴⁴ W. Haj Ahmad^{44,z} T. Kress⁴⁴ A. Nowack⁴⁴ O. Pooth⁴⁴ A. Stahl⁴⁴ T. Ziemons⁴⁴ A. Zotz⁴⁴ H. Aarup Petersen⁴⁵ M. Aldaya Martin⁴⁵ J. Alimena⁴⁵ S. Amoroso⁴⁵ Y. An⁴⁵ S. Baxter⁴⁵ M. Bayatmakou⁴⁵ H. Becerril Gonzalez⁴⁵ O. Behnke⁴⁵ A. Belvedere⁴⁵ S. Bhattacharya⁴⁵ F. Blekman^{45,aa} K. Borras^{45,bb} D. Brunner⁴⁵ A. Campbell⁴⁵ A. Cardini⁴⁵ C. Cheng⁴⁵ F. Colombina⁴⁵ S. Consuegra Rodríguez⁴⁵ G. Correia Silva⁴⁵ M. De Silva⁴⁵ G. Eckerlin⁴⁵ D. Eckstein⁴⁵ L. I. Estevez Banos⁴⁵ O. Filatov⁴⁵ E. Gallo^{45,aa} A. Geiser⁴⁵ A. Giralddi⁴⁵ G. Greau⁴⁵ V. Guglielmi⁴⁵ M. Guthoff⁴⁵ A. Hinzmann⁴⁵ A. Jafari^{45,cc} L. Jeppe⁴⁵ N. Z. Jomhari⁴⁵ B. Kaech⁴⁵ M. Kasemann⁴⁵ H. Kaveh⁴⁵ C. Kleinwort⁴⁵ R. Kogler⁴⁵ M. Komm⁴⁵ D. Krücker⁴⁵ W. Lange⁴⁵ D. Leyva Pernia⁴⁵ K. Lipka^{45,dd} W. Lohmann^{45,ee} R. Mankel⁴⁵

- I.-A. Melzer-Pellmann⁴⁵, M. Mendizabal Morentin⁴⁵, J. Metwally⁴⁵, A. B. Meyer⁴⁵, G. Milella⁴⁵, A. Mussgiller⁴⁵,
 A. Nürnberg⁴⁵, Y. Otari⁴⁵, J. Park⁴⁵, D. Pérez Adán⁴⁵, E. Ranken⁴⁵, A. Raspereza⁴⁵, B. Ribeiro Lopes⁴⁵,
 J. Rübenach⁴⁵, A. Saggio⁴⁵, M. Scham^{45,ff,bb}, S. Schnake^{45,bb}, P. Schütze⁴⁵, C. Schwanenberger^{45,aa},
 D. Selivanova⁴⁵, M. Shchedrolosiev⁴⁵, R. E. Sosa Ricardo⁴⁵, L. P. Sreelatha Pramod⁴⁵, D. Stafford⁴⁵, F. Vazzoler⁴⁵,
 A. Ventura Barroso⁴⁵, R. Walsh⁴⁵, Q. Wang⁴⁵, Y. Wen⁴⁵, K. Wichmann⁴⁵, L. Wiens^{45,bb}, C. Wissing⁴⁵,
 Y. Yang⁴⁵, A. Zimmermann Castro Santos⁴⁵, A. Albrecht⁴⁶, S. Albrecht⁴⁶, M. Antonello⁴⁶, S. Bein⁴⁶,
 L. Benato⁴⁶, M. Bonanomi⁴⁶, P. Connor⁴⁶, M. Eich⁴⁶, K. El Morabit⁴⁶, Y. Fischer⁴⁶, A. Fröhlich⁴⁶, C. Garbers⁴⁶,
 E. Garutti⁴⁶, A. Grohsjean⁴⁶, M. Hajheidari⁴⁶, J. Haller⁴⁶, H. R. Jabusch⁴⁶, G. Kasieczka⁴⁶, P. Keicher⁴⁶,
 R. Klanner⁴⁶, W. Korcari⁴⁶, T. Kramer⁴⁶, V. Kutzner⁴⁶, F. Labe⁴⁶, J. Lange⁴⁶, A. Lobanov⁴⁶, C. Matthies⁴⁶,
 A. Mehta⁴⁶, L. Moureaux⁴⁶, M. Mrowietz⁴⁶, A. Nigamova⁴⁶, Y. Nissan⁴⁶, A. Paasch⁴⁶, K. J. Pena Rodriguez⁴⁶,
 T. Quadfasel⁴⁶, B. Raciti⁴⁶, M. Rieger⁴⁶, D. Savoie⁴⁶, J. Schindler⁴⁶, P. Schleper⁴⁶, M. Schröder⁴⁶,
 J. Schwandt⁴⁶, M. Sommerhalder⁴⁶, H. Stadie⁴⁶, G. Steinbrück⁴⁶, A. Tews⁴⁶, M. Wolf⁴⁶, S. Brommer⁴⁷,
 M. Burkart⁴⁷, E. Butz⁴⁷, T. Chwalek⁴⁷, A. Dierlamm⁴⁷, A. Droll⁴⁷, N. Faltermann⁴⁷, M. Giffels⁴⁷, A. Gottmann⁴⁷,
 F. Hartmann^{47,gg}, R. Hofsaess⁴⁷, M. Horzela⁴⁷, U. Husemann⁴⁷, J. Kieseler⁴⁷, M. Klute⁴⁷, R. Koppenhöfer⁴⁷,
 J. M. Lawhorn⁴⁷, M. Link⁴⁷, A. Lintuluoto⁴⁷, S. Maier⁴⁷, S. Mitra⁴⁷, M. Mormile⁴⁷, Th. Müller⁴⁷, M. Neukum⁴⁷,
 M. Oh⁴⁷, M. Presilla⁴⁷, G. Quast⁴⁷, K. Rabbertz⁴⁷, B. Regnery⁴⁷, N. Shadskiy⁴⁷, I. Shvetsov⁴⁷,
 H. J. Simonis⁴⁷, N. Trevisani⁴⁷, R. Ulrich⁴⁷, J. van der Linden⁴⁷, R. F. Von Cube⁴⁷, M. Wassmer⁴⁷, S. Wieland⁴⁷,
 F. Wittig⁴⁷, R. Wolf⁴⁷, S. Wunsch⁴⁷, X. Zuo⁴⁷, G. Anagnostou⁴⁸, P. Assiouras⁴⁸, G. Daskalakis⁴⁸, A. Kyriakis⁴⁸,
 A. Papadopoulos^{48,gg}, A. Stakia⁴⁸, P. Kontaxakis⁴⁹, G. Melachroinos⁴⁹, A. Panagiotou⁴⁹, I. Papavergou⁴⁹,
 I. Paraskevas⁴⁹, N. Saoulidou⁴⁹, K. Theofilatos⁴⁹, E. Tziaferi⁴⁹, K. Vellidis⁴⁹, I. Zisopoulos⁴⁹, G. Bakas⁵⁰,
 T. Chatzistavrou⁵⁰, G. Karapostoli⁵⁰, K. Kousouris⁵⁰, I. Papakrivopoulos⁵⁰, E. Siamarkou⁵⁰, G. Tsiopolitis⁵⁰,
 A. Zacharopoulou⁵⁰, K. Adamidis⁵¹, I. Bestintzanos⁵¹, I. Evangelou⁵¹, C. Foudas⁵¹, P. Gianneios⁵¹, C. Kamtsikis⁵¹,
 P. Katsoulis⁵¹, P. Kokkas⁵¹, P. G. Kosmoglou Kioseoglou⁵¹, N. Manthos⁵¹, I. Papadopoulos⁵¹, J. Strologas⁵¹,
 M. Bartók^{52,hh}, C. Hajdu⁵², D. Horvath^{52,ii,jj}, F. Sikler⁵², V. Veszpremi⁵², M. Csanád⁵³, K. Farkas⁵³,
 M. M. A. Gadallah^{53,kk}, Á. Kadlecik⁵³, P. Major⁵³, K. Mandal⁵³, G. Pásztor⁵³, A. J. Rádl^{53,ll}, G. I. Veres⁵³,
 P. Raics⁵⁴, B. Ujvari^{54,mm}, G. Zilizi⁵⁴, G. Bencze⁵⁵, S. Czellar⁵⁵, J. Karancsi^{55,hh}, J. Molnar⁵⁵, Z. Szillasi⁵⁵,
 T. Csorgo^{56,ll}, F. Nemes^{56,ll}, T. Novak⁵⁶, J. Babbar⁵⁷, S. Bansal⁵⁷, S. B. Beri⁵⁷, V. Bhatnagar⁵⁷, G. Chaudhary⁵⁷,
 S. Chauhan⁵⁷, N. Dhingra^{57,nn}, A. Kaur⁵⁷, A. Kaur⁵⁷, H. Kaur⁵⁷, M. Kaur⁵⁷, S. Kumar⁵⁷, M. Meena⁵⁷,
 K. Sandeep⁵⁷, T. Sheokand⁵⁷, J. B. Singh⁵⁷, A. Singla⁵⁷, A. Ahmed⁵⁸, A. Bhardwaj⁵⁸, A. Chhetri⁵⁸,
 B. C. Choudhary⁵⁸, A. Kumar⁵⁸, M. Naimuddin⁵⁸, K. Ranjan⁵⁸, S. Saumya⁵⁸, S. Acharya^{59,oo}, S. Baradia⁵⁹,
 S. Barman^{59,pp}, S. Bhattacharya⁵⁹, D. Bhowmik⁵⁹, S. Dutta⁵⁹, S. Dutta⁵⁹, B. Gomber^{59,oo}, P. Palit⁵⁹, B. Sahu^{59,oo},
 S. Sarkar⁵⁹, M. M. Ameen⁶⁰, P. K. Behera⁶⁰, S. C. Behera⁶⁰, S. Chatterjee⁶⁰, P. Jana⁶⁰, P. Kalbhor⁶⁰,
 J. R. Komaragiri^{60,qq}, D. Kumar^{60,qq}, L. Panwar^{60,qq}, R. Pradhan⁶⁰, P. R. Pujahari⁶⁰, N. R. Saha⁶⁰, A. Sharma⁶⁰,
 A. K. Sikdar⁶⁰, S. Verma⁶⁰, T. Aziz⁶¹, I. Das⁶¹, S. Dugad⁶¹, M. Kumar⁶¹, G. B. Mohanty⁶¹, P. Suryadevara⁶¹,
 A. Bala⁶², S. Banerjee⁶², R. M. Chatterjee⁶², M. Guchait⁶², Sh. Jain⁶², S. Karmakar⁶², S. Kumar⁶²,
 G. Majumder⁶², K. Mazumdar⁶², S. Mukherjee⁶², S. Parolia⁶², A. Thachayath⁶², S. Bahinipati^{63,rr}, A. K. Das⁶³,
 C. Kar⁶³, D. Maity^{63,ss}, P. Mal⁶³, T. Mishra⁶³, V. K. Muraleedharan Nair Bindhu^{63,ss}, K. Naskar^{63,ss},
 A. Nayak^{63,ss}, P. Sadangi⁶³, P. Saha⁶³, S. K. Swain⁶³, S. Varghese^{63,ss}, D. Vats^{63,ss}, A. Alpina⁶⁴, S. Dube⁶⁴,
 B. Kansal⁶⁴, A. Laha⁶⁴, A. Rastogi⁶⁴, S. Sharma⁶⁴, H. Bakhshiansohi^{65,tt}, E. Khazaie^{65,uu}, M. Zeinali^{65,vv},
 S. Chenarani^{66,ww}, S. M. Etesami⁶⁶, M. Khakzad⁶⁶, M. Mohammadi Najafabadi⁶⁶, M. Grunewald⁶⁷,
 M. Abbrescia^{68a,68b}, R. Aly^{68a,68c,xx}, A. Colaleo^{68a,68b}, D. Creanza^{68a,68c}, B. D'Anzi^{68a,68b}, N. De Filippis^{68a,68c},
 M. De Palma^{68a,68b}, A. Di Florio^{68a,68c}, W. Elmetenawee^{68a,68b,xx}, L. Fiore^{68a}, G. Iaselli^{68a,68c}, M. Louka^{68a,68b},
 G. Maggi^{68a,68c}, M. Maggi^{68a}, I. Margjeka^{68a,68b}, V. Mastrapasqua^{68a,68b}, S. My^{68a,68b}, S. Nuzzo^{68a,68b},
 A. Pellecchia^{68a,68b}, A. Pompili^{68a,68b}, G. Pugliese^{68a,68c}, R. Radogna^{68a}, G. Ramirez-Sanchez^{68a,68c}, D. Ramos^{68a},
 A. Ranieri^{68a}, L. Silvestris^{68a}, F. M. Simone^{68a,68b}, Ü. Sözbilir^{68a}, A. Stamerra^{68a}, R. Venditti^{68a},
 P. Verwilligen^{68a}, A. Zaza^{68a,68b}, G. Abbiendi^{69a}, C. Battilana^{69a,69b}, D. Bonacorsi^{69a,69b}, L. Borgonovi^{69a},
 R. Campanini^{69a,69b}, P. Capiluppi^{69a,69b}, A. Castro^{69a,69b}, F. R. Cavallo^{69a}, M. Cuffiani^{69a,69b}, G. M. Dallavalle^{69a},
 T. Diotallevi^{69a,69b}, F. Fabbri^{69a}, A. Fanfani^{69a,69b}, D. Fasanella^{69a,69b}, P. Giacomelli^{69a}, L. Giommi^{69a,69b},
 C. Grandi^{69a}, S. Lo Meo^{69a,yy}, L. Lunerti^{69a,69b}, S. Marcellini^{69a}, G. Masetti^{69a}, F. L. Navarria^{69a,69b}

- A. Perrotta^{69a} F. Primavera^{69a,69b} A. M. Rossi^{69a,69b} T. Rovelli^{69a,69b} G. P. Siroli^{69a,69b} S. Costa^{70a,70b,zz}
A. Di Mattia^{70a} R. Potenza^{70a,70b} A. Tricomi^{70a,70b,zz} C. Tuve^{70a,70b} G. Barbagli^{71a} G. Bardelli^{71a,71b}
B. Camaiani^{71a,71b} A. Cassese^{71a} R. Ceccarelli^{71a} V. Ciulli^{71a,71b} C. Civinini^{71a} R. D'Alessandro^{71a,71b}
E. Focardi^{71a,71b} T. Kello^{71a} G. Latino^{71a,71b} P. Lenzi^{71a,71b} M. Lizzo^{71a} M. Meschini^{71a} S. Paoletti^{71a}
A. Papanastassiou^{71a,71b} G. Sguazzoni^{71a} L. Viliani^{71a} L. Benussi⁷² S. Bianco⁷² S. Meola^{72,aaa} D. Piccolo⁷²
P. Chatagnon^{73a} F. Ferro^{73a} E. Robutti^{73a} S. Tosi^{73a,73b} A. Benaglia^{74a} G. Boldrini^{74a,74b} F. Brivio^{74a}
F. Cetorelli^{74a} F. De Guio^{74a,74b} M. E. Dinardo^{74a,74b} P. Dini^{74a} S. Gennai^{74a} R. Gerosa^{74a,74b} A. Ghezzi^{74a,74b}
P. Govoni^{74a,74b} L. Guzzi^{74a} M. T. Lucchini^{74a,74b} M. Malberti^{74a} S. Malvezzi^{74a} A. Massironi^{74a}
D. Menasce^{74a} L. Moroni^{74a} M. Paganoni^{74a,74b} D. Pedrini^{74a} B. S. Pinolini^{74a} S. Ragazzi^{74a,74b}
T. Tabarelli de Fatis^{74a,74b} D. Zuolo^{74a} S. Buontempo^{75a} A. Cagnotta^{75a,75b} F. Carnevali^{75a,75b} N. Cavallo^{75a,75c}
A. De Iorio^{75a,75b} F. Fabozzi^{75a,75c} A. O. M. Iorio^{75a,75b} L. Lista^{75a,75b,bbb} P. Paolucci^{75a,gg} B. Rossi^{75a}
C. Sciacca^{75a,75b} R. Ardino^{76a} P. Azzi^{76a} N. Bacchetta^{76a,ccc} D. Bisello^{76a,76b} P. Bortignon^{76a}
A. Bragagnolo^{76a,76b} R. Carlin^{76a,76b} P. Checchia^{76a} T. Dorigo^{76a} F. Gasparini^{76a,76b} U. Gasparini^{76a,76b}
G. Grosso^{76a} L. Layer^{76a,ddd} E. Lusiani^{76a} M. Margoni^{76a,76b} A. T. Meneguzzo^{76a,76b} M. Michelotto^{76a}
M. Migliorini^{76a,76b} J. Pazzini^{76a,76b} P. Ronchese^{76a,76b} R. Rossin^{76a,76b} F. Simonetto^{76a,76b} G. Strong^{76a}
M. Tosi^{76a,76b} A. Triossi^{76a,76b} H. Yarar^{76a,76b} M. Zanetti^{76a,76b} P. Zotto^{76a,76b} A. Zucchetta^{76a,76b}
G. Zumerle^{76a,76b} S. Abu Zeid^{77a,eee} C. Aimè^{77a,77b} A. Braghieri^{77a} S. Calzaferri^{77a,77b} D. Fiorina^{77a,77b}
P. Montagna^{77a,77b} V. Re^{77a} C. Riccardi^{77a,77b} P. Salvini^{77a} I. Vai^{77a,77b} P. Vitulo^{77a,77b} S. Ajmal^{78a,78b}
P. Asenov^{78a,fff} G. M. Bilei^{78a} D. Ciangottini^{78a,78b} L. Fanò^{78a,78b} M. Magherini^{78a,78b} G. Mantovani^{78a,78b}
V. Mariani^{78a,78b} M. Menichelli^{78a} F. Moscatelli^{78a,fff} A. Rossi^{78a,78b} A. Santocchia^{78a,78b} D. Spiga^{78a}
T. Tedeschi^{78a,78b} P. Azzurri^{79a} G. Bagliesi^{79a} R. Bhattacharya^{79a} L. Bianchini^{79a,79b} T. Boccali^{79a}
E. Bossini^{79a} D. Bruschini^{79a,79c} R. Castaldi^{79a} M. A. Ciocci^{79a,79b} M. Cipriani^{79a,79b} V. D'Amante^{79a,79d}
R. Dell'Orso^{79a} S. Donato^{79a} A. Giassi^{79a} F. Ligabue^{79a,79c} D. Matos Figueiredo^{79a} A. Messineo^{79a,79b}
M. Musich^{79a,79b} F. Palla^{79a} A. Rizzi^{79a,79b} G. Rolandi^{79a,79c} S. Roy Chowdhury^{79a} T. Sarkar^{79a}
A. Scribano^{79a} P. Spagnolo^{79a} R. Tenchini^{79a} G. Tonelli^{79a,79b} N. Turini^{79a,79d} A. Venturi^{79a} P. G. Verdini^{79a}
P. Barria^{80a} M. Campana^{80a,80b} F. Cavallari^{80a} L. Cunqueiro Mendez^{80a,80b} D. Del Re^{80a,80b} E. Di Marco^{80a}
M. Diemoz^{80a} F. Errico^{80a,80b} E. Longo^{80a,80b} P. Meridiani^{80a} J. Mijuskovic^{80a,80b} G. Organtini^{80a,80b}
F. Pandolfi^{80a} R. Paramatti^{80a,80b} C. Quaranta^{80a,80b} S. Rahatlou^{80a,80b} C. Rovelli^{80a} F. Santanastasio^{80a,80b}
L. Soffi^{80a} N. Amapane^{81a,81b} R. Arcidiacono^{81a,81c} S. Argiro^{81a,81b} M. Arneodo^{81a,81c} N. Bartosik^{81a}
R. Bellan^{81a,81b} A. Bellora^{81a,81b} C. Biino^{81a} N. Cartiglia^{81a} M. Costa^{81a,81b} R. Covarelli^{81a,81b} N. Demaria^{81a}
L. Finco^{81a} M. Grippo^{81a,81b} B. Kiani^{81a,81b} F. Legger^{81a} F. Luongo^{81a,81b} C. Mariotti^{81a} S. Maselli^{81a}
A. Mecca^{81a,81b} E. Migliore^{81a,81b} M. Monteno^{81a} R. Mulargia^{81a} M. M. Obertino^{81a,81b} G. Ortona^{81a}
L. Pacher^{81a,81b} N. Pastrone^{81a} M. Pelliccioni^{81a} M. Ruspà^{81a,81c} F. Siviero^{81a,81b} V. Sola^{81a,81b}
A. Solano^{81a,81b} D. Soldi^{81a,81b} A. Staiano^{81a} C. Tarricone^{81a,81b} D. Trocino^{81a} G. Umoret^{81a,81b}
E. Vlasov^{81a,81b} S. Belforte^{82a} V. Candelise^{82a,82b} M. Casarsa^{82a} F. Cossutti^{82a} K. De Leo^{82a,82b}
G. Della Ricca^{82a,82b} S. Dogra⁸³ J. Hong⁸³ C. Huh⁸³ B. Kim⁸³ D. H. Kim⁸³ J. Kim⁸³ H. Lee⁸³ S. W. Lee⁸³
C. S. Moon⁸³ Y. D. Oh⁸³ M. S. Ryu⁸³ S. Sekmen⁸³ Y. C. Yang⁸³ G. Bak⁸⁴ P. Gwak⁸⁴ H. Kim⁸⁴
D. H. Moon⁸⁴ E. Asilar⁸⁵ D. Kim⁸⁵ T. J. Kim⁸⁵ J. A. Merlin⁸⁵ S. Choi⁸⁶ S. Han⁸⁶ B. Hong⁸⁶ K. Lee⁸⁶
K. S. Lee⁸⁶ S. Lee⁸⁶ J. Park⁸⁶ S. K. Park⁸⁶ J. Yoo⁸⁶ J. Goh⁸⁷ H. S. Kim⁸⁸ Y. Kim⁸⁸ S. Lee⁸⁸ J. Almond⁸⁹
J. H. Bhyun⁸⁹ J. Choi⁸⁹ W. Jun⁸⁹ J. Kim⁸⁹ J. S. Kim⁸⁹ S. Ko⁸⁹ H. Kwon⁸⁹ H. Lee⁸⁹ J. Lee⁸⁹ J. Lee⁸⁹
B. H. Oh⁸⁹ S. B. Oh⁸⁹ H. Seo⁸⁹ U. K. Yang⁸⁹ I. Yoon⁸⁹ W. Jang⁹⁰ D. Y. Kang⁹⁰ Y. Kang⁹⁰ S. Kim⁹⁰
B. Ko⁹⁰ J. S. H. Lee⁹⁰ Y. Lee⁹⁰ I. C. Park⁹⁰ Y. Roh⁹⁰ I. J. Watson⁹⁰ S. Yang⁹⁰ S. Ha⁹¹ H. D. Yoo⁹¹
M. Choi⁹² M. R. Kim⁹² H. Lee⁹² Y. Lee⁹² I. Yu⁹² T. Beyrouthy⁹³ Y. Maghrbi⁹³ K. Dreimanis⁹⁴ A. Gaile⁹⁴
G. Pikurs⁹⁴ A. Potrebko⁹⁴ M. Seidel⁹⁴ V. Veckalns^{94,ggg} N. R. Strautnieks⁹⁵ M. Ambrozys⁹⁶ A. Juodagalvis⁹⁶
A. Rinkevicius⁹⁶ G. Tamulaitis⁹⁶ N. Bin Norjoharuddeen⁹⁷ I. Yusuff^{97,hhh} Z. Zolkapli⁹⁷ J. F. Benitez⁹⁸
A. Castaneda Hernandez⁹⁸ H. A. Encinas Acosta⁹⁸ L. G. Gallegos Maríñez⁹⁸ M. León Coello⁹⁸
J. A. Murillo Quijada⁹⁸ A. Sehwat⁹⁸ L. Valencia Palomo⁹⁸ G. Ayala⁹⁹ H. Castilla-Valdez⁹⁹
E. De La Cruz-Burelo⁹⁹ I. Heredia-De La Cruz^{99,iii} R. Lopez-Fernandez⁹⁹ C. A. Mondragon Herrera⁹⁹
A. Sánchez Hernández⁹⁹ C. Oropeza Barrera¹⁰⁰ M. Ramírez García¹⁰⁰ I. Bautista¹⁰¹ I. Pedraza¹⁰¹

H. A. Salazar Ibarguen¹⁰¹, C. Uribe Estrada¹⁰¹, I. Bujanja¹⁰², N. Raicevic¹⁰², P. H. Butler¹⁰³, A. Ahmad¹⁰⁴,
M. I. Asghar¹⁰⁴, A. Awais¹⁰⁴, M. I. M. Awan¹⁰⁴, H. R. Hoorani¹⁰⁴, W. A. Khan¹⁰⁴, V. Avati¹⁰⁵, L. Grzanka¹⁰⁵,
M. Malawski¹⁰⁵, H. Bialkowska¹⁰⁶, M. Bluj¹⁰⁶, B. Boimska¹⁰⁶, M. Górski¹⁰⁶, M. Kazana¹⁰⁶, M. Szleper¹⁰⁶,
P. Zalewski¹⁰⁶, K. Bunkowski¹⁰⁷, K. Doroba¹⁰⁷, A. Kalinowski¹⁰⁷, M. Konecki¹⁰⁷, J. Krolikowski¹⁰⁷,
A. Muhammad¹⁰⁷, K. Pozniak¹⁰⁸, W. Zabolotny¹⁰⁸, M. Araujo¹⁰⁹, D. Bastos¹⁰⁹, C. Beirão Da Cruz E Silva¹⁰⁹,
A. Boletti¹⁰⁹, M. Bozzo¹⁰⁹, G. Da Molin¹⁰⁹, P. Faccioli¹⁰⁹, M. Gallinaro¹⁰⁹, J. Hollar¹⁰⁹, N. Leonardo¹⁰⁹,
T. Niknejad¹⁰⁹, A. Petrilli¹⁰⁹, M. Pisano¹⁰⁹, J. Seixas¹⁰⁹, J. Varela¹⁰⁹, J. W. Wulff¹⁰⁹, P. Adzic¹¹⁰, P. Milenovic¹¹⁰,
M. Dordevic¹¹¹, J. Milosevic¹¹¹, V. Rekovic¹¹¹, M. Aguilar-Benitez¹¹², J. Alcaraz Maestre¹¹², Cristina F. Bedoya¹¹²,
M. Cepeda¹¹², M. Cerrada¹¹², N. Colino¹¹², B. De La Cruz¹¹², A. Delgado Peris¹¹², D. Fernández Del Val¹¹²,
J. P. Fernández Ramos¹¹², J. Flix¹¹², M. C. Fouz¹¹², O. Gonzalez Lopez¹¹², S. Goy Lopez¹¹², J. M. Hernandez¹¹²,
M. I. Josa¹¹², J. León Holgado¹¹², D. Moran¹¹², C. M. Morcillo Perez¹¹², Á. Navarro Tobar¹¹²,
C. Perez Dengra¹¹², A. Pérez-Calero Yzquierdo¹¹², J. Puerta Pelayo¹¹², I. Redondo¹¹², D. D. Redondo Ferrero¹¹²,
L. Romero¹¹², S. Sánchez Navas¹¹², L. Urda Gómez¹¹², J. Vazquez Escobar¹¹², C. Willmott¹¹², J. F. de Trocóniz¹¹³,
B. Alvarez Gonzalez¹¹⁴, J. Cuevas¹¹⁴, J. Fernandez Menendez¹¹⁴, S. Folgueras¹¹⁴, I. Gonzalez Caballero¹¹⁴,
J. R. González Fernández¹¹⁴, E. Palencia Cortezon¹¹⁴, C. Ramón Álvarez¹¹⁴, V. Rodríguez Bouza¹¹⁴,
A. Soto Rodríguez¹¹⁴, A. Trapote¹¹⁴, C. Vico Villalba¹¹⁴, P. Vischia¹¹⁴, S. Bhowmik¹¹⁵, S. Blanco Fernández¹¹⁵,
J. A. Brochero Cifuentes¹¹⁵, I. J. Cabrillo¹¹⁵, A. Calderon¹¹⁵, J. Duarte Campderros¹¹⁵, M. Fernandez¹¹⁵,
C. Fernandez Madrazo¹¹⁵, G. Gomez¹¹⁵, C. Lasaosa García¹¹⁵, C. Martinez Rivero¹¹⁵,
P. Martinez Ruiz del Arbol¹¹⁵, F. Matorras¹¹⁵, P. Matorras Cuevas¹¹⁵, E. Navarrete Ramos¹¹⁵, J. Piedra Gomez¹¹⁵,
L. Scodellaro¹¹⁵, I. Vila¹¹⁵, J. M. Vizan Garcia¹¹⁵, M. K. Jayananda¹¹⁶, B. Kailasapathy^{116,ijj},
D. U. J. Sonnadara¹¹⁶, D. D. C. Wickramaratna¹¹⁶, W. G. D. Dharmaratna¹¹⁷, K. Liyanage¹¹⁷, N. Perera¹¹⁷,
N. Wickramage¹¹⁷, D. Abbaneo¹¹⁸, C. Amendola¹¹⁸, E. Auffray¹¹⁸, G. Auzinger¹¹⁸, J. Baechler¹¹⁸, D. Barney¹¹⁸,
A. Bermúdez Martínez¹¹⁸, M. Bianco¹¹⁸, B. Bilin¹¹⁸, A. A. Bin Anuar¹¹⁸, A. Bocci¹¹⁸, E. Brondolin¹¹⁸,
C. Caillol¹¹⁸, T. Camporesi¹¹⁸, G. Cerminara¹¹⁸, N. Chernyavskaya¹¹⁸, D. d'Enterria¹¹⁸, A. Dabrowski¹¹⁸,
A. David¹¹⁸, A. De Roeck¹¹⁸, M. M. Defranchis¹¹⁸, M. Deile¹¹⁸, M. Dobson¹¹⁸, F. Fallavollita^{118,kkk},
L. Forthomme¹¹⁸, G. Franzoni¹¹⁸, W. Funk¹¹⁸, S. Giani¹¹⁸, D. Gigi¹¹⁸, K. Gill¹¹⁸, F. Glege¹¹⁸, L. Gouskos¹¹⁸,
M. Haranko¹¹⁸, J. Hegeman¹¹⁸, B. Huber¹¹⁸, V. Innocente¹¹⁸, T. James¹¹⁸, P. Janot¹¹⁸, S. Laurila¹¹⁸, P. Lecoq¹¹⁸,
E. Leutgeb¹¹⁸, C. Lourenço¹¹⁸, B. Maier¹¹⁸, L. Malgeri¹¹⁸, M. Mannelli¹¹⁸, A. C. Marini¹¹⁸, M. Matthewman¹¹⁸,
F. Meijers¹¹⁸, S. Mersi¹¹⁸, E. Meschi¹¹⁸, V. Milosevic¹¹⁸, F. Moortgat¹¹⁸, M. Mulders¹¹⁸, S. Orfanelli¹¹⁸,
F. Pantaleo¹¹⁸, G. Petrucciani¹¹⁸, A. Pfeiffer¹¹⁸, M. Pierini¹¹⁸, D. Piparo¹¹⁸, H. Qu¹¹⁸, D. Rabady¹¹⁸,
G. Reales Gutiérrez¹¹⁸, M. Rovere¹¹⁸, H. Sakulin¹¹⁸, S. Scarfi¹¹⁸, C. Schwick¹¹⁸, M. Selvaggi¹¹⁸, A. Sharma¹¹⁸,
K. Shchelina¹¹⁸, P. Silva¹¹⁸, P. Sphicas^{118,lll}, A. G. Stahl Leiton¹¹⁸, A. Steen¹¹⁸, S. Summers¹¹⁸, D. Treille¹¹⁸,
P. Tropea¹¹⁸, A. Tsiros¹¹⁸, D. Walter¹¹⁸, J. Wanczyk^{118,mmm}, K. A. Wozniak^{118,nnn}, S. Wuchterl¹¹⁸, P. Zehetner¹¹⁸,
P. Zejdl¹¹⁸, W. D. Zeuner¹¹⁸, T. Bevilacqua^{119,ooo}, L. Caminada^{119,ooo}, A. Ebrahimi¹¹⁹, W. Erdmann¹¹⁹,
R. Horisberger¹¹⁹, Q. Ingram¹¹⁹, H. C. Kaestli¹¹⁹, D. Kotlinski¹¹⁹, C. Lange¹¹⁹, M. Missiroli^{119,ooo},
L. Noehte^{119,ooo}, T. Rohe¹¹⁹, T. K. Aarrestad¹²⁰, K. Androsov^{120,mmm}, M. Backhaus¹²⁰, A. Calandri¹²⁰,
C. Cazzaniga¹²⁰, K. Datta¹²⁰, A. De Cosa¹²⁰, G. Dissertori¹²⁰, M. Dittmar¹²⁰, M. Donegà¹²⁰, F. Eble¹²⁰,
M. Galli¹²⁰, K. Gedia¹²⁰, F. Glessgen¹²⁰, C. Grab¹²⁰, D. Hits¹²⁰, W. Lustermann¹²⁰, A.-M. Lyon¹²⁰,
R. A. Manzoni¹²⁰, M. Marchegiani¹²⁰, L. Marchese¹²⁰, C. Martin Perez¹²⁰, A. Mascellani^{120,mmm},
F. Nessi-Tedaldi¹²⁰, F. Pauss¹²⁰, V. Perovic¹²⁰, S. Pigazzini¹²⁰, M. G. Ratti¹²⁰, M. Reichmann¹²⁰, C. Reissel¹²⁰,
T. Reitenspiess¹²⁰, B. Ristic¹²⁰, F. Riti¹²⁰, D. Ruini¹²⁰, D. A. Sanz Becerra¹²⁰, R. Seidita¹²⁰, J. Steggemann^{120,mmm},
D. Valsecchi¹²⁰, R. Wallny¹²⁰, C. Amsler^{121,ppp}, P. Bärttschi¹²¹, C. Botta¹²¹, D. Brzhechko¹²¹, M. F. Canelli¹²¹,
K. Cormier¹²¹, R. Del Burgo¹²¹, J. K. Heikkilä¹²¹, M. Huwiler¹²¹, W. Jin¹²¹, A. Jofrehei¹²¹, B. Kilminster¹²¹,
S. Leontsinis¹²¹, S. P. Liechti¹²¹, A. Macchiolo¹²¹, P. Meiring¹²¹, V. M. Mikuni¹²¹, U. Molinatti¹²¹,
I. Neutelings¹²¹, A. Reimers¹²¹, P. Robmann¹²¹, S. Sanchez Cruz¹²¹, K. Schweiger¹²¹, M. Senger¹²¹,
Y. Takahashi¹²¹, R. Tramontano¹²¹, C. Adloff^{122,qqq}, C. M. Kuo¹²², W. Lin¹²², P. K. Rout¹²², P. C. Tiwari^{122,qq},
S. S. Yu¹²², L. Ceard¹²³, Y. Chao¹²³, K. F. Chen¹²³, P. s. Chen¹²³, Z. g. Chen¹²³, W.-S. Hou¹²³, T. h. Hsu¹²³,
Y. w. Kao¹²³, R. Khurana¹²³, G. Kole¹²³, Y. y. Li¹²³, R.-S. Lu¹²³, E. Paganis¹²³, A. Psallidas¹²³, X. f. Su¹²³,
J. Thomas-Wilsker¹²³, L. s. Tsai¹²³, H. y. Wu¹²³, E. Yazgan¹²³, C. Asawatangkuldee¹²⁴, N. Srimanobhas¹²⁴

V. Wachirapusanand¹²⁴ D. Agyel¹²⁵ F. Boran¹²⁵ Z. S. Demiroglu¹²⁵ F. Dolek¹²⁵ I. Dumanoglu^{125,rrr}
 E. Eskut¹²⁵ Y. Guler^{125,sss} E. Gurpinar Guler^{125,sss} C. Isik¹²⁵ O. Kara¹²⁵ A. Kayis Topaksu¹²⁵ U. Kiminsu¹²⁵
 G. Onengut¹²⁵ K. Ozdemir^{125,ttt} A. Polatoz¹²⁵ B. Tali^{125,uuu} U. G. Tok¹²⁵ S. Turkcapar¹²⁵ E. Uslan¹²⁵
 I. S. Zorbakir¹²⁵ M. Yalvac^{126,vvv} B. Akgun¹²⁷ I. O. Atakisi¹²⁷ E. Gülmez¹²⁷ M. Kaya^{127,www} O. Kaya^{127,xxx}
 S. Tekten^{127,yyy} A. Cakir¹²⁸ K. Cankocak^{128,rrr,zzz} Y. Komurcu¹²⁸ S. Sen^{128,aaaa} O. Aydilek¹²⁹ S. Cerci^{129,uuu}
 V. Epshteyn¹²⁹ B. Haciasahinoglu¹²⁹ I. Hos^{129,bbbb} B. Isildak^{129,cccc} B. Kaynak¹²⁹ S. Ozkorucuklu¹²⁹
 O. Potok¹²⁹ H. Sert¹²⁹ C. Simsek¹²⁹ D. Sunar Cerci^{129,uuu} C. Zorbilmez¹²⁹ A. Boyaryntsev¹³⁰ B. Grynyov¹³⁰
 L. Levchuk¹³¹ D. Anthony¹³² J. J. Brooke¹³² A. Bundock¹³² F. Bury¹³² E. Clement¹³² D. Cussans¹³²
 H. Flacher¹³² M. Glowacki¹³² J. Goldstein¹³² H. F. Heath¹³² L. Kreczko¹³² B. Krikler¹³² S. Paramesvaran¹³²
 S. Seif El Nasr-Storey¹³² V. J. Smith¹³² N. Stylianou^{132,dddd} K. Walkingshaw Pass¹³² R. White¹³² A. H. Ball¹³³
 K. W. Bell¹³³ A. Belyaev^{133,eeee} C. Brew¹³³ R. M. Brown¹³³ D. J. A. Cockerill¹³³ C. Cooke¹³³ K. V. Ellis¹³³
 K. Harder¹³³ S. Harper¹³³ M.-L. Holmberg^{133,ffff} J. Linacre¹³³ K. Manolopoulos¹³³ D. M. Newbold¹³³
 E. Olaiya¹³³ D. Petyt¹³³ T. Reis¹³³ G. Salvi¹³³ T. Schuh¹³³ C. H. Shepherd-Themistocleous¹³³ I. R. Tomalin¹³³
 T. Williams¹³³ R. Bainbridge¹³⁴ P. Bloch¹³⁴ C. E. Brown¹³⁴ O. Buchmuller¹³⁴ V. Cacchio¹³⁴
 C. A. Carrillo Montoya¹³⁴ G. S. Chahal^{134,gggg} D. Colling¹³⁴ J. S. Dancu¹³⁴ P. Dauncey¹³⁴ G. Davies¹³⁴
 J. Davies¹³⁴ M. Della Negra¹³⁴ S. Fayer¹³⁴ G. Fedi¹³⁴ G. Hall¹³⁴ M. H. Hassanshahi¹³⁴ A. Howard¹³⁴ G. Iles¹³⁴
 M. Knight¹³⁴ J. Langford¹³⁴ L. Lyons¹³⁴ A.-M. Magnan¹³⁴ S. Malik¹³⁴ A. Martelli¹³⁴ M. Mieskolainen¹³⁴
 J. Nash^{134,hhhh} M. Pesaresi¹³⁴ B. C. Radburn-Smith¹³⁴ A. Richards¹³⁴ A. Rose¹³⁴ C. Seez¹³⁴ R. Shukla¹³⁴
 A. Tapper¹³⁴ K. Uchida¹³⁴ G. P. Uttley¹³⁴ L. H. Vage¹³⁴ T. Virdee^{134,gg} M. Vojinovic¹³⁴ N. Wardle¹³⁴
 D. Winterbottom¹³⁴ K. Coldham¹³⁵ J. E. Cole¹³⁵ A. Khan¹³⁵ P. Kyberd¹³⁵ I. D. Reid¹³⁵ S. Abdullin¹³⁶
 A. Brinkerhoff¹³⁶ B. Caraway¹³⁶ J. Dittmann¹³⁶ K. Hatakeyama¹³⁶ J. Hiltbrand¹³⁶ A. R. Kanuganti¹³⁶
 B. McMaster¹³⁶ M. Saunders¹³⁶ S. Sawant¹³⁶ C. Sutantawibul¹³⁶ M. Toms^{136,q} J. Wilson¹³⁶ R. Bartek¹³⁷
 A. Dominguez¹³⁷ C. Huerta Escamilla¹³⁷ A. E. Simsek¹³⁷ R. Uniyal¹³⁷ A. M. Vargas Hernandez¹³⁷
 R. Chudasama¹³⁸ S. I. Cooper¹³⁸ S. V. Gleyzer¹³⁸ C. U. Perez¹³⁸ P. Rumerio^{138,iiiii} E. Usai¹³⁸ C. West¹³⁸
 R. Yi¹³⁸ A. Akpinar¹³⁹ A. Albert¹³⁹ D. Arcaro¹³⁹ C. Cosby¹³⁹ Z. Demiragli¹³⁹ C. Erice¹³⁹ E. Fontanesi¹³⁹
 D. Gastler¹³⁹ S. Jeon¹³⁹ J. Rohlf¹³⁹ K. Salyer¹³⁹ D. Sperka¹³⁹ D. Spitzbart¹³⁹ I. Suarez¹³⁹ A. Tsatsos¹³⁹
 S. Yuan¹³⁹ G. Benelli¹⁴⁰ X. Coubez^{140,bb} D. Cutts¹⁴⁰ M. Hadley¹⁴⁰ U. Heintz¹⁴⁰ J. M. Hogan^{140,jjjj}
 T. Kwon¹⁴⁰ G. Landsberg¹⁴⁰ K. T. Lau¹⁴⁰ D. Li¹⁴⁰ J. Luo¹⁴⁰ S. Mondal¹⁴⁰ M. Narain^{140,a} N. Pervan¹⁴⁰
 S. Sagir^{140,kkkk} F. Simpson¹⁴⁰ M. Stamenkovic¹⁴⁰ W. Y. Wong¹⁴⁰ X. Yan¹⁴⁰ W. Zhang¹⁴⁰ S. Abbott¹⁴¹
 J. Bonilla¹⁴¹ C. Brainerd¹⁴¹ R. Breedon¹⁴¹ M. Calderon De La Barca Sanchez¹⁴¹ M. Chertok¹⁴¹ M. Citron¹⁴¹
 J. Conway¹⁴¹ P. T. Cox¹⁴¹ R. Erbacher¹⁴¹ F. Jensen¹⁴¹ O. Kukral¹⁴¹ G. Mocellin¹⁴¹ M. Mulhearn¹⁴¹
 D. Pellett¹⁴¹ W. Wei¹⁴¹ Y. Yao¹⁴¹ F. Zhang¹⁴¹ M. Bachtis¹⁴² R. Cousins¹⁴² A. Datta¹⁴² J. Hauser¹⁴²
 M. Ignatenko¹⁴² M. A. Iqbal¹⁴² T. Lam¹⁴² E. Manca¹⁴² D. Saltzberg¹⁴² V. Valuev¹⁴² R. Clare¹⁴³
 J. W. Gary¹⁴³ M. Gordon¹⁴³ G. Hanson¹⁴³ W. Si¹⁴³ S. Wimpenny^{143,a} J. G. Branson¹⁴⁴ S. Cittolin¹⁴⁴
 S. Cooperstein¹⁴⁴ D. Diaz¹⁴⁴ J. Duarte¹⁴⁴ L. Giannini¹⁴⁴ J. Guiang¹⁴⁴ R. Kansal¹⁴⁴ V. Krutelyov¹⁴⁴
 R. Lee¹⁴⁴ J. Letts¹⁴⁴ M. Masciovecchio¹⁴⁴ F. Mokhtar¹⁴⁴ M. Pieri¹⁴⁴ M. Quinnan¹⁴⁴
 B. V. Sathia Narayanan¹⁴⁴ V. Sharma¹⁴⁴ M. Tadel¹⁴⁴ E. Vourliotis¹⁴⁴ F. Würthwein¹⁴⁴ Y. Xiang¹⁴⁴
 A. Yagil¹⁴⁴ A. Barzdukas¹⁴⁵ L. Brennan¹⁴⁵ C. Campagnari¹⁴⁵ G. Collura¹⁴⁵ A. Dorsett¹⁴⁵ J. Incandela¹⁴⁵
 M. Kilpatrick¹⁴⁵ J. Kim¹⁴⁵ A. J. Li¹⁴⁵ P. Masterson¹⁴⁵ H. Mei¹⁴⁵ M. Oshiro¹⁴⁵ J. Richman¹⁴⁵ U. Sarica¹⁴⁵
 R. Schmitz¹⁴⁵ F. Setti¹⁴⁵ J. Sheplock¹⁴⁵ D. Stuart¹⁴⁵ S. Wang¹⁴⁵ A. Bornheim¹⁴⁶ O. Cerri¹⁴⁶ A. Latorre¹⁴⁶
 J. Mao¹⁴⁶ H. B. Newman¹⁴⁶ T. Q. Nguyen¹⁴⁶ M. Spiropulu¹⁴⁶ J. R. Vlimant¹⁴⁶ C. Wang¹⁴⁶ S. Xie¹⁴⁶
 R. Y. Zhu¹⁴⁶ J. Alison¹⁴⁷ S. An¹⁴⁷ M. B. Andrews¹⁴⁷ P. Bryant¹⁴⁷ V. Dutta¹⁴⁷ T. Ferguson¹⁴⁷ A. Harilal¹⁴⁷
 C. Liu¹⁴⁷ T. Mudholkar¹⁴⁷ S. Murthy¹⁴⁷ M. Paulini¹⁴⁷ A. Roberts¹⁴⁷ A. Sanchez¹⁴⁷ W. Terrill¹⁴⁷
 J. P. Cumalat¹⁴⁸ W. T. Ford¹⁴⁸ A. Hassani¹⁴⁸ G. Karathanasis¹⁴⁸ E. MacDonald¹⁴⁸ N. Manganelli¹⁴⁸
 F. Marini¹⁴⁸ A. Perloff¹⁴⁸ C. Savard¹⁴⁸ N. Schonbeck¹⁴⁸ K. Stenson¹⁴⁸ K. A. Ulmer¹⁴⁸ S. R. Wagner¹⁴⁸
 N. Zipper¹⁴⁸ J. Alexander¹⁴⁹ S. Bright-Thonney¹⁴⁹ X. Chen¹⁴⁹ D. J. Cranshaw¹⁴⁹ J. Fan¹⁴⁹ X. Fan¹⁴⁹
 D. Gadkari¹⁴⁹ S. Hogan¹⁴⁹ J. Monroy¹⁴⁹ J. R. Patterson¹⁴⁹ J. Reichert¹⁴⁹ M. Reid¹⁴⁹ A. Ryd¹⁴⁹ J. Thom¹⁴⁹
 P. Wittich¹⁴⁹ R. Zou¹⁴⁹ M. Albrow¹⁵⁰ M. Alyari¹⁵⁰ O. Amram¹⁵⁰ G. Apollinari¹⁵⁰ A. Apresyan¹⁵⁰
 L. A. T. Bauerdick¹⁵⁰ D. Berry¹⁵⁰ J. Berryhill¹⁵⁰ P. C. Bhat¹⁵⁰ K. Burkett¹⁵⁰ J. N. Butler¹⁵⁰ A. Canepa¹⁵⁰

G. B. Cerati¹⁵⁰, H. W. K. Cheung¹⁵⁰, F. Chlebana¹⁵⁰, G. Cummings¹⁵⁰, J. Dickinson¹⁵⁰, I. Dutta¹⁵⁰, V. D. Elvira¹⁵⁰, Y. Feng¹⁵⁰, J. Freeman¹⁵⁰, A. Gandrakota¹⁵⁰, Z. Gecse¹⁵⁰, L. Gray¹⁵⁰, D. Green¹⁵⁰, A. Grummer¹⁵⁰, S. Grünendahl¹⁵⁰, D. Guerrero¹⁵⁰, O. Gutsche¹⁵⁰, R. M. Harris¹⁵⁰, R. Heller¹⁵⁰, T. C. Herwig¹⁵⁰, J. Hirschauer¹⁵⁰, L. Horyn¹⁵⁰, B. Jayatilaka¹⁵⁰, S. Jindariani¹⁵⁰, M. Johnson¹⁵⁰, U. Joshi¹⁵⁰, T. Klijnsma¹⁵⁰, B. Klima¹⁵⁰, K. H. M. Kwok¹⁵⁰, S. Lammel¹⁵⁰, D. Lincoln¹⁵⁰, R. Lipton¹⁵⁰, T. Liu¹⁵⁰, C. Madrid¹⁵⁰, K. Maeshima¹⁵⁰, C. Mantilla¹⁵⁰, D. Mason¹⁵⁰, P. McBride¹⁵⁰, P. Merkel¹⁵⁰, S. Mrenna¹⁵⁰, S. Nahn¹⁵⁰, J. Ngadiuba¹⁵⁰, D. Noonan¹⁵⁰, V. Papadimitriou¹⁵⁰, N. Pastika¹⁵⁰, K. Pedro¹⁵⁰, C. Pena^{150,III}, F. Ravera¹⁵⁰, A. Reinsvold Hall^{150,mmmm}, L. Ristori¹⁵⁰, E. Sexton-Kennedy¹⁵⁰, N. Smith¹⁵⁰, A. Soha¹⁵⁰, L. Spiegel¹⁵⁰, S. Stoynev¹⁵⁰, J. Strait¹⁵⁰, L. Taylor¹⁵⁰, S. Tkaczyk¹⁵⁰, N. V. Tran¹⁵⁰, L. Uplegger¹⁵⁰, E. W. Vaandering¹⁵⁰, I. Zoi¹⁵⁰, C. Aruta¹⁵¹, P. Avery¹⁵¹, D. Bourilkov¹⁵¹, L. Cadamuro¹⁵¹, P. Chang¹⁵¹, V. Cherepanov¹⁵¹, R. D. Field¹⁵¹, E. Koenig¹⁵¹, M. Kolosova¹⁵¹, J. Konigsberg¹⁵¹, A. Korytov¹⁵¹, K. H. Lo¹⁵¹, K. Matchev¹⁵¹, N. Menendez¹⁵¹, G. Mitselmakher¹⁵¹, K. Mohrman¹⁵¹, A. Muthirakalayil Madhu¹⁵¹, N. Rawal¹⁵¹, D. Rosenzweig¹⁵¹, S. Rosenzweig¹⁵¹, K. Shi¹⁵¹, J. Wang¹⁵¹, T. Adams¹⁵², A. Al Kadhimi¹⁵², A. Askew¹⁵², N. Bower¹⁵², R. Habibullah¹⁵², V. Hagopian¹⁵², R. Hashmi¹⁵², R. S. Kim¹⁵², S. Kim¹⁵², T. Kolberg¹⁵², G. Martinez¹⁵², H. Prosper¹⁵², P. R. Prova¹⁵², O. Viazlo¹⁵², M. Wulansatib¹⁵², R. Yohay¹⁵², J. Zhang¹⁵², B. Alsufyani¹⁵³, M. M. Baarmand¹⁵³, S. Butalla¹⁵³, T. Elkafrawy^{153,eee}, M. Hohlmann¹⁵³, R. Kumar Verma¹⁵³, M. Rahmani¹⁵³, M. R. Adams¹⁵⁴, C. Bennett¹⁵⁴, R. Cavanaugh¹⁵⁴, S. Dittmer¹⁵⁴, R. Escobar Franco¹⁵⁴, O. Evdokimov¹⁵⁴, C. E. Gerber¹⁵⁴, D. J. Hofman¹⁵⁴, J. h. Lee¹⁵⁴, D. S. Lemos¹⁵⁴, A. H. Merrit¹⁵⁴, C. Mills¹⁵⁴, S. Nanda¹⁵⁴, G. Oh¹⁵⁴, B. Ozek¹⁵⁴, D. Pilipovic¹⁵⁴, T. Roy¹⁵⁴, S. Rudrabhatla¹⁵⁴, M. B. Tonjes¹⁵⁴, N. Varelas¹⁵⁴, X. Wang¹⁵⁴, Z. Ye¹⁵⁴, J. Yoo¹⁵⁴, M. Alhusseini¹⁵⁵, D. Blend¹⁵⁵, K. Dilsiz^{155,nnnn}, L. Emediato¹⁵⁵, G. Karaman¹⁵⁵, O. K. Köseyan¹⁵⁵, J.-P. Merlo¹⁵⁵, A. Mestvirishvili^{155,oooo}, J. Nachtman¹⁵⁵, O. Neogi¹⁵⁵, H. Ogul^{155,pppp}, Y. Onel¹⁵⁵, A. Penzo¹⁵⁵, C. Snyder¹⁵⁵, E. Tiras^{155,qqqq}, B. Blumenfeld¹⁵⁶, L. Corcodilos¹⁵⁶, J. Davis¹⁵⁶, A. V. Gritsan¹⁵⁶, L. Kang¹⁵⁶, S. Kyriacou¹⁵⁶, P. Maksimovic¹⁵⁶, M. Roguljic¹⁵⁶, J. Roskes¹⁵⁶, S. Sekhar¹⁵⁶, M. Swartz¹⁵⁶, T. Á. Vami¹⁵⁶, A. Abreu¹⁵⁷, L. F. Alcerro Alcerro¹⁵⁷, J. Anguiano¹⁵⁷, P. Baringer¹⁵⁷, A. Bean¹⁵⁷, Z. Flowers¹⁵⁷, D. Grove¹⁵⁷, J. King¹⁵⁷, G. Krintiras¹⁵⁷, M. Lazarovits¹⁵⁷, C. Le Mahieu¹⁵⁷, C. Lindsey¹⁵⁷, J. Marquez¹⁵⁷, N. Minafra¹⁵⁷, M. Murray¹⁵⁷, M. Nickel¹⁵⁷, M. Pitt¹⁵⁷, S. Popescu^{157,rrrr}, C. Rogan¹⁵⁷, C. Royon¹⁵⁷, R. Salvatico¹⁵⁷, S. Sanders¹⁵⁷, C. Smith¹⁵⁷, Q. Wang¹⁵⁷, G. Wilson¹⁵⁷, B. Allmond¹⁵⁸, A. Ivanov¹⁵⁸, K. Kaadze¹⁵⁸, A. Kalogeropoulos¹⁵⁸, D. Kim¹⁵⁸, Y. Maravin¹⁵⁸, K. Nam¹⁵⁸, J. Natoli¹⁵⁸, D. Roy¹⁵⁸, G. Sorrentino¹⁵⁸, F. Rebassoo¹⁵⁹, D. Wright¹⁵⁹, A. Baden¹⁶⁰, A. Belloni¹⁶⁰, A. Bethani¹⁶⁰, Y. M. Chen¹⁶⁰, S. C. Eno¹⁶⁰, N. J. Hadley¹⁶⁰, S. Jabeen¹⁶⁰, R. G. Kellogg¹⁶⁰, T. Koeth¹⁶⁰, Y. Lai¹⁶⁰, S. Lascio¹⁶⁰, A. C. Mignerey¹⁶⁰, S. Nabili¹⁶⁰, C. Palmer¹⁶⁰, C. Papageorgakis¹⁶⁰, M. M. Paranjpe¹⁶⁰, L. Wang¹⁶⁰, J. Bendavid¹⁶¹, W. Busza¹⁶¹, I. A. Cali¹⁶¹, Y. Chen¹⁶¹, M. D'Alfonso¹⁶¹, J. Eysermans¹⁶¹, C. Freer¹⁶¹, G. Gomez-Ceballos¹⁶¹, M. Goncharov¹⁶¹, P. Harris¹⁶¹, D. Hoang¹⁶¹, D. Kovalskyi¹⁶¹, J. Krupa¹⁶¹, L. Lavezzo¹⁶¹, Y.-J. Lee¹⁶¹, K. Long¹⁶¹, C. Mironov¹⁶¹, C. Paus¹⁶¹, D. Rankin¹⁶¹, C. Roland¹⁶¹, G. Roland¹⁶¹, S. Rothman¹⁶¹, Z. Shi¹⁶¹, G. S. F. Stephens¹⁶¹, J. Wang¹⁶¹, Z. Wang¹⁶¹, B. Wyslouch¹⁶¹, T. J. Yang¹⁶¹, B. Crossman¹⁶², B. M. Joshi¹⁶², C. Kapsiak¹⁶², M. Krohn¹⁶², D. Mahon¹⁶², J. Mans¹⁶², B. Marzocchi¹⁶², S. Pandey¹⁶², M. Revering¹⁶², R. Rusack¹⁶², R. Saradhy¹⁶², N. Schroeder¹⁶², N. Strobbe¹⁶², M. A. Wadud¹⁶², L. M. Cremaldi¹⁶³, K. Bloom¹⁶⁴, M. Bryson¹⁶⁴, D. R. Claes¹⁶⁴, C. Fangmeier¹⁶⁴, F. Golf¹⁶⁴, G. Haza¹⁶⁴, J. Hossain¹⁶⁴, C. Joo¹⁶⁴, I. Kravchenko¹⁶⁴, I. Reed¹⁶⁴, J. E. Siado¹⁶⁴, W. Tabb¹⁶⁴, A. Vagnerini¹⁶⁴, A. Wightman¹⁶⁴, F. Yan¹⁶⁴, D. Yu¹⁶⁴, A. G. Zecchinelli¹⁶⁴, G. Agarwal¹⁶⁵, H. Bandyopadhyay¹⁶⁵, L. Hay¹⁶⁵, I. Iashvili¹⁶⁵, A. Kharchilava¹⁶⁵, M. Morris¹⁶⁵, D. Nguyen¹⁶⁵, S. Rappoccio¹⁶⁵, H. Rejeb Sfar¹⁶⁵, A. Williams¹⁶⁵, E. Barberis¹⁶⁶, Y. Haddad¹⁶⁶, Y. Han¹⁶⁶, A. Krishna¹⁶⁶, J. Li¹⁶⁶, M. Lu¹⁶⁶, G. Madigan¹⁶⁶, R. Mccarthy¹⁶⁶, D. M. Morse¹⁶⁶, V. Nguyen¹⁶⁶, T. Orimoto¹⁶⁶, A. Parker¹⁶⁶, L. Skinnari¹⁶⁶, A. Tishelman-Charny¹⁶⁶, B. Wang¹⁶⁶, D. Wood¹⁶⁶, S. Bhattacharya¹⁶⁷, J. Bueghly¹⁶⁷, Z. Chen¹⁶⁷, K. A. Hahn¹⁶⁷, Y. Liu¹⁶⁷, Y. Miao¹⁶⁷, D. G. Monk¹⁶⁷, M. H. Schmitt¹⁶⁷, A. Taliencio¹⁶⁷, M. Velasco¹⁶⁷, R. Band¹⁶⁸, R. Bucci¹⁶⁸, S. Castells¹⁶⁸, M. Cremonesi¹⁶⁸, A. Das¹⁶⁸, R. Goldouzian¹⁶⁸, M. Hildreth¹⁶⁸, K. W. Ho¹⁶⁸, K. Hurtado Anampa¹⁶⁸, T. Ivanov¹⁶⁸, C. Jessop¹⁶⁸, K. Lannon¹⁶⁸, J. Lawrence¹⁶⁸, N. Loukas¹⁶⁸, L. Lutton¹⁶⁸, J. Mariano¹⁶⁸, N. Marinelli¹⁶⁸, I. Mcalister¹⁶⁸, T. McCauley¹⁶⁸, C. Mcgrady¹⁶⁸, C. Moore¹⁶⁸, Y. Musienko^{168,q}, H. Nelson¹⁶⁸, M. Osherson¹⁶⁸, A. Piccinelli¹⁶⁸, R. Ruchti¹⁶⁸, A. Townsend¹⁶⁸, Y. Wan¹⁶⁸, M. Wayne¹⁶⁸, H. Yockey¹⁶⁸, M. Zarucki¹⁶⁸

L. Zygala¹⁶⁸, A. Basnet¹⁶⁹, B. Bylsma¹⁶⁹, M. Carrigan¹⁶⁹, L. S. Durkin¹⁶⁹, C. Hill¹⁶⁹, M. Joyce¹⁶⁹,
 A. Lesauvage¹⁶⁹, M. Nunez Ornelas¹⁶⁹, K. Wei¹⁶⁹, B. L. Winer¹⁶⁹, B. R. Yates¹⁶⁹, F. M. Addesa¹⁷⁰,
 H. Bouchamaoui¹⁷⁰, P. Das¹⁷⁰, G. Dezoort¹⁷⁰, P. Elmer¹⁷⁰, A. Frankenthal¹⁷⁰, B. Greenberg¹⁷⁰, N. Haubrich¹⁷⁰,
 S. Higginbotham¹⁷⁰, G. Kopp¹⁷⁰, S. Kwan¹⁷⁰, D. Lange¹⁷⁰, A. Loeliger¹⁷⁰, D. Marlow¹⁷⁰, I. Ojalvo¹⁷⁰,
 J. Olsen¹⁷⁰, A. Shevelev¹⁷⁰, D. Stickland¹⁷⁰, C. Tully¹⁷⁰, S. Malik¹⁷¹, A. S. Bakshi¹⁷², V. E. Barnes¹⁷²,
 S. Chandra¹⁷², R. Chawla¹⁷², S. Das¹⁷², A. Gu¹⁷², L. Gutay¹⁷², M. Jones¹⁷², A. W. Jung¹⁷², D. Kondratyev¹⁷²,
 A. M. Koshy¹⁷², M. Liu¹⁷², G. Negro¹⁷², N. Neumeister¹⁷², G. Paspalaki¹⁷², S. Piperov¹⁷², V. Scheurer¹⁷²,
 J. F. Schulte¹⁷², M. Stojanovic¹⁷², J. Thieman¹⁷², A. K. Virdi¹⁷², F. Wang¹⁷², W. Xie¹⁷², J. Dolen¹⁷³,
 N. Parashar¹⁷³, A. Pathak¹⁷³, D. Acosta¹⁷⁴, A. Baty¹⁷⁴, T. Carnahan¹⁷⁴, K. M. Ecklund¹⁷⁴,
 P. J. Fernández Manteca¹⁷⁴, S. Freed¹⁷⁴, P. Gardner¹⁷⁴, F. J. M. Geurts¹⁷⁴, A. Kumar¹⁷⁴, W. Li¹⁷⁴,
 O. Miguel Colin¹⁷⁴, B. P. Padley¹⁷⁴, R. Redjimi¹⁷⁴, J. Rotter¹⁷⁴, E. Yigitbasi¹⁷⁴, Y. Zhang¹⁷⁴, A. Bodek¹⁷⁵,
 P. de Barbaro¹⁷⁵, R. Demina¹⁷⁵, J. L. Dulemba¹⁷⁵, C. Fallon¹⁷⁵, A. Garcia-Bellido¹⁷⁵, O. Hindrichs¹⁷⁵,
 A. Khukhunaishvili¹⁷⁵, P. Parygin^{175,q}, E. Popova^{175,q}, R. Taus¹⁷⁵, G. P. Van Onsem¹⁷⁵, K. Goulianos¹⁷⁶,
 B. Chiarito¹⁷⁷, J. P. Chou¹⁷⁷, Y. Gershtein¹⁷⁷, E. Halkiadakis¹⁷⁷, A. Hart¹⁷⁷, M. Heindl¹⁷⁷, D. Jaroslawski¹⁷⁷,
 O. Karacheban^{177,ee}, I. Laflotte¹⁷⁷, A. Lath¹⁷⁷, R. Montalvo¹⁷⁷, K. Nash¹⁷⁷, H. Routray¹⁷⁷, S. Salur¹⁷⁷,
 S. Schnetzer¹⁷⁷, S. Somalwar¹⁷⁷, R. Stone¹⁷⁷, S. A. Thayil¹⁷⁷, S. Thomas¹⁷⁷, J. Vora¹⁷⁷, H. Wang¹⁷⁷, H. Acharya¹⁷⁸,
 D. Ally¹⁷⁸, A. G. Delannoy¹⁷⁸, S. Fiorendi¹⁷⁸, T. Holmes¹⁷⁸, N. Karunarathna¹⁷⁸, L. Lee¹⁷⁸, E. Nibigira¹⁷⁸,
 S. Spanier¹⁷⁸, D. Aebi¹⁷⁹, M. Ahmad¹⁷⁹, O. Bouhali^{179,ssss}, M. Dalchenko¹⁷⁹, R. Eusebi¹⁷⁹, J. Gilmore¹⁷⁹,
 T. Huang¹⁷⁹, T. Kamon^{179,ttt}, H. Kim¹⁷⁹, S. Luo¹⁷⁹, S. Malhotra¹⁷⁹, R. Mueller¹⁷⁹, D. Overton¹⁷⁹,
 D. Rathjens¹⁷⁹, A. Safonov¹⁷⁹, N. Akchurin¹⁸⁰, J. Damgov¹⁸⁰, V. Hegde¹⁸⁰, A. Hussain¹⁸⁰, Y. Kazhykarim¹⁸⁰,
 K. Lamichhane¹⁸⁰, S. W. Lee¹⁸⁰, A. Mankel¹⁸⁰, T. Mengke¹⁸⁰, S. Muthumuni¹⁸⁰, T. Peltola¹⁸⁰, I. Volobouev¹⁸⁰,
 A. Whitbeck¹⁸⁰, E. Appelt¹⁸¹, S. Greene¹⁸¹, A. Gurrola¹⁸¹, W. Johns¹⁸¹, R. Kunnawalkam Elayavalli¹⁸¹,
 A. Melo¹⁸¹, F. Romeo¹⁸¹, P. Sheldon¹⁸¹, S. Tuo¹⁸¹, J. Velkovska¹⁸¹, J. Viinikainen¹⁸¹, B. Cardwell¹⁸²,
 B. Cox¹⁸², J. Hakala¹⁸², R. Hirosky¹⁸², A. Ledovsky¹⁸², A. Li¹⁸², C. Neu¹⁸², C. E. Perez Lara¹⁸²,
 P. E. Karchin¹⁸³, A. Aravind¹⁸⁴, S. Banerjee¹⁸⁴, K. Black¹⁸⁴, T. Bose¹⁸⁴, S. Dasu¹⁸⁴, I. De Bruyn¹⁸⁴,
 P. Everaerts¹⁸⁴, C. Galloni¹⁸⁴, H. He¹⁸⁴, M. Herndon¹⁸⁴, A. Herve¹⁸⁴, C. K. Koraka¹⁸⁴, A. Lanaro¹⁸⁴,
 R. Loveless¹⁸⁴, J. Madhusudanan Sreekala¹⁸⁴, A. Mallampalli¹⁸⁴, A. Mohammadi¹⁸⁴, S. Mondal¹⁸⁴, G. Parida¹⁸⁴,
 D. Pinna¹⁸⁴, A. Savin¹⁸⁴, V. Shang¹⁸⁴, V. Sharma¹⁸⁴, W. H. Smith¹⁸⁴, D. Teague¹⁸⁴, H. F. Tsoi¹⁸⁴, W. Vetens¹⁸⁴,
 A. Warden¹⁸⁴, S. Afanasiev¹⁸⁵, V. Andreev¹⁸⁵, Yu. Andreev¹⁸⁵, T. Aushev¹⁸⁵, M. Azarkin¹⁸⁵, A. Babaev¹⁸⁵,
 A. Belyaev¹⁸⁵, V. Blinov^{185,q}, E. Boos¹⁸⁵, V. Borshch¹⁸⁵, D. Budkouski¹⁸⁵, V. Bunichev¹⁸⁵, V. Chekhovsky¹⁸⁵,
 R. Chistov^{185,q}, M. Danilov^{185,q}, A. Dermenev¹⁸⁵, T. Dimova^{185,q}, D. Druzhkin^{185,uuuu}, M. Dubinin^{185,llll},
 L. Dudko¹⁸⁵, A. Ershov¹⁸⁵, G. Gavrilo¹⁸⁵, V. Gavrilo¹⁸⁵, S. Gninenko¹⁸⁵, V. Golovtcov¹⁸⁵, N. Golubev¹⁸⁵,
 I. Golutvin¹⁸⁵, I. Gorbunov¹⁸⁵, A. Gribushin¹⁸⁵, Y. Ivanov¹⁸⁵, V. Kachanov¹⁸⁵, L. Kardapoltsev^{185,q},
 V. Karjavine¹⁸⁵, A. Karneyeu¹⁸⁵, V. Kim^{185,q}, M. Kirakosyan¹⁸⁵, D. Kirpichnikov¹⁸⁵, M. Kirsanov¹⁸⁵,
 V. Klyukhin¹⁸⁵, O. Kodolova^{185,vvvv}, D. Konstantinov¹⁸⁵, V. Korenkov¹⁸⁵, A. Kozyrev^{185,q}, N. Krasnikov¹⁸⁵,
 A. Lanev¹⁸⁵, P. Levchenko^{185,www}, N. Lychkovskaya¹⁸⁵, V. Makarenko¹⁸⁵, A. Malakhov¹⁸⁵, V. Matveev^{185,q},
 V. Murzin¹⁸⁵, A. Nikitenko^{185,xxxx,vvvv}, S. Obraztsov¹⁸⁵, V. Oreshkin¹⁸⁵, V. Palichik¹⁸⁵, V. Perelygin¹⁸⁵,
 S. Petrushanko¹⁸⁵, S. Polikarpov^{185,q}, V. Popov¹⁸⁵, O. Radchenko^{185,q}, M. Savina¹⁸⁵, V. Savrin¹⁸⁵,
 V. Shalaev¹⁸⁵, S. Shmatov¹⁸⁵, S. Shulha¹⁸⁵, Y. Skovpen^{185,q}, S. Slabospitskii¹⁸⁵, V. Smirnov¹⁸⁵, D. Sosnov¹⁸⁵,
 V. Sulimov¹⁸⁵, E. Tcherniaev¹⁸⁵, A. Terkulov¹⁸⁵, O. Teryaev¹⁸⁵, I. Tlisova¹⁸⁵, A. Toropin¹⁸⁵, L. Uvarov¹⁸⁵,
 A. Uzunian¹⁸⁵, A. Vorobyev^{185,a}, G. Vorotnikov¹⁸⁵, N. Voytishin¹⁸⁵, B. S. Yuldashev^{185,yyyy}, A. Zarubin¹⁸⁵,
 I. Zhizhin¹⁸⁵ and A. Zhokin¹⁸⁵

(CMS Collaboration)

¹Yerevan Physics Institute, Yerevan, Armenia²Institut für Hochenergiephysik, Vienna, Austria³Universiteit Antwerpen, Antwerpen, Belgium⁴Vrije Universiteit Brussel, Brussel, Belgium⁵Université Libre de Bruxelles, Bruxelles, Belgium

- ⁶Ghent University, Ghent, Belgium
⁷Université Catholique de Louvain, Louvain-la-Neuve, Belgium
⁸Centro Brasileiro de Pesquisas Físicas, Rio de Janeiro, Brazil
⁹Universidade do Estado do Rio de Janeiro, Rio de Janeiro, Brazil
¹⁰Universidade Estadual Paulista, Universidade Federal do ABC, São Paulo, Brazil
¹¹Institute for Nuclear Research and Nuclear Energy, Bulgarian Academy of Sciences, Sofia, Bulgaria
¹²University of Sofia, Sofia, Bulgaria
¹³Instituto De Alta Investigación, Universidad de Tarapacá, Casilla 7 D, Arica, Chile
¹⁴Beihang University, Beijing, China
¹⁵Department of Physics, Tsinghua University, Beijing, China
¹⁶Institute of High Energy Physics, Beijing, China
¹⁷State Key Laboratory of Nuclear Physics and Technology, Peking University, Beijing, China
¹⁸Sun Yat-Sen University, Guangzhou, China
¹⁹University of Science and Technology of China, Hefei, China
²⁰Institute of Modern Physics and Key Laboratory of Nuclear Physics and Ion-beam Application (MOE)—Fudan University, Shanghai, China
²¹Zhejiang University, Hangzhou, Zhejiang, China
²²Universidad de Los Andes, Bogota, Colombia
²³Universidad de Antioquia, Medellin, Colombia
²⁴University of Split, Faculty of Electrical Engineering, Mechanical Engineering and Naval Architecture, Split, Croatia
²⁵University of Split, Faculty of Science, Split, Croatia
²⁶Institute Rudjer Boskovic, Zagreb, Croatia
²⁷University of Cyprus, Nicosia, Cyprus
²⁸Charles University, Prague, Czech Republic
²⁹Escuela Politecnica Nacional, Quito, Ecuador
³⁰Universidad San Francisco de Quito, Quito, Ecuador
³¹Academy of Scientific Research and Technology of the Arab Republic of Egypt, Egyptian Network of High Energy Physics, Cairo, Egypt
³²Center for High Energy Physics (CHEP-FU), Fayoum University, El-Fayoum, Egypt
³³National Institute of Chemical Physics and Biophysics, Tallinn, Estonia
³⁴Department of Physics, University of Helsinki, Helsinki, Finland
³⁵Helsinki Institute of Physics, Helsinki, Finland
³⁶Lappeenranta-Lahti University of Technology, Lappeenranta, Finland
³⁷IRFU, CEA, Université Paris-Saclay, Gif-sur-Yvette, France
³⁸Laboratoire Leprince-Ringuet, CNRS/IN2P3, Ecole Polytechnique, Institut Polytechnique de Paris, Palaiseau, France
³⁹Université de Strasbourg, CNRS, IPHC UMR 7178, Strasbourg, France
⁴⁰Institut de Physique des 2 Infinis de Lyon (IP2I), Villeurbanne, France
⁴¹Georgian Technical University, Tbilisi, Georgia
⁴²RWTH Aachen University, I. Physikalisches Institut, Aachen, Germany
⁴³RWTH Aachen University, III. Physikalisches Institut A, Aachen, Germany
⁴⁴RWTH Aachen University, III. Physikalisches Institut B, Aachen, Germany
⁴⁵Deutsches Elektronen-Synchrotron, Hamburg, Germany
⁴⁶University of Hamburg, Hamburg, Germany
⁴⁷Karlsruher Institut fuer Technologie, Karlsruhe, Germany
⁴⁸Institute of Nuclear and Particle Physics (INPP), NCSR Demokritos, Aghia Paraskevi, Greece
⁴⁹National and Kapodistrian University of Athens, Athens, Greece
⁵⁰National Technical University of Athens, Athens, Greece
⁵¹University of Ioánnina, Ioánnina, Greece
⁵²HUN-REN Wigner Research Centre for Physics, Budapest, Hungary
⁵³MTA-ELTE Lendület CMS Particle and Nuclear Physics Group, Eötvös Loránd University, Budapest, Hungary
⁵⁴Faculty of Informatics, University of Debrecen, Debrecen, Hungary
⁵⁵Institute of Nuclear Research ATOMKI, Debrecen, Hungary
⁵⁶Karoly Robert Campus, MATE Institute of Technology, Gyongyos, Hungary
⁵⁷Panjab University, Chandigarh, India
⁵⁸University of Delhi, Delhi, India
⁵⁹Saha Institute of Nuclear Physics, HBNI, Kolkata, India
⁶⁰Indian Institute of Technology Madras, Madras, India

- ⁶¹*Tata Institute of Fundamental Research-A, Mumbai, India*
⁶²*Tata Institute of Fundamental Research-B, Mumbai, India*
⁶³*National Institute of Science Education and Research, An OCC of Homi Bhabha National Institute, Bhubaneswar, Odisha, India*
⁶⁴*Indian Institute of Science Education and Research (IISER), Pune, India*
⁶⁵*Isfahan University of Technology, Isfahan, Iran*
⁶⁶*Institute for Research in Fundamental Sciences (IPM), Tehran, Iran*
⁶⁷*University College Dublin, Dublin, Ireland*
^{68a}*INFN Sezione di Bari, Bari, Italy*
^{68b}*Università di Bari, Bari, Italy*
^{68c}*Politecnico di Bari, Bari, Italy*
^{69a}*INFN Sezione di Bologna, Bologna, Italy*
^{69b}*Università di Bologna, Bologna, Italy*
^{70a}*INFN Sezione di Catania, Catania, Italy*
^{70b}*Università di Catania, Catania, Italy*
^{71a}*INFN Sezione di Firenze, Firenze, Italy*
^{71b}*Università di Firenze, Firenze, Italy*
⁷²*INFN Laboratori Nazionali di Frascati, Frascati, Italy*
^{73a}*INFN Sezione di Genova, Genova, Italy*
^{73b}*Università di Genova, Genova, Italy*
^{74a}*INFN Sezione di Milano-Bicocca, Milano, Italy*
^{74b}*Università di Milano-Bicocca, Milano, Italy*
^{75a}*INFN Sezione di Napoli, Napoli, Italy*
^{75b}*Università di Napoli 'Federico II', Napoli, Italy*
^{75c}*Università della Basilicata, Potenza, Italy*
^{75d}*Scuola Superiore Meridionale (SSM), Napoli, Italy*
^{76a}*INFN Sezione di Padova, Padova, Italy*
^{76b}*Università di Padova, Padova, Italy*
^{76c}*Università di Trento, Trento, Italy*
^{77a}*INFN Sezione di Pavia, Pavia, Italy*
^{77b}*Università di Pavia, Pavia, Italy*
^{78a}*INFN Sezione di Perugia, Perugia, Italy*
^{78b}*Università di Perugia, Perugia, Italy*
^{79a}*INFN Sezione di Pisa, Pisa, Italy*
^{79b}*Università di Pisa, Pisa, Italy*
^{79c}*Scuola Normale Superiore di Pisa, Pisa, Italy*
^{79d}*Università di Siena, Siena, Italy*
^{80a}*INFN Sezione di Roma, Roma, Italy*
^{80b}*Sapienza Università di Roma, Roma, Italy*
^{81a}*INFN Sezione di Torino, Torino, Italy*
^{81b}*Università di Torino, Torino, Italy*
^{81c}*Università del Piemonte Orientale, Novara, Italy*
^{82a}*INFN Sezione di Trieste, Trieste, Italy*
^{82b}*Università di Trieste, Trieste, Italy*
⁸³*Kyungpook National University, Daegu, Korea*
⁸⁴*Chonnam National University, Institute for Universe and Elementary Particles, Kwangju, Korea*
⁸⁵*Hanyang University, Seoul, Korea*
⁸⁶*Korea University, Seoul, Korea*
⁸⁷*Kyung Hee University, Department of Physics, Seoul, Korea*
⁸⁸*Sejong University, Seoul, Korea*
⁸⁹*Seoul National University, Seoul, Korea*
⁹⁰*University of Seoul, Seoul, Korea*
⁹¹*Yonsei University, Department of Physics, Seoul, Korea*
⁹²*Sungkyunkwan University, Suwon, Korea*
⁹³*College of Engineering and Technology, American University of the Middle East (AUM), Dasman, Kuwait*
⁹⁴*Riga Technical University, Riga, Latvia*
⁹⁵*University of Latvia (LU), Riga, Latvia*
⁹⁶*Vilnius University, Vilnius, Lithuania*
⁹⁷*National Centre for Particle Physics, Universiti Malaya, Kuala Lumpur, Malaysia*

- ⁹⁸*Universidad de Sonora (UNISON), Hermosillo, Mexico*
⁹⁹*Centro de Investigacion y de Estudios Avanzados del IPN, Mexico City, Mexico*
¹⁰⁰*Universidad Iberoamericana, Mexico City, Mexico*
¹⁰¹*Benemerita Universidad Autonoma de Puebla, Puebla, Mexico*
¹⁰²*University of Montenegro, Podgorica, Montenegro*
¹⁰³*University of Canterbury, Christchurch, New Zealand*
¹⁰⁴*National Centre for Physics, Quaid-I-Azam University, Islamabad, Pakistan*
¹⁰⁵*AGH University of Krakow, Faculty of Computer Science, Electronics and Telecommunications, Krakow, Poland*
¹⁰⁶*National Centre for Nuclear Research, Swierk, Poland*
¹⁰⁷*Institute of Experimental Physics, Faculty of Physics, University of Warsaw, Warsaw, Poland*
¹⁰⁸*Warsaw University of Technology, Warsaw, Poland*
¹⁰⁹*Laboratório de Instrumentação e Física Experimental de Partículas, Lisboa, Portugal*
¹¹⁰*Faculty of Physics, University of Belgrade, Belgrade, Serbia*
¹¹¹*VINCA Institute of Nuclear Sciences, University of Belgrade, Belgrade, Serbia*
¹¹²*Centro de Investigaciones Energéticas Medioambientales y Tecnológicas (CIEMAT), Madrid, Spain*
¹¹³*Universidad Autónoma de Madrid, Madrid, Spain*
¹¹⁴*Universidad de Oviedo, Instituto Universitario de Ciencias y Tecnologías Espaciales de Asturias (ICTEA), Oviedo, Spain*
¹¹⁵*Instituto de Física de Cantabria (IFCA), CSIC-Universidad de Cantabria, Santander, Spain*
¹¹⁶*University of Colombo, Colombo, Sri Lanka*
¹¹⁷*University of Ruhuna, Department of Physics, Matara, Sri Lanka*
¹¹⁸*CERN, European Organization for Nuclear Research, Geneva, Switzerland*
¹¹⁹*Paul Scherrer Institut, Villigen, Switzerland*
¹²⁰*ETH Zurich—Institute for Particle Physics and Astrophysics (IPA), Zurich, Switzerland*
¹²¹*Universität Zürich, Zurich, Switzerland*
¹²²*National Central University, Chung-Li, Taiwan*
¹²³*National Taiwan University (NTU), Taipei, Taiwan*
¹²⁴*High Energy Physics Research Unit, Department of Physics, Faculty of Science, Chulalongkorn University, Bangkok, Thailand*
¹²⁵*Çukurova University, Physics Department, Science and Art Faculty, Adana, Turkey*
¹²⁶*Middle East Technical University, Physics Department, Ankara, Turkey*
¹²⁷*Bogazici University, Istanbul, Turkey*
¹²⁸*Istanbul Technical University, Istanbul, Turkey*
¹²⁹*Istanbul University, Istanbul, Turkey*
¹³⁰*Institute for Scintillation Materials of National Academy of Science of Ukraine, Kharkiv, Ukraine*
¹³¹*National Science Centre, Kharkiv Institute of Physics and Technology, Kharkiv, Ukraine*
¹³²*University of Bristol, Bristol, United Kingdom*
¹³³*Rutherford Appleton Laboratory, Didcot, United Kingdom*
¹³⁴*Imperial College, London, United Kingdom*
¹³⁵*Brunel University, Uxbridge, United Kingdom*
¹³⁶*Baylor University, Waco, Texas, USA*
¹³⁷*Catholic University of America, Washington, DC, USA*
¹³⁸*The University of Alabama, Tuscaloosa, Alabama, USA*
¹³⁹*Boston University, Boston, Massachusetts, USA*
¹⁴⁰*Brown University, Providence, Rhode Island, USA*
¹⁴¹*University of California, Davis, Davis, California, USA*
¹⁴²*University of California, Los Angeles, California, USA*
¹⁴³*University of California, Riverside, Riverside, California, USA*
¹⁴⁴*University of California, San Diego, La Jolla, California, USA*
¹⁴⁵*University of California, Santa Barbara—Department of Physics, Santa Barbara, California, USA*
¹⁴⁶*California Institute of Technology, Pasadena, California, USA*
¹⁴⁷*Carnegie Mellon University, Pittsburgh, Pennsylvania, USA*
¹⁴⁸*University of Colorado Boulder, Boulder, Colorado, USA*
¹⁴⁹*Cornell University, Ithaca, New York, USA*
¹⁵⁰*Fermi National Accelerator Laboratory, Batavia, Illinois, USA*
¹⁵¹*University of Florida, Gainesville, Florida, USA*
¹⁵²*Florida State University, Tallahassee, Florida, USA*
¹⁵³*Florida Institute of Technology, Melbourne, Florida, USA*
¹⁵⁴*University of Illinois Chicago, Chicago, USA*

- ¹⁵⁵*The University of Iowa, Iowa City, Iowa, USA*
¹⁵⁶*Johns Hopkins University, Baltimore, Maryland, USA*
¹⁵⁷*The University of Kansas, Lawrence, Kansas, USA*
¹⁵⁸*Kansas State University, Manhattan, Kansas, USA*
¹⁵⁹*Lawrence Livermore National Laboratory, Livermore, California, USA*
¹⁶⁰*University of Maryland, College Park, Maryland, USA*
¹⁶¹*Massachusetts Institute of Technology, Cambridge, Massachusetts, USA*
¹⁶²*University of Minnesota, Minneapolis, Minnesota, USA*
¹⁶³*University of Mississippi, Oxford, Mississippi, USA*
¹⁶⁴*University of Nebraska-Lincoln, Lincoln, Nebraska, USA*
¹⁶⁵*State University of New York at Buffalo, Buffalo, New York, USA*
¹⁶⁶*Northeastern University, Boston, Massachusetts, USA*
¹⁶⁷*Northwestern University, Evanston, Illinois, USA*
¹⁶⁸*University of Notre Dame, Notre Dame, Indiana, USA*
¹⁶⁹*The Ohio State University, Columbus, Ohio, USA*
¹⁷⁰*Princeton University, Princeton, New Jersey, USA*
¹⁷¹*University of Puerto Rico, Mayaguez, Puerto Rico, USA*
¹⁷²*Purdue University, West Lafayette, Indiana, USA*
¹⁷³*Purdue University Northwest, Hammond, Indiana, USA*
¹⁷⁴*Rice University, Houston, Texas, USA*
¹⁷⁵*University of Rochester, Rochester, New York, USA*
¹⁷⁶*The Rockefeller University, New York, New York, USA*
¹⁷⁷*Rutgers, The State University of New Jersey, Piscataway, New Jersey, USA*
¹⁷⁸*University of Tennessee, Knoxville, Tennessee, USA*
¹⁷⁹*Texas A&M University, College Station, Texas, USA*
¹⁸⁰*Texas Tech University, Lubbock, Texas, USA*
¹⁸¹*Vanderbilt University, Nashville, Tennessee, USA*
¹⁸²*University of Virginia, Charlottesville, Virginia, USA*
¹⁸³*Wayne State University, Detroit, Michigan, USA*
¹⁸⁴*University of Wisconsin—Madison, Madison, Wisconsin, USA*
¹⁸⁵*An institute or international laboratory covered by a cooperation agreement with CERN*

^aDeceased.

^bAlso at Yerevan State University, Yerevan, Armenia.

^cAlso at TU Wien, Vienna, Austria.

^dAlso at Institute of Basic and Applied Sciences, Faculty of Engineering, Arab Academy for Science, Technology and Maritime Transport, Alexandria, Egypt.

^eAlso at Ghent University, Ghent, Belgium.

^fAlso at Universidade Estadual de Campinas, Campinas, Brazil.

^gAlso at Federal University of Rio Grande do Sul, Porto Alegre, Brazil.

^hAlso at UFMS, Nova Andradina, Brazil.

ⁱAlso at Nanjing Normal University, Nanjing, China.

^jAlso at Henan Normal University, Xinxiang, China.

^kAlso at The University of Iowa, Iowa City, Iowa, USA.

^lAlso at University of Chinese Academy of Sciences, Beijing, China.

^mAlso at China Center of Advanced Science and Technology, Beijing, China.

ⁿAlso at University of Chinese Academy of Sciences, Beijing, China.

^oAlso at China Spallation Neutron Source, Guangdong, China.

^pAlso at Université Libre de Bruxelles, Bruxelles, Belgium.

^qAlso at Another institute or international laboratory covered by a cooperation agreement with CERN.

^rAlso at Cairo University, Cairo, Egypt.

^sAlso at Suez University, Suez, Egypt.

^tAlso at British University in Egypt, Cairo, Egypt.

^uAlso at Birla Institute of Technology, Mesra, Mesra, India.

^vAlso at Purdue University, West Lafayette, Indiana, USA.

^wAlso at Université de Haute Alsace, Mulhouse, France.

^xAlso at Department of Physics, Tsinghua University, Beijing, China.

^yAlso at The University of the State of Amazonas, Manaus, Brazil.

^zAlso at Erzincan Binali Yildirim University, Erzincan, Turkey.

^{aa}Also at University of Hamburg, Hamburg, Germany.

- ^{bb}Also at RWTH Aachen University, III. Physikalisches Institut A, Aachen, Germany.
- ^{cc}Also at Isfahan University of Technology, Isfahan, Iran.
- ^{dd}Also at Bergische University Wuppertal (BUW), Wuppertal, Germany.
- ^{ee}Also at Brandenburg University of Technology, Cottbus, Germany.
- ^{ff}Also at Forschungszentrum Jülich, Juelich, Germany.
- ^{gg}Also at CERN, European Organization for Nuclear Research, Geneva, Switzerland.
- ^{hh}Also at Institute of Physics, University of Debrecen, Debrecen, Hungary.
- ⁱⁱAlso at Institute of Nuclear Research ATOMKI, Debrecen, Hungary.
- ^{jj}Also at Universitatea Babes-Bolyai—Facultatea de Fizica, Cluj-Napoca, Romania.
- ^{kk}Also at Physics Department, Faculty of Science, Assiut University, Assiut, Egypt.
- ^{ll}Also at HUN-REN Wigner Research Centre for Physics, Budapest, Hungary.
- ^{mm}Also at Faculty of Informatics, University of Debrecen, Debrecen, Hungary.
- ⁿⁿAlso at Punjab Agricultural University, Ludhiana, India.
- ^{oo}Also at University of Hyderabad, Hyderabad, India.
- ^{pp}Also at University of Visva-Bharati, Santiniketan, India.
- ^{qq}Also at Indian Institute of Science (IISc), Bangalore, India.
- ^{rr}Also at IIT Bhubaneswar, Bhubaneswar, India.
- ^{ss}Also at Institute of Physics, Bhubaneswar, India.
- ^{tt}Also at Deutsches Elektronen-Synchrotron, Hamburg, Germany.
- ^{uu}Also at Department of Physics, Isfahan University of Technology, Isfahan, Iran.
- ^{vv}Also at Sharif University of Technology, Tehran, Iran.
- ^{ww}Also at Department of Physics, University of Science and Technology of Mazandaran, Behshahr, Iran.
- ^{xx}Also at Helwan University, Cairo, Egypt.
- ^{yy}Also at Italian National Agency for New Technologies, Energy and Sustainable Economic Development, Bologna, Italy.
- ^{zz}Also at Centro Siciliano di Fisica Nucleare e di Struttura Della Materia, Catania, Italy.
- ^{aaa}Also at Università degli Studi Guglielmo Marconi, Roma, Italy.
- ^{bbb}Also at Scuola Superiore Meridionale, Università di Napoli 'Federico II', Napoli, Italy.
- ^{ccc}Also at Fermi National Accelerator Laboratory, Batavia, Illinois, USA.
- ^{ddd}Also at Università di Napoli 'Federico II', Napoli, Italy.
- ^{eee}Also at Ain Shams University, Cairo, Egypt.
- ^{fff}Also at Consiglio Nazionale delle Ricerche—Istituto Officina dei Materiali, Perugia, Italy.
- ^{ggg}Also at Riga Technical University, Riga, Latvia.
- ^{hhh}Also at Department of Applied Physics, Faculty of Science and Technology, Universiti Kebangsaan Malaysia, Bangi, Malaysia.
- ⁱⁱⁱAlso at Consejo Nacional de Ciencia y Tecnología, Mexico City, Mexico.
- ^{jjj}Also at Trincomalee Campus, Eastern University, Sri Lanka, Nilaveli, Sri Lanka.
- ^{kkk}Also at INFN Sezione di Pavia, Università di Pavia, Pavia, Italy.
- ^{lll}Also at National and Kapodistrian University of Athens, Athens, Greece.
- ^{mmm}Also at Ecole Polytechnique Fédérale Lausanne, Lausanne, Switzerland.
- ⁿⁿⁿAlso at University of Vienna Faculty of Computer Science, Vienna, Austria.
- ^{ooo}Also at Universität Zürich, Zurich, Switzerland.
- ^{ppp}Also at Stefan Meyer Institute for Subatomic Physics, Vienna, Austria.
- ^{qqq}Also at Laboratoire d'Annecy-le-Vieux de Physique des Particules, IN2P3-CNRS, Annecy-le-Vieux, France.
- ^{rrr}Also at Near East University, Research Center of Experimental Health Science, Mersin, Turkey.
- ^{sss}Also at Konya Technical University, Konya, Turkey.
- ^{ttt}Also at Izmir Bakircay University, Izmir, Turkey.
- ^{uuu}Also at Adiyaman University, Adiyaman, Turkey.
- ^{vvv}Also at Bozok Universitetesi Rektörlüğü, Yozgat, Turkey.
- ^{www}Also at Marmara University, Istanbul, Turkey.
- ^{xxx}Also at Milli Savunma University, Istanbul, Turkey.
- ^{yyy}Also at Kafkas University, Kars, Turkey.
- ^{zzz}Also at Istanbul Okan University, Istanbul, Turkey.
- ^{aaaa}Also at Hacettepe University, Ankara, Turkey.
- ^{bbbb}Also at Istanbul University—Cerrahpasa, Faculty of Engineering, Istanbul, Turkey.
- ^{cccc}Also at Yildiz Technical University, Istanbul, Turkey.
- ^{dddd}Also at Vrije Universiteit Brussel, Brussel, Belgium.
- ^{eeee}Also at School of Physics and Astronomy, University of Southampton, Southampton, United Kingdom.
- ^{ffff}Also at University of Bristol, Bristol, United Kingdom.
- ^{gggg}Also at IPPP Durham University, Durham, United Kingdom.
- ^{hhhh}Also at Monash University, Faculty of Science, Clayton, Australia.
- ⁱⁱⁱⁱAlso at Università di Torino, Torino, Italy.

- ^{jjjj} Also at Bethel University, St. Paul, Minnesota, USA.
- ^{kkkk} Also at Karamanoğlu Mehmetbey University, Karaman, Turkey.
- ^{llll} Also at California Institute of Technology, Pasadena, California, USA.
- ^{mmmm} Also at United States Naval Academy, Annapolis, Maryland, USA.
- ⁿⁿⁿⁿ Also at Bingöl University, Bingöl, Turkey.
- ^{oooo} Also at Georgian Technical University, Tbilisi, Georgia.
- ^{pppp} Also at Sinop University, Sinop, Turkey.
- ^{qqqq} Also at Erciyes University, Kayseri, Turkey.
- ^{rrrr} Also at Horia Hulubei National Institute of Physics and Nuclear Engineering (IFIN-HH), Bucharest, Romania.
- ^{ssss} Also at Texas A&M University at Qatar, Doha, Qatar.
- ^{tttt} Also at Kyungpook National University, Daegu, Korea.
- ^{uuuu} Also at Universiteit Antwerpen, Antwerpen, Belgium.
- ^{vvvv} Also at Yerevan Physics Institute, Yerevan, Armenia.
- ^{wwww} Also at Northeastern University, Boston, Massachusetts, USA.
- ^{xxxx} Also at Imperial College, London, United Kingdom.
- ^{yyyy} Also at Institute of Nuclear Physics of the Uzbekistan Academy of Sciences, Tashkent, Uzbekistan.